IAS-2021-005: Improving Consumptive Use Estimates within the Lower Colorado River Basin using Satellite-Derived Determinations of Crop Growth Stage Lengths

Andrew N. French

Yuma Center of Excellence for Desert Agriculture
University of Arizona
899 E. Plaza Cir. #2, Yuma, AZ 85365

Elzbieta H. Wisniewski

U.S. Arid Land Agricultural Research Center
U.S. Department of Agriculture,
21881 N. Cardon Lane, Maricopa, AZ 85138

Troy Wirth, John W. Shields, and Andrew Scott

U.S. Bureau of Reclamation
500 Date St., Boulder City, NV 89005

April 8, 2025

Contents

1 Summary **1**

2 Introduction **2**

3 Evapotranspiration Modeling **3**

4 Objective 1: Scripts for Growth Stage Tracking **9**
- 4.1 Assemble crop type information . . . 11
- 4.2 Retrieve NDVI times series . . . 11
- 4.3 Filter the NDVI data . . . 11
- 4.4 Convert NDVI to K_c . . . 14
- 4.5 Compute ET_c . . . 15
- 4.6 Script for Alfalfa . . . 20
- 4.7 Script for Bermudagrass and Kleingrass . . . 22
- 4.8 Script for Sudangrass . . . 24
- 4.9 Script for Citrus . . . 24
- 4.10 Scripts for Dates and Olives . . . 31
- 4.11 Scripts for Carrot, Lettuce, Sugar beet and Wheat . . . 33
- 4.12 Scripts for Cotton, Corn and Grapes . . . 33

5 Objective 2: Application of Scripts **34**
- 5.1 Alfalfa . . . 37
- 5.2 Bermudagrass and Kleingrass . . . 43
- 5.3 Citrus . . . 47
- 5.4 Carrots . . . 55
- 5.5 Corn . . . 58
- 5.6 Cotton . . . 62
- 5.7 Dates . . . 66
- 5.8 Grapes . . . 69
- 5.9 Kleingrass . . . 72
- 5.10 Lettuce . . . 75
- 5.11 Olives . . . 79
- 5.12 Sudangrass . . . 82
- 5.13 Sugar beet . . . 85
- 5.14 Wheat . . . 89

6 Objective 3: Compare ET_c Estimates **93**
6.1 Coachella . . . 93
6.2 CRIT . . . 97
6.3 IID . . . 100
6.4 Mohave . . . 102
6.5 PVID . . . 103
6.6 Yuma . . . 105

7 Extending ET_c estimation with Radar Remote Sensing **111**

8 Implications, Comments, and Recommendations **117**
8.1 Implications . . . 117
8.2 Comments on the NDVI growth stage methodology . . . 117
8.2.1 Remote Sensing Data . . . 118
8.2.2 NDVI Processing . . . 118
8.2.3 Growth Stage Modeling Outcomes . . . 119
8.3 Comments on using LCRAS, NDVI, and K_c for ET_c estimation . . . 120
8.3.1 ET_c from LCRAS . . . 120
8.3.2 ET_c from NDVI . . . 121
8.3.3 ET_c from K_c . . . 122
8.3.4 ET_c from Land Surface Temperatures . . . 122
8.4 Recommendations . . . 123

9 Acknowledgements **125**

References **126**

List of Figures

1 LCRAS K_c curves at IID & Coachella vs. Yuma 5
2 LCRAS weather station locations 7
3 Reference evapotranspiration (ET_{os}) 8
4 Converting NDVI to ET_c using growth stages 13
5 Testing NDVI threshold values for Bermudagrass and Kleingrass . . 23
6 NDVI response to day of year and tree maturity for citrus at Yuma . 25
7 Growth stage delineation for citrus 27
8 Average citrus NDVI trends for young, mature, and declining trees . 29
9 Adaptive K_c for young to mature citrus 30
10 Dates maturity vs. NDVI and Day of Year at Yuma 31
11 Olives vs. NDVI and Day of Year at IID 32
12 Alfalfa ET_c estimation from NDVI 38
13 Total field-wise ET_c for alfalfa 39
14 Number of alfalfa cuttings per year 41
15 Maximum NDVI each week for alfalfa 42
16 Bermudagrass /Kleingrass NDVI tresholding for IID 44
17 Example of Bermudagrass /Kleingrass thresholding for Yuma sites . 45
18 Total ET_c for combined Bermudagrass and Kleingrass 46
19 Mature citrus ET_c estimation from NDVI 49
20 Young citrus ET_c estimation from NDVI 50
21 Declining citrus ET_c estimation from NDVI 51
22 Total ET_c for Yuma citrus 2019-2022 computed for three tree maturities 52
23 Total ET_c for IID citrus 2019-2022 computed for three tree maturities 53
24 Total ET_c for Coachella citrus 2019-2022 computed for three tree maturities 54
25 Carrot ET_c estimation from NDVI 56
26 Distribution of ET_c for carrots 57
27 Corn ET_c estimation from NDVI 59
28 Growth stage estimation from NDVI and LCRAS for corn 60
29 Total ET_c for corn at Yuma 61
30 Cotton ET_c estimation from NDVI 63
31 Growth stage estimation from NDVI and LCRAS for cotton 64
32 Total ET_c for cotton 2019-2022 65
33 Mature dates ET_c estimation from NDVI 67
34 Total ET_c for dates 68
35 Grapes ET_c estimation from NDVI 70

36 Total ET_c for grape 2019-2022 71
37 Kleingrass ET_c estimation from NDVI 73
38 Total ET_c for Kleingrass 2019-2022 74
39 Lettuce ET_c estimation from NDVI 76
40 Growth stage estimation from NDVI and LCRAS for lettuce 77
41 Total ET_c (mm/year) for lettuce at Yuma 78
42 Olives ET_c estimation from NDVI 80
43 Total ET_c for olive 2019-2022 81
44 Sudangrass ET_c estimation from NDVI 83
45 Total ET_c (mm/year) for Sudangrass 2019-2022 84
46 Sugar beet ET_c estimation from NDVI 86
47 Growth stage estimation from NDVI and LCRAS for sugar beet . . 87
48 Total ET_c (mm/year) for sugar beet 2019-2022 88
49 Wheat ET_c estimation from NDVI 90
50 Growth stage estimation from NDVI and LCRAS for wheat at Yuma 91
51 Total ET_c (mm/year) for wheat 2019-2022 92
52 NDVI for grapes at Coachella 94
53 Comparing Sudangrass growth at CRIT in 2020 and 2022 98
54 Tracking alfalfa cuttings with Sentinel-2 NDVI and and Sentinel-1 VH/VV from active radar 111
55 Citrus maturity vs. day of year using NDVI and radar VH/VV . . . 113
56 Lettuce time series at Yuma 115
57 Total ET_c (mm/year) for lettuce at Yuma using radar 116

List of Tables

1 Scripts to convert NDVI to ET_c . . . 10
2 LCRAS K_c values, Part 1 . . . 16
3 LCRAS K_c values, Part 2 . . . 17
4 LCRAS K_c values, Part 3 . . . 18
5 LCRAS K_c values, Part 4 . . . 19
6 LCRAS K_c values, Part 5 . . . 20
7 Parameter settings for analyzing Alfalfa NDVI time series . . . 21
8 Significant crops for LCRAS areas, 2019-2022, Part 1 of 2 . . . 35
9 Significant crops for LCRAS areas, 2019-2022, Part 2 of 2 . . . 36
10 Alfalfa Annual ET_c (mm/year) . . . 37
11 NDVI results for combined Bermudagrass and Kleingrass . . . 43
12 NDVI results for Citrus Annual ET_c . . . 47
13 Carrots Annual ET_c . . . 55
14 Corn Annual ET_c . . . 58
15 Cotton ET_c . . . 62
16 Dates Annual ET_c (mm/year) . . . 66
17 Grapes ET_c . . . 69
18 Kleingrass ET_c . . . 72
19 Lettuce ET_c (mm/year) . . . 75
20 Olives ET_c . . . 79
21 Sudangrass ET_c . . . 82
22 Sugar beet ET_c . . . 85
23 Wheat Annual ET_c (mm/year) . . . 89
24 Coachella ET_c Results Part 1 . . . 96
25 Coachella ET_c Results Part 2 . . . 97
26 CRIT ET_c Results . . . 99
27 IID ET_c Results . . . 101
28 Mohave ET_c Results . . . 102
29 PVID ET_c Results . . . 104
30 Yuma ET_c Results Part 1 . . . 106
31 Yuma ET_c Results Part 2 . . . 107
32 LCRAS Annual ET_c (mm/year): Coachella, CRIT . . . 108
33 LCRAS Annual ET_c (mm/year): IID, Mohave . . . 109
34 LCRAS Annual ET_c (mm/year): PVID, Yuma . . . 110
35 Lettuce ET_c (mm/year) from radar observation . . . 114
36 NDVI Growth Stage Tracking Outcome Groups . . . 119

1 Summary

The U.S. Bureau of Reclamation is tasked with estimating agricultural water use throughout the Lower Colorado River Basin. Its accounting system, LCRAS, has facilitated this responsibility since 2003 by using reference evapotranspiration data, crop coefficients, and remotely sensed land cover information to estimate crop-specific water use for all of the irrigation areas. Implementation of LCRAS was a significant advance in water accounting by Reclamation because the approach provided estimates of crop evapotranspiration (ET_c) directly instead of inferring it from differences between the total water budget and returned flows. However, LCRAS accuracy is not as good as it could be because it specifies when crops are planted, growth development rates, and how long they are grown. Those specifications constrain LCRAS to conditions that do not match actual farm practice and lead to ET_c inaccuracy.

This report presents results from a project that addresses these limitations. The study uses satellite remote sensing methodology to determine crop growth stages that improves estimation accuracy for planting time, growth rates, and length of growing seasons. The stages are determined by collecting images of normalized difference vegetation indices (NDVI), over all irrigated areas, assembling them with Reclamation-verified crop type maps, partitioning fields individually into FAO-56-style crop growth stages, and converting these into field-averaged daily ET_c data sets.

Prior to 2018 this methodology would have been difficult. Earlier, satellite observations were too infrequent ($>$7 days), or had spatial resolutions that were too coarse ($\geq$30 m). Software tools needed to manage very large data sets were also missing. Today, observations and tools needed are freely and readily available. Satellite data from the Sentinel-2 sensor are provided at 10 m resolution every 3-5 days. Software provided by the web-based Google Earth Engine delivers access to vegetation index data in minutes. Together, the data and software make the satellite remote sensing methodology feasible and practical.

Results from the growth stage project showed how ET_c estimates over irrigated areas in the Lower Colorado River Basin can be improved. Crop growth stages were accurately tracked, and the resulting total ET_c values reasonably estimated. Modeling outcomes fell into three groups: 'fully-successful', 'alternative-identified', and 'undetermined'. Most annual crops were part of the 'fully successful' group– examples include alfalfa, lettuce, wheat, and cotton. Growth stages were reliably tracked, and the satellite data highlighted instances when LCRAS was inaccurate. For perennial crops– citrus and date trees – an alternative vegetation index approach was identified and used to estimate ET_c. For these it was more important to track growth based on annual averages instead of day-to-day changes. Reclamation practice of clas-

sifying tree maturity enabled use of NDVI and crop coefficients to estimate ET_c. Three crops– Bermudagrass, Kleingrass, and Sudangrass – fell into the 'undetermined' group. These could not be consistently tracked in the same way as for other annual crops because they are managed in hard-to-predict and episodic ways that varied by irrigation area. In these cases, a simple NDVI-thresholding approach returned reasonable ET_c.

The project also demonstrated how an additional tool, active radar remote sensing, could be employed to make the approach still more effective by providing observations regardless of cloudiness.

Outcomes from this study show that the LCRAS model can be advanced and improved by using satellite data to track crop growth stages and annual growth trends. The growth stage model would lead to ET_c estimates that are more accurate than LCRAS. Adoption by Reclamation could facilitate a more rapid and comprehensive water accounting system.

2 Introduction

The Lower Colorado River is a vital source of freshwater for agricultural users across the U.S. Southwest. This report presents final results from the U.S. Bureau of Reclamation's WaterSmart-funded study IAS-2021-005 that seeks to improve the effectiveness and accuracy of agricultural water use accounting.

The U.S. Bureau of Reclamation (Reclamation), Water Master for the Colorado River below Hoover Dam, has been required to account for annual water use pursuant to a decree of the Supreme Court of the United States (547 U.S. 150, 1964, consolidated 2006). Because of this role, it is vital for Reclamation to accurately quantify how much and where water is used. Annual water use is summarized in a report entitled "Colorado River Accounting and Water Use Report: Arizona, California, and Nevada (Water Report)". Reclamation water use reports were augmented by detailed reports of crop evapotranspiration (ET_c) and evaporation (Lower Colorado River Annual Summary of Evapotranspiration and Evaporation (LCRAS)). These reports provide crop cover type maps derived from remote sensing observations, predominantly from Landsat (https://usgs.gov/landsat-missions/data), that were not previously available. These crop maps, along with a standardized approach for estimating ET_c, enabled improved accuracy and consistency. More recently, expansion and increased availability of remotely sensed image data has made possible additional improvement of the LCRAS Report. Whereas the ET_c approach established by Jensen (1998, 2003) used remote sensing solely for crop classification, it became possible

with the more frequent data to track crop growth patterns at close to daily time steps. This approach- which adjusted growth stages, while utilizing existing LCRAS coefficients (described below)- enabled estimation of ET_c for all fields individually, or in aggregate, throughout the entire growing season. Documentation for the new application (French et al., 2023), showed that when crop type data are provided, the method is quick, practical, and more accurate than the existing LCRAS approach.

3 Evapotranspiration Modeling

Current Reclamation ET_c modeling uses the single crop coefficient approach (K_c) as described in FAO-56 (Allen et al., 1998). It is based on the scaling of reference evapotranspiration (ET_{os} [1]) by crop coefficients:

$$ET_c = K_c \times ET_{os} \tag{1}$$

The coefficients are specific to each crop type or crop category and represent daily ET_c expected for the entire growing season. The season for each crop is partitioned into 4 or fewer growth stages. Modeling inputs are reference evapotranspiration (ET_{os}), crop coefficient curves, and crop growth observations.

ET_{os} is the amount of water transported into the atmosphere from a uniform surface of dense, actively growing vegetation with 0.12 m height, where soil water is ample and the spatial extent of vegetation is at least 100 m in all directions. In Allen et al. (2005) standardized ET (ET_{os}) is set forth for computing:

$$ET_{os} = \frac{0.48\Delta(R_n - G) + \gamma \frac{C_n}{T+273} u_2 (e_s - e_a)}{\Delta + \gamma(1 + C_d u_2)} \tag{2}$$

where Δ is the slope of the saturation vapor pressure curve, R_n is net radiation, G is soil heat flux, γ is the psychrometric constant, T is mean daily air temperature at $\sim$2 m height above the ground, u_2 is mean wind speed at 2 m height, and e_s and e_a are saturation and ambient water vapor pressure, respectively. The constants C_n and C_d are set according to calculation time steps and height of the reference crop. For this project, time steps were daily and reference crop height was 0.12 m. Accordingly, C_n was set to 900, and C_d set to 0.34. Equation 2 is comprised of two components. One consists of radiative fluxes, which are determined by solar radiation, atmospheric radiation, and soil heat flux (R_n and G). The other consists of advective fluxes determined by near surface wind speed and water vapor pressure (u_2, e_s, and e_a). ET_{os} data

[1] The 'os' subscript is used to denote that the short-crop (0.12 m height) reference value is used.

used in this project are derived from Arizona (azmet.arizona.edu) and California (cimis.water.ca.gov) weather stations. Each website provides ET_{os} , meaning that use of Eq. 2 was not needed. Locations of the weather stations are denoted by red dots within the LCRAS irrigation districts (Figure 2).

Crop coefficient curves represent the crop-specific scaling term that transforms ET_{os} into ET_c at a daily time step. FAO-56 describes two different methodologies for generating the coefficient curves. The dual crop coefficient method develops separate time series for evaporation and transpiration scale factors, while the single crop coefficient method consolidates evaporation and transpiration into one daily value. Reclamation adopts the single coefficient approach. As defined in Jensen (2003), Reclamation further constrains the curves to be static in time. This means that each observed crop is presumed to be planted, grown, and harvested in a pre-defined time interval.

The single crop coefficient approach has sub-components that partition the growing season into four stages: initial, development, mid, and end, respectively denoted as INI, DEV, MID, and END. Because the stages are linearly connected, only three reference coefficients are needed: K_cINI , K_cMID , and K_cEND . Reclamation follows this construct for all irrigation districts except for IID and Coachella, where the K_c patterns are more curvilinear. These more complicated patterns cannot be easily modeled with three reference coefficients, so simplification of the K_c curves for those two districts was conducted. The resulting standard K_c curves for crops considered in this project are listed in Tables 2, 3, and 4.

The Reclamation approach adopted in 2003 (Jensen, 2003) was a significant advance in ET_c estimation because it adopted use of remote sensing imagery to map crop type distributions in all 6 of the Lower Colorado irrigated regions. By combining images with ground-based crop validation data sets- obtained 4 times a year- the Reclamation-defined K_c curves could be assigned, multiplied by weather-station based ET_{os} , and the resulting daily ET_c values summed to obtained annual ET_c . The static K_c patterns are generalized based on actual cropping patterns in the areas where those crops are typically grown but do not resolve between-field or seasonal variations due to changes in agricultural operations such as planting and harvest dates.

Beginning around 2018, satellite remote sensing data became increasingly available, making possible a better way to track crop water use. Instead of using only Landsat data, which collected every 16 days (now 8-16 days) at 30 m resolution, Reclamation could begin using the European Space Agency's Sentinel 2 satellite, which observes the Southwest USA every 3-5 days at 10 m resolution. This meant that multispectral satellite data could be used for more than crop classification: it could track crop growth. The Normalized Difference Vegetation Index (NDVI, Rouse et al.,

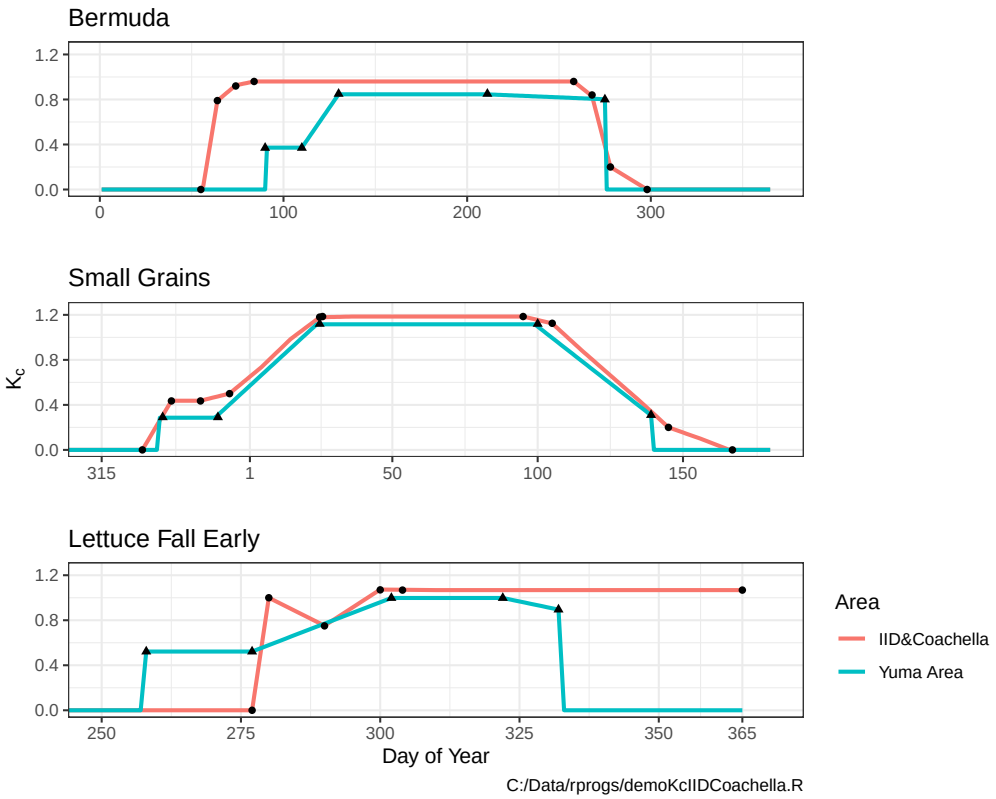

Figure 1. LCRAS K_c curves at IID & Coachella vs. Yuma. Plots for Bermudagrass (top), Small Grains (middle), and Lettuce Fall Early (bottom) are shown to illustrate the differences between K_c definitions for different irrigation areas. IID & Coachella are curvilinear. For lettuce, the K_c pattern includes an early season spike to represent pre-emergent irrigation. The Yuma area follows the FAO-56 pattern of only needing three K_c values (INI, MID, END) to define the seasonal curve. The other irrigation areas – CRIT, PVID and Mohave – also follow the FAO-56 pattern.

1974) is pivotal for this task (Equation 3), the index being computed from near infrared reflectance (NIR) and red reflectance (Red) bands:

$$NDVI = \frac{NIR - Red}{NIR + Red} \tag{3}$$

Green vegetation is dark in Red reflected light and bright in NIR reflected light, while soils- with some exceptions- are similarly reflective in both bands. Consequently, NDVI can be a surrogate for vegetation canopy density. Multiple functional relationships can be used to estimate fractional cover. An example of one is shown in Equation 4 (Carlson and Ripley, 1997):

$$F = [NDVI_{\star}]^2 \tag{4}$$

where F is fractional cover and $NDVI_{\star}$ is $NDVI$ normalized between 0 and 1.

For this study, it is important to know that $NDVI$ is closely related to F and that mapping NDVI images can be a surrogate for green vegetation biomass and K_c. This project's goal is to demonstrate how mapping of K_c can be done reliably, and to document the resulting effect upon ET_c estimates across all of the irrigated areas within the Lower Colorado River region.

Figure 2. LCRAS weather station locations serving the six Lower Colorado River irrigation areas.

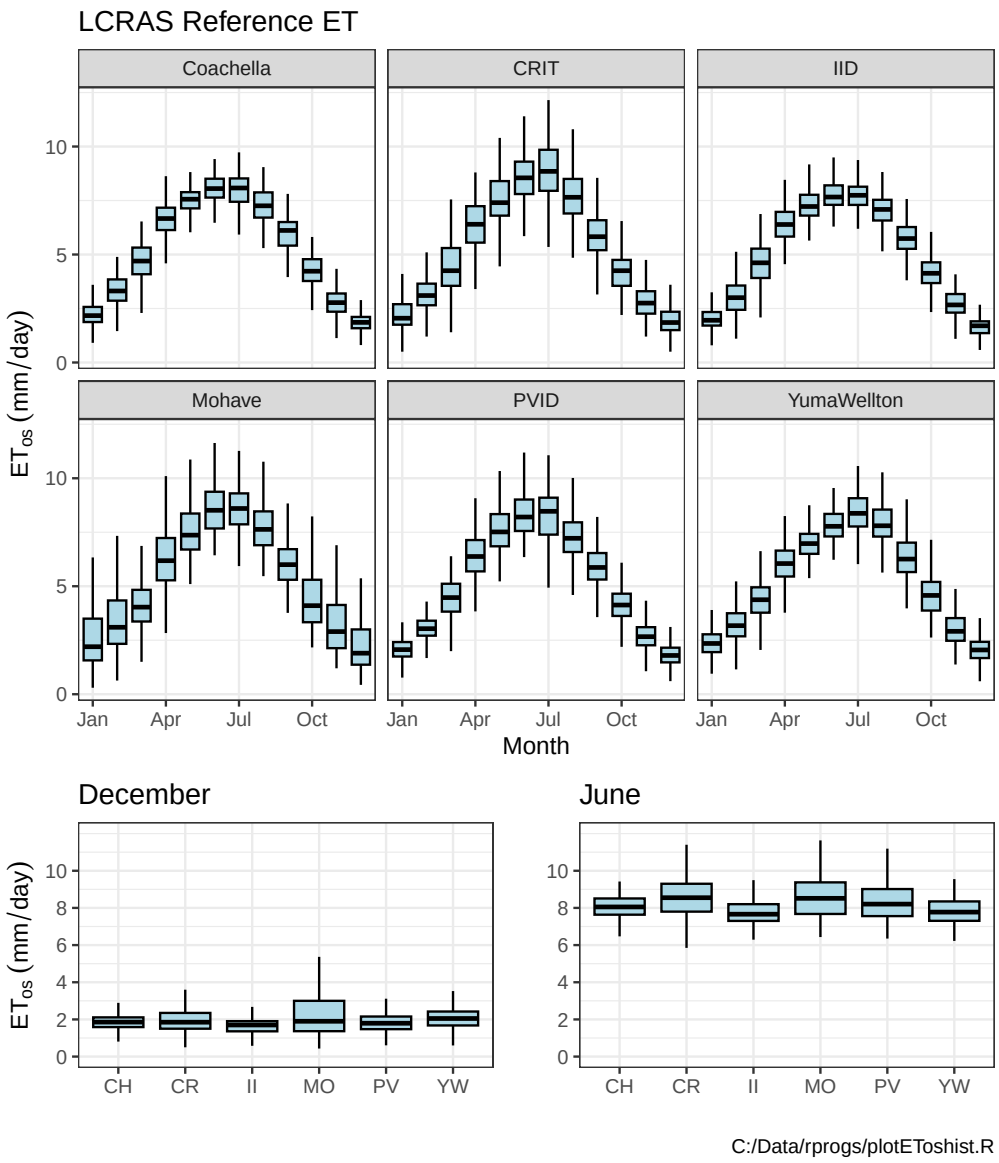

Figure 3. Monthly reference evapotranspiration (ET_{os}) for the LCRAS study period, 2018-2022. Abbreviations in bottom plots correspond to irrigation areas as follow: CH (Coachella), CR (CRIT), II (IID), MO (Mohave), PV (PVID), and YW (Yuma-Wellton).

4 Objective 1: Scripts for Growth Stage Tracking

The tasks for Objective 1 are to review, test, and document R scripts needed for growth stage tracking.

At the start of WaterSmart project IAS-2021-005, prototype R scripts had been available as part of the research presented in French et al. (2023) [2]. This section provides details on revised versions of those prototypes and on scripts not previously written. 'R' is a general-purpose, open-source, programming language (v4.4.0, R Core Team, 2021). Script implementation was done within the development environment 'RStudio' (RStudio Team, 2020).[3]

The initial scripts demonstrated feasibility for four crop types: 1) a short season crop, broccoli, 2) a mid-length season crop, wheat, 3) a long season crop, cotton, and 4) an episodic season crop, alfalfa. Each script was designed to implement Eq. 1, where K_c curves were defined by inflection time points determined from NDVI observations. ET_{os} values were derived from averaged weather station data. There are 21 core weather stations used for ET_{os} estimation (Figure 2). Historical averages show how ET_{os} varies within each irrigation area (top of Figure 3). Seasonal differences range $\sim$2 mm/day in December and $\sim$8 mm/day in June (bottom, Figure 3). .

The script collections were revised using two approaches: one that used multiple scripts customized by crop type, and another that used one script that can process all crop types. Script names are listed in Table 1. Two approaches were done to create processing options and flexibility for future use by Reclamation. The first approach is advantageous for code simplicity, easier code debugging, and rapid processing. Its disadvantage is that separate script executions are needed for each crop type. The advantage for the second approach is implementation simplicity– namely only one script is needed to produce ET_c results. However, that script is lengthy, complex, and sometimes requires long (>20 minutes) execution times.

[1] Mention of tradenames and commercial products is for reader convenience and does not imply endorsement. USBR and USDA do not endorse or recommend products.

[2] Posit, RStudio, and Shiny are trademarks of Posit Software, PBC, all rights reserved, and may be registered in the United States Patent and Trademark Office and in other countries.

Table 1. Scripts to convert NDVI to ET_c

Crop	R Script
Alfalfa[†]	Alfalfa_NDVI_to_Kc_and_ETc.R
Bermudagrass [*]	Bermuda_NDVI_to_ETc_threshmethod.R
Citrus[‡]	Citrus_AdaptiveNDVI_to_Kc_and_ETc.R
Corn	Corn_NDVI_to_Kc_and_ETc.R
Cotton	Cotton_NDVI_to_Kc_and_ETc.R
Dates	Dates_NDVI_to_Kc_and_ETc.R
Carrot[§]	Carrot_NDVI_to_Kc_and_ETc.R
Grapes	Grape_NDVI_to_Kc_and_ETc.R
Kleingrass [*]	Bermuda_NDVI_to_ETc_threshmethod.R
Lettuce[§]	HeadLettuce_NDVI_to_Kc_and_ETc.R
Olives	Olive_NDVI_to_Kc_and_ETc.R
Sudangrass [*]	Sudan_NDVI_to_Kc_and_ETc.R
Sugar beet[§]	Sugar_NDVI_to_Kc_and_ETc.R
Wheat[§]	Wheat_NDVI_to_Kc_and_ETc.R
All[°]	Crop_growth_stages_detection.R

[†] Multiple cycles per year.

[*] Binary classification into MID or fallow, with Bermudagrass and Kleingrass combined.

[‡] K_c adapts to maturity via NDVI.

[§] Stages may start and end in different years.

[°] Unified script handles all crop types.

Generally both script collections use the same algorithms to convert NDVI data into growth stages and transform those into field-by-field ET_c values. There are five main steps.

4.1 Assemble crop type information

In step 1, shapefiles are collected for all irrigation areas for the target year, and split into crop specific data sets. The collections are derived from the field validation campaigns, usually done in February, April, July, and December. For this project, approximately 144 GIS 'shapefiles' were derived from the 2019-2022 collection: six discrete irrigation areas, four years, and six crop types per district. Each shapefile contains the standard LCRAS crop name, crop code, area id, field id, and geographic bounds in UTM zone 11 projection. The shapefiles include file components: shp, prj, shx, and dbf.

4.2 Retrieve NDVI times series

In step 2, the shapefiles are uploaded and processed on the Google Earth Engine (GEE, `https://code.earthengine.google.com`) platform. Processing times usually range from a few seconds to <10 minutes. The maximum query limit on GEE is 10 MB. See Gorelick et al. (2017) and GEE Developers Guide for details. Operation of the GEE application (not detailed in this report), uses a javascript file to direct which satellite sensor and spectral bands to use, the date-time window to query, and the geographic positions of the fields as determined by the shapefiles. The javascript file template for this report (*Sen2NDVI_TW.js*, available from Reclamation), uses 'Harmonized' 10-m Sentinel-2 bands 4 (red) and 8 (NIR), applies cloud masking to remove bad data, computes NDVI, and assembles a field-by-field time-series table. Note that 'Harmonized' data in this context indicates that band-dependent offsets in observations after January 24, 2022 have been removed (Earth Engine Catalog). The other use of harmonization, not applicable for this report, indicates the joint calibration of Landsat and Sentinel 2 sensors and results in 30 m resolution data sets (Claverie et al., 2018). Output data from GEE processing are downloaded to cloud storage and then transferred to local computers for further analysis.

4.3 Filter the NDVI data

In step 3, the NDVI data files are prepared and formatted for use with the R scripts. First the NDVI are transposed with the script *transposeGEE_NDVI_proj.R* to con-

vert the GEE output to values ordered row-wise by time. Second, the NDVI are de-spiked, smoothed, and interpolated to daily time steps. Because of differences in script design, output formats from this step differ for the two scripting pathways. For the crop-specific processing, the script *interpol_filter_GEEVI_proj.R* is used. The input and output files have 8 data fields (Crop, District,Site, Date, Year, DOY,NDVI,Interpflag). The name for the unified processing script is *GEE_NDVI_matrix_tran_inter_fill_header.R*. Its implementation is similar to the crop-specific script, and mainly differs in the output file format, which retains the crop identifications annotated in the shapefiles.

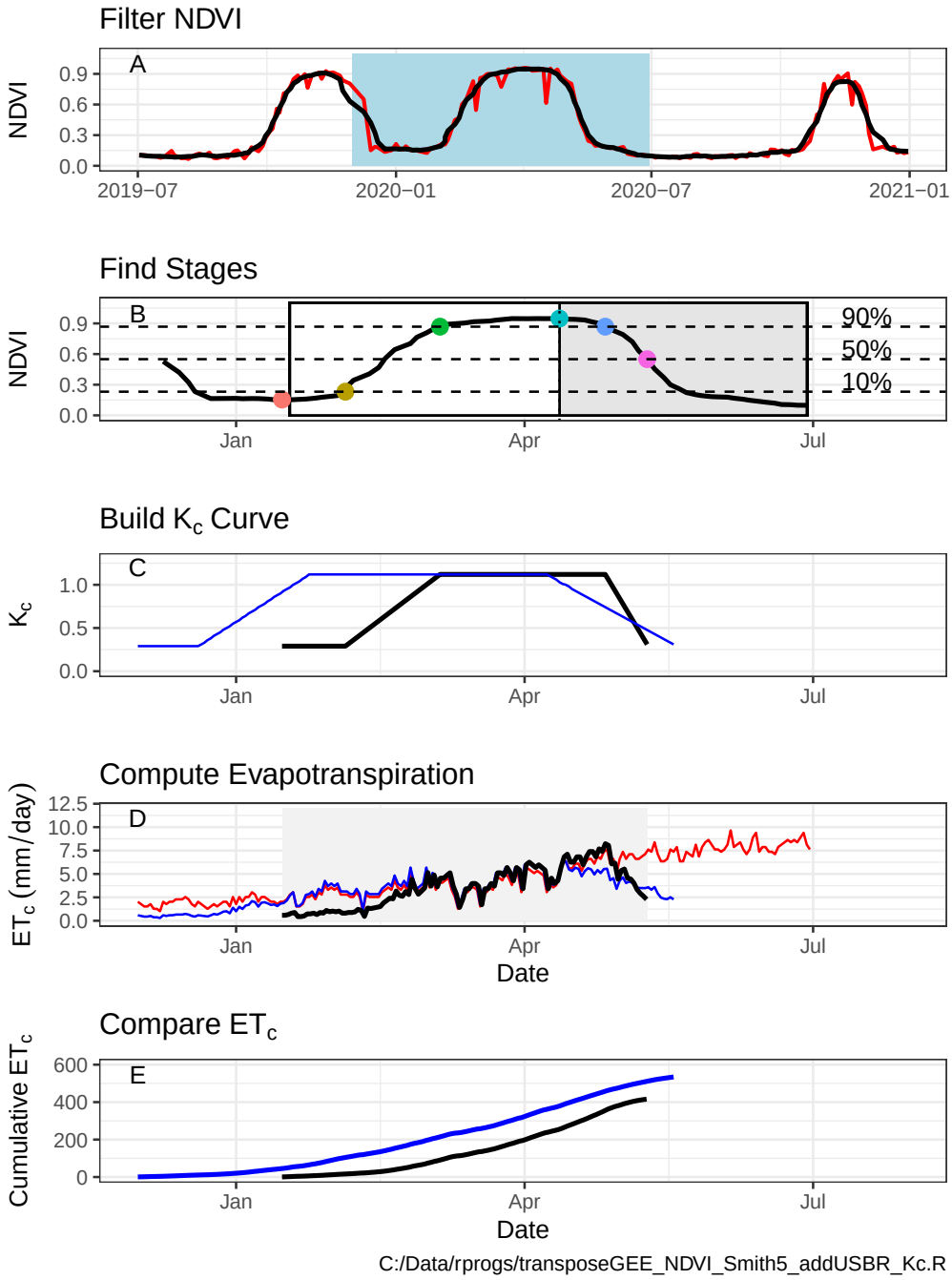

Figure 4. Converting NDVI to ET_c using growth stages. Data for small grains are used to illustrate the procedure. See details in Section 4.4, page 14.

4.4 Convert NDVI to K_c

In step 4, the NDVI are converted to crop growth stages and daily K_c values assigned for every field. The following procedure, used for most crops, is illustrated in Fig. 4. The unified script *Crop_growth_stages_detection_final.R* follows the same general guidelines for stage partitioning of annual crops, but uses a different set of internal coding. For details see comments within the script. The procedures for analyzing NDVI for Bermudagrass and Kleingrass are described in section 4.7. Processing details for citrus and date trees are noted in section 5.3.

1. Select time window. The chosen window depends on the likely range of dates for the particular crop (blue shading, Figure 4A).

2. Find maximum NDVI in the time window. Identifying this date is crucial for the following elements as it constrains selection of early and late growth stages (light blue circle, Figure 4B).

3. Partition the time window into early and late season. The early season begins on the first day of the time window and ends at the day at maximum NDVI. The late season begins from the maximum NDVI day to the end of the time window (white and gray boxes, Figure 4B).

4. Find minimum NDVI in the early season (orange circle, Figure 4B).

5. Compute early season NDVI range. Done by differencing the maximum and minimum NDVI (light blue and orange circles, Figure 4B).

6. Set percentiles (X) for stage transitions. Usually set as follows: 10% for INI/DEV, 90% for DEV/MID, 90% for MID/END, and 50% for END (dashed horizontal lines, Figure 4B).

7. Compute NDVI quantiles at the transitions. Done using this equation: $NDVI_q = NDVI_{range} * X + NDVI_{minimum}$ where $NDVI_q$ is the NDVI value at the selected stage transition (brown, green, pale blue, pink circles, Figure 4B).

8. Set length of INI period and compute day of planting. The FAO-56 values (listed in Table 11, pp. 104-108 therein) are used (orange to brown circle, Figure 4B).

9. Compute day of year for the stage transitions. This is done by linear interpolation. The NDVI curve needs to be smooth and monotonically increasing or decreasing.

10. Compute K_c values. K_c INI and K_c MID are assigned directly by using the corresponding days previously identified. K_c DEV and K_c MID are computed by linear interpolation (black line, Figure 4C). Standardized K_c values used for all districts are listed in Tables 2-6. Coefficients for two districts–IID and Coachella– are not defined in LCRAS using the standard K_c triplet from FAO-56. They are more curvilinear, and so are incompatible with the NDVI-based growth stage model. Consequently, approximate triplet K_c coefficients (for INI, MID, END) were created.

4.5 Compute ET_c

In step 5, ET_c values are determined:

1. Extract ET_{os} from weather station files (red line, Figure 4D).
2. Compute ET_c (black line, Figure 4D).
3. Compute total ET_c (black line, Figure 4E).

Table 2. LCRAS K_c values, Part 1. Values for Coachella and IID are modifications of the source K_c values to conform with the FAO-56 growth stage modeling. Early season spikes in LCRAS were not used in the remote sensing analyses.

		K_c		
Crop	District	INI	MID	END
Alfalfa	Coachella	0.30	1.16	0.30
	CRIT	0.37	1.11	0.37
	IID	0.30	1.16	0.30
	Mohave	0.37	1.11	0.37
	PVID	0.37	1.10	0.37
	Yuma	0.37	1.10	0.37
Bermudagrass	Coachella	0.80	0.96	0.83
	CRIT	0.37	0.85	0.80
	IID	0.80	0.96	0.83
	Mohave	0.37	0.85	0.80
	PVID	0.37	0.85	0.80
	Yuma	0.37	0.85	0.80
Citrus-Young	Coachella	0.43	0.34	0.43
	CRIT	0.43	0.34	0.44
	IID	0.43	0.34	0.43
	Mohave	0.43	0.34	0.44
	PVID	0.43	0.34	0.44
	Yuma	0.43	0.34	0.44
Citrus-Mature	Coachella	0.71	0.57	0.71
	CRIT	0.71	0.57	0.73
	IID	0.71	0.57	0.71
	Mohave	0.71	0.57	0.73
	PVID	0.71	0.57	0.73
	Yuma	0.71	0.57	0.73
Citrus-Declining	Coachella	0.50	0.40	0.51
	CRIT	0.50	0.40	0.51
	IID	0.50	0.40	0.51
	Mohave	0.50	0.40	0.51
	PVID	0.50	0.40	0.51
	Yuma	0.50	0.40	0.51

Table 3. LCRAS K_c values, Part 2

		K_c		
Crop	District	INI	MID	END
Corn	Coachella	0.37	1.20	0.46
	CRIT	0.29	1.20	0.46
	IID	0.37	1.20	0.46
	Mohave	0.29	1.20	0.46
	PVID	0.29	1.20	0.46
	Yuma	0.34	1.19	0.46
Cotton	Coachella	0.20	1.12	0.56
	CRIT	0.20	1.12	0.56
	IID	0.20	1.12	0.56
	Mohave	0.20	1.12	0.56
	PVID	0.20	1.12	0.56
	Yuma	0.26	1.12	0.57
Dates	Coachella	0.82	0.98	0.94
	CRIT	0.88	1.01	0.92
	IID	0.83	0.98	0.94
	Mohave	0.88	0.88	0.88
	PVID	0.88	1.01	0.92
	Yuma	0.82	0.98	0.94
Deciduous Orchards	Coachella	0.38	0.85	0.50
	CRIT	0.45	0.87	0.49
	IID	0.38	0.85	0.50
	Mohave	0.45	0.87	0.49
	PVID	0.45	0.87	0.49
	Yuma	0.38	0.85	0.50
Field Grains	Coachella	0.37	1.20	0.46
	CRIT	0.29	1.20	0.46
	IID	0.37	1.20	0.46
	Mohave	0.29	1.20	0.46
	PVID	0.29	1.20	0.46
	Yuma	0.34	1.19	0.46

Table 4. LCRAS K_c values, Part 3. Undefined stages are denoted by dashes.

		K_c		
Crop	District	INI	MID	END
Grapes	Coachella	0.11	0.85	0.27
	CRIT	0.11	0.85	0.27
	IID	0.11	0.85	0.27
	Mohave	0.11	0.85	0.27
	PVID	0.11	0.85	0.27
	Yuma	0.11	0.85	0.27
Kleingrass	Coachella	0.80	0.96	0.83
	CRIT	0.37	0.85	0.80
	IID	0.80	0.96	0.83
	Mohave	0.37	0.85	0.80
	PVID	0.37	0.85	0.80
	Yuma	0.37	0.85	0.80
Lettuce Fall Early	Coachella	0.578	0.998	-
	CRIT	0.578	0.998	-
	IID	0.578	0.998	-
	Mohave	0.578	0.998	-
	PVID	0.578	0.998	-
	Yuma	0.522	0.998	0.895
Lettuce Fall Late	Coachella	0.788	1.08	-
	CRIT	-	-	-
	IID	0.788	1.08	-
	Mohave	-	-	-
	PVID	-	-	-
	Yuma	0.788	-	0.895
Lettuce Spring Early	Coachella	-	1.068	-
	CRIT	-	-	-
	IID	-	1.068	-
	Mohave	-	-	-
	PVID	-	-	-
	Yuma	-	1.00	0.888

Table 5. LCRAS K_c values, Part 4. Undefined stages are denoted by dashes.

		K_c		
Crop	District	INI	MID	END
Lettuce Spring Late	Coachella	-	1.068	-
	CRIT	0.856	1.002	0.879
	IID	-	1.068	-
	Mohave	0.856	1.002	0.879
	PVID	0.856	1.002	0.879
	Yuma	0.788	1.000	0.888
Olives	Coachella	0.60	0.55	0.60
	CRIT	0.60	0.55	0.60
	IID	0.60	0.55	0.60
	Mohave	0.60	0.55	0.60
	PVID	0.60	0.55	0.60
	Yuma	0.60	0.55	0.60
Small Grains	Coachella	0.44	1.18	0.20
	CRIT	0.30	1.13	0.31
	IID	0.44	1.18	0.20
	Mohave	0.30	1.13	0.31
	PVID	0.30	1.13	0.31
	Yuma	0.29	1.12	0.31
Small Vegetables Fall	Coachella	0.44	1.06	-
	CRIT	0.34	1.00	-
	IID	0.44	1.06	-
	Mohave	0.34	1.00	-
	PVID	0.34	1.00	-
	Yuma	0.57	1.00	-
Small Vegetables Spring	Coachella	-	1.06	0.77
	CRIT	-	1.00	0.77
	IID	-	1.06	0.77
	Mohave	-	1.00	0.77
	PVID	-	1.00	0.77
	Yuma	-	1.00	0.79

Table 6. LCRAS K_c values, Part 5. Values for sugar beet are provided only for areas where grown. Undefined stages are denoted by dashes.

		K_c		
Crop	District	INI	MID	END
Sudangrass	Coachella	0.24	1.20	0.61
	CRIT	0.46	1.14	1.04
	IID	0.24	1.20	0.61
	Mohave	0.46	1.14	1.04
	PVID	0.46	1.14	1.04
	Yuma	0.37	1.13	1.04
Sugar beet	Coachella	0.20	1.14	0.93
	CRIT	-	-	-
	IID	0.20	1.14	0.93
	Mohave	-	-	-
	PVID	-	-	-
	Yuma	-	-	-

4.6 Script for Alfalfa

The script for alfalfa growth stage mapping creates K_c curves that model multiple cutting cycles per year. Delineating growth stages for multiple harvests is a more complicated and difficult task than doing so for single-harvest crops. The stages for alfalfa have short durations that can be difficult to resolve for three reasons: there can be interfering clouds that make remote sensing impossible, the times between satellite overpasses are too long, or the images are noisy for unknown reasons. For this study region, however, cloud cover is less common, while Sentinel 2 data overpasses are frequent – usually 3-5 days between observations. To minimize other problems with noisy NDVI observations, the time-series are smoothed and data spikes are removed with replacement using adjacent values (e.g., Brock, 1986).

Constraints for the alfalfa model are listed in Table 7.

Table 7. Parameter settings for analyzing Alfalfa NDVI time series.

Attribute	Values
Low NDVI threshold	0.5
ggpmisc::find_peaks parameters	Span window: 15
oce::despike parameters	n=4, k=15
stats::filter width	13
Minimum days between NDVI peaks	20
Stage length constraints	L_INI=5, L_DEV>=20 L_MID>=10, L_END>=5

4.7 Script for Bermudagrass and Kleingrass

Scripts for Bermudagrass and Kleingrass were combined because separate analyses for each would not be representative: field discrimination of the two is difficult and potentially inaccurate. Fortunately, corresponding K_c values for these are identical, making the combined analysis the same as if results from Bermudagrass and Kleingrass were averaged. Although these grasses are cut multiple times in a year, suggesting an alfalfa-like analysis, that approach was not taken because cutting patterns for Bermudagrass and Kleingrass were much more irregular and inconsistent- as reflected in the NDVI values- than observed for alfalfa. Consequently an alternative thresholding approach was adopted. Here those grass crops were partitioned into two stages: MID or no-growth. The K_c MID value is taken as listed in Table 2, and K_c is set to zero for the no-growth stage. Partitioning is done by selecting an NDVI value that separates NDVI peaks from troughs. A range of reasonable threshold values can be found by modeling ET_c site-by-site, creating total ET_c histograms vs. chosen NDVI threshold, and then seeking inflection points (Figure 5). Optimal threshold values were usually found between 0.5 and 0.6. For consistency with the alfalfa algorithm, NDVI threshold was set to 0.5. This binary categorization assumes no significant ET_c during INI stages (consistent with dormancy) and minimal duration of DEV and END stages.

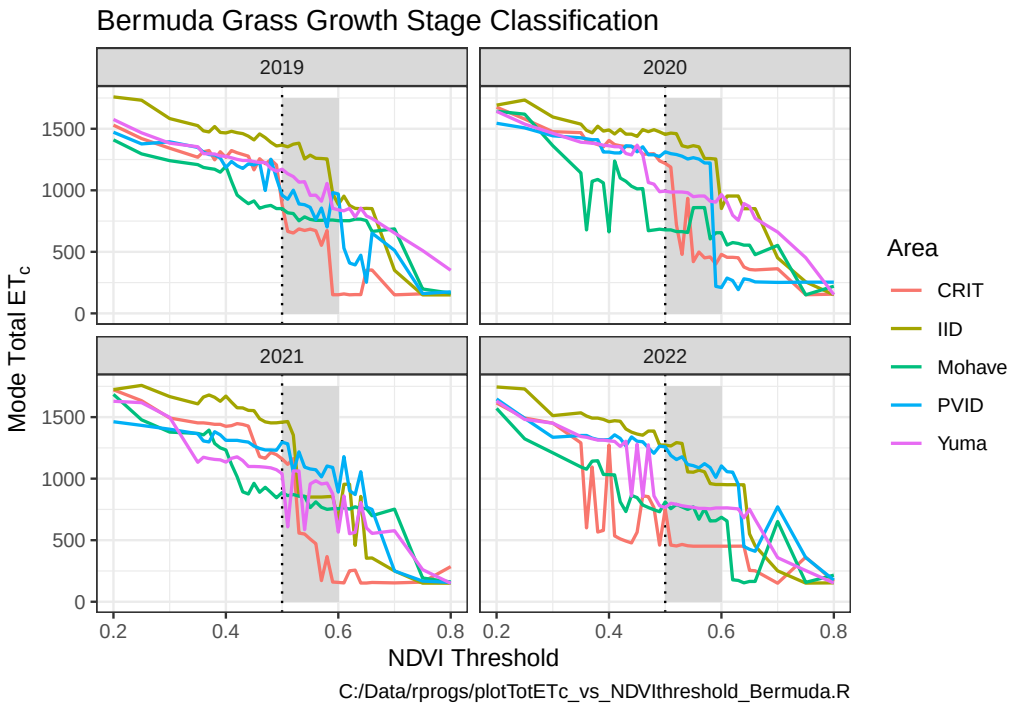

Figure 5. Testing NDVI threshold values for Bermudagrass and Kleingrass . Total ET_c is computed for every instance of Bermudagrass in each of five irrigation districts: CRIT, IID, Mohave, PVID, and Yuma. Then the mode of the ET_c distribution is plotted vs. NDVI threshold value. The optimal threshold is assumed to lie within the region (gray zone) where the mode of the ET_c distribution changes most rapidly. This generally falls between NDVI of 0.5 to 0.6.

4.8 Script for Sudangrass

The script for Sudangrass models crop growth as one season, as does the Reclamation approach. There are multiple cuttings per year, but the NDVI patterns generally show small amplitude drops when cuttings occur. This means that despite reduction in biomass, grass cover typically remains close to full cover after cuttings. In turn, this indicates that averaging of the NDVI over the MID period is representative of ET_c .

4.9 Script for Citrus

For citrus crops, the growth stage delineation approach used for crops such as Sudangrass had to be modified because citrus season growth cycles are represented by NDVI in a different way from annual crops. Specifically, NDVI over citrus is a composite of one signal due to vegetation canopy density changes, and another signal due to changes in solar illumination. During winter months the sub-canopy soil is shaded, while during summer months its shading is minimal. Even though satellite view angles are nearly nadir throughout the year, these changing solar elevation angles affect NDVI (Wang et al., 2022; Mu et al., 2024). Hence for citrus there are two temporal NDVI patterns to distinguish, as illustrated by examples in Figure 6. Shown are NDVI patterns for mature citrus (black) and young citrus (gray). Parabolic lines (gray) delineate quadratic fits used to partition within-year growth stages. The blue arrow highlights the seasonal NDVI that decreases as solar elevation angles increase. The red arrow represents the average NDVI displacement due to citrus maturity. Adjustment of K_c values is based on magnitude of the displacement as described below (Page 28).

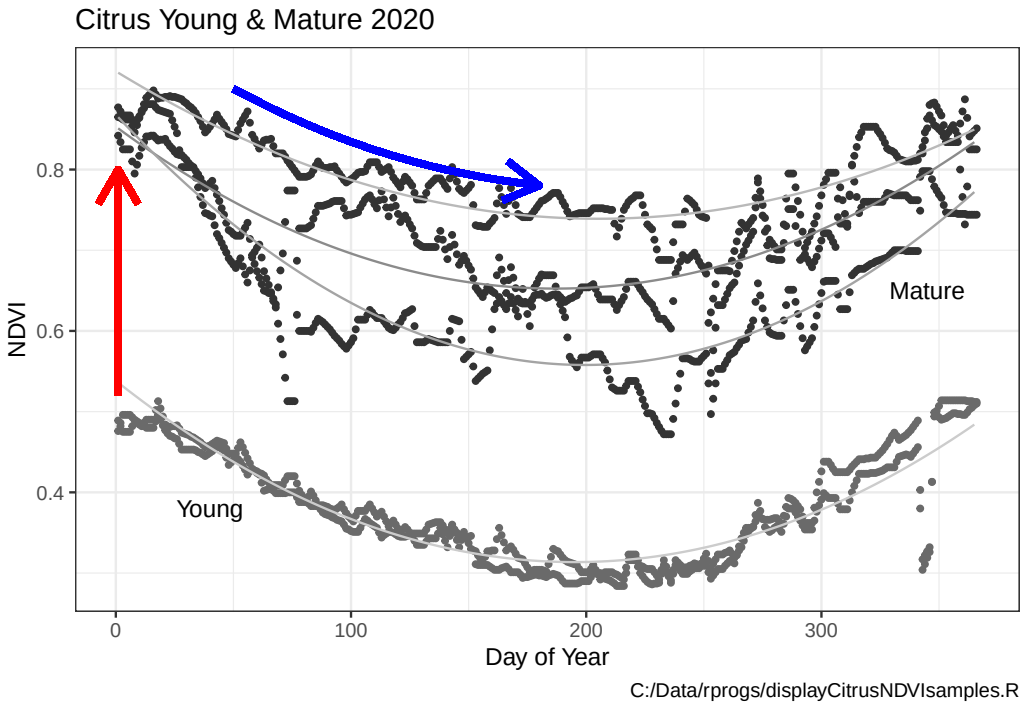

Figure 6. NDVI response to day of year and tree maturity for citrus at Yuma. Two patterns are shown: a quadratic shape (trend denoted by blue arrow) and an overall amplitude change (denoted by red arrow). The growth stage approach selects quantiles by the quadratic fits (gray lines). The K_c values are then determined by the relative NDVI magnitude between the young and mature trees.

For citrus, NDVI values consisting of two components: annual averages, which are a function of tree maturity, and quadratic daily changes, that are due partly (possibly largely) by changes in solar elevation angles. The scope of this WaterSMART study did not allow analysis of the relative importance of tree maturity and solar angles on the NDVI signal. An initial evaluation of LCRAS observations suggests that citrus maturity, and its corresponding ET_c , is mostly represented by annual NDVI averages, while the parabolic NDVI patterns are dominantly an artifact of temporal changes in the bidirectional reflection distribution function (BRDF; for explanation see MODIS BRDF).However, some of the parabolic characteristics may be contributed by seasonal changes in relative ET_c . Note, for example, that existing K_c values for citrus (blue line in Figure 7) mimic the concave-up parabolic shape. The parabolic NDVI pattern is strong for mature citrus, and weak, to nearly flat, for young citrus.

Because information on how to separate tree maturity from illumination effects was not evaluated, this study constructed K_c values in two steps: first by following Reclamation practice for growth stages, and second by modifying K_c values according to tree maturity.

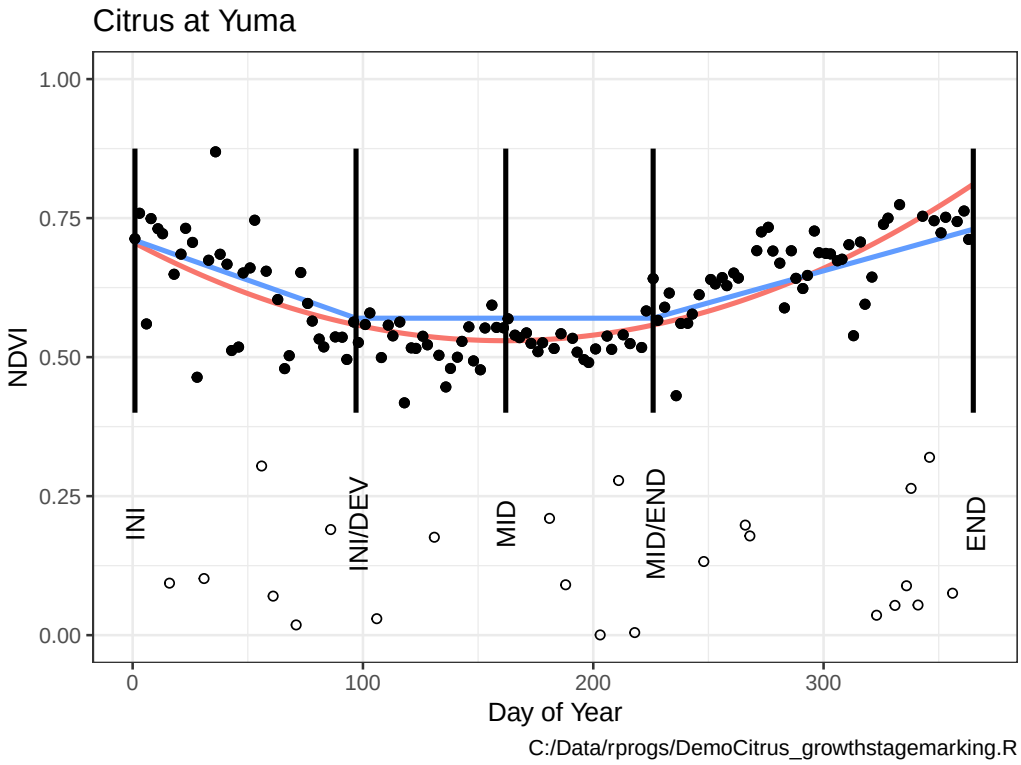

Figure 7. Growth stage delineation for citrus. Shown are field-averaged NDVI samples from Yuma citrus vs. day of year. Valid data points are shown in black and outliers as open symbols. Growth stages (delineated by vertical black lines) are calculated in two steps: first a quadratic curve (red line) is fit to the valid points, then the lower 10^{th}-percentile NDVI values are found. Growth stages (blue line) are linearly interpolated from Jan 1 to the first 10^{th}-percentile, and again from the second 10^{th}-percentile to Dec 31. The MID stage is bound by the INI/DEV and MID/END transition days.

In step one, citrus growth stages were partitioned into three parts (DEV, MID, END) using NDVI quantiles. Start of INI and end of END stages were defined as being on 1 January of each year. The NDVI 10^{th}-percentile was used to locate the DEV/MID and MID/END transitions. For the example in Figure 7, the INI/DEV, DEV/MID, mean of MID, MID/END, and END transitions are delineated by vertical black lines. A quadratic curve (red line) was then fit to the NDVI points after removal of outlier values (open symbols).

In step two, K_c values were calculated with respect to citrus end members, i.e., the K_c components defined for 'Young' and 'Mature' citrus. Reclamation prescribes three sets of K_c values dependent upon tree heights: Young (height 1-3 m), Mature (height >3 m), and Declining (Table 2). Analysis of Sentinel 2 data shows that the magnitude of NDVI is a strong indicator of tree height. Options for quantifying NDVI magnitude include using either annual or seasonal averages. Because the dynamic range of NDVI is greatest when mid-winter values are chosen, they were used for this study. NDVI values are lowest for young trees, highest for mature trees, and slightly less than maximal for declining trees (Figure 8). Using area-specific NDVI from the first two weeks of January for a given year allows creation of a K_c curve that is adaptive to tree height. As shown in Figure 9 (top), median, early January NDVI values from all fields define the K_c bounds for the INI to MID growth stages. The K_c values at each day of year that are derived from these bounds are shown Figure 9 (bottom). Discrimination between declining trees and trees transitioning from young to mature status is not feasible with NDVI annual data, but might be resolved by tracking NDVI for each field over multiple years and noting when maximal NDVI values are less than a preceding year of observations.

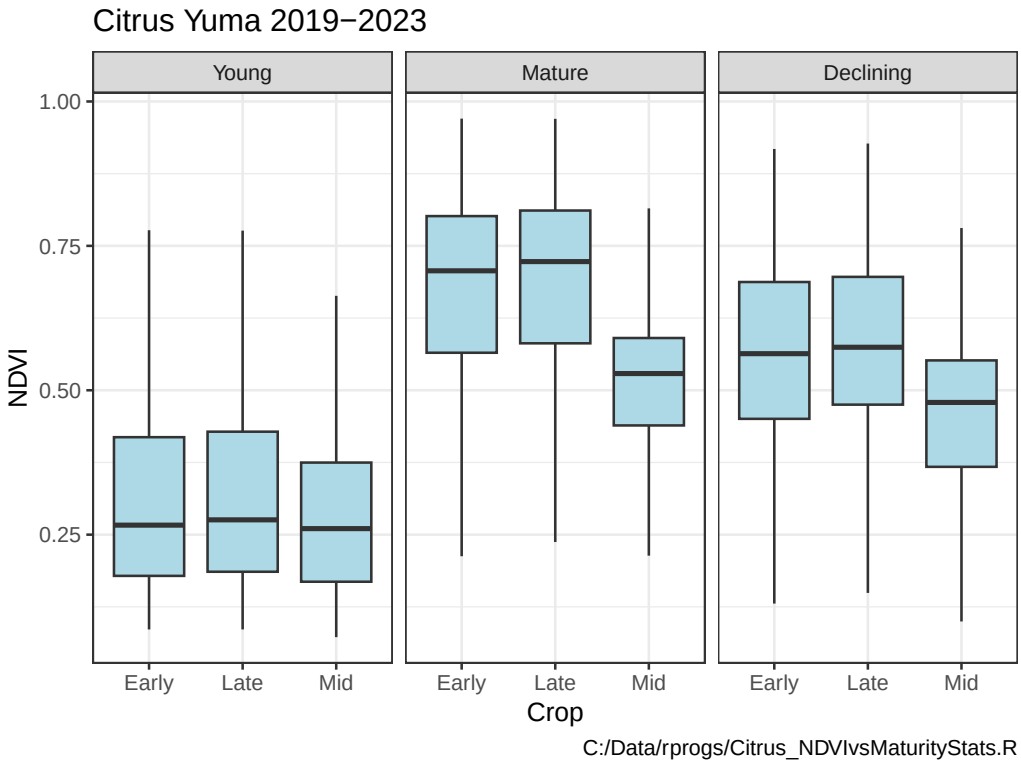

Figure 8. Average citrus NDVI trends for young, mature, and declining trees. Three time periods are considered: early (first two weeks in January), late (last two weeks in December), and mid (June). The boxplots show that average NDVI values closely correspond to tree maturity. When considering only young and mature trees the averages are diagnostic, but confusion exists when considering declining citrus.

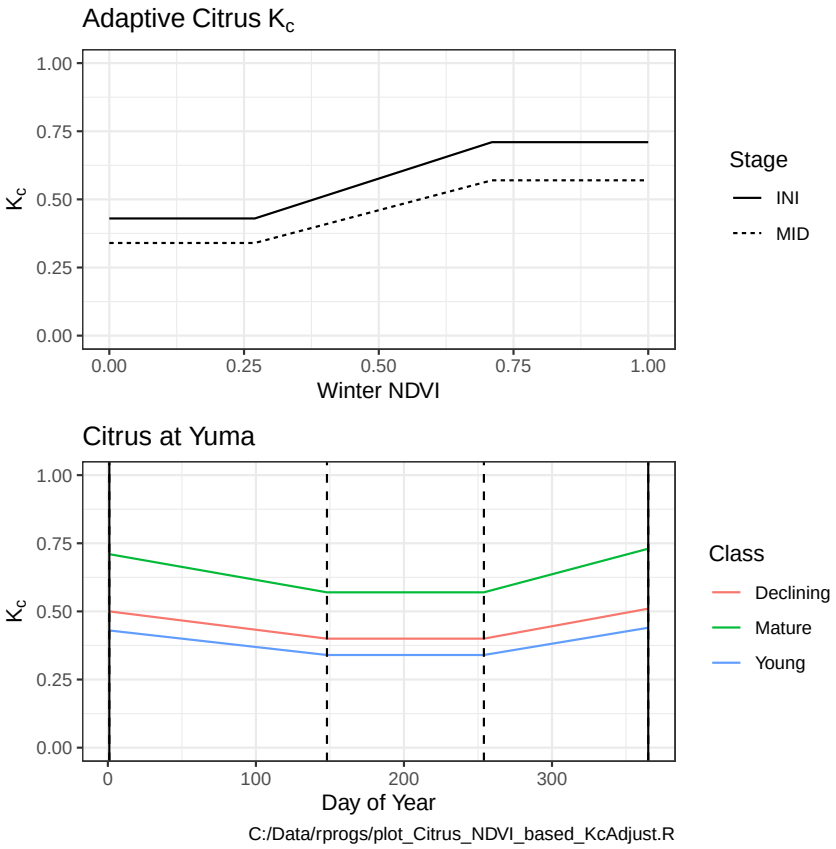

Figure 9. Adaptive K_c for young to mature citrus. K_c values for initial and mid-season growth stages (top) are used to create full-season K_c values. Reference K_c curves (bottom) define the lower and upper K_c limits. Declining citrus trees cannot be distinguished from trees between minimal and maximal maturity.

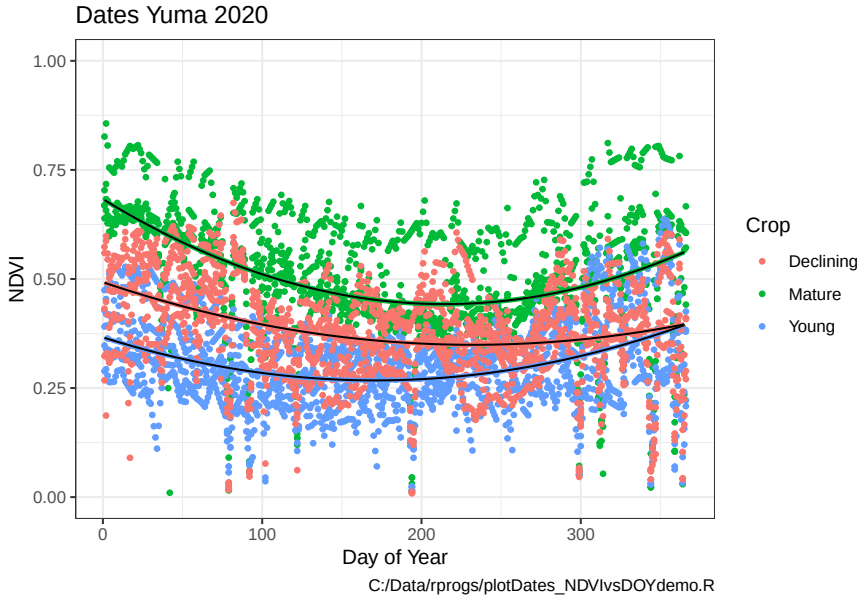

Figure 10. Dates maturity vs. NDVI and Day of Year at Yuma. Colored symbols represent maturity as classified by LCRAS. The black lines are quadratic best-fit lines modeling all instances in each maturity class. Downward spikes close to zero-NDVI are likely remote sensing artifacts from cloudy skies.

4.10 Scripts for Dates and Olives

The script for dates and olives follow the same K_c-delineation approach used for the first part of the citrus algorithm: quadratic curves are fit to daily NDVI values, and bounds for the DEV-MID-END transitions are located using the 10^{th}-percentiles. Reclamation data discriminate dates by maturity, as illustrated in Figure 10, but do not vary the K_c curves, so an adaptive approach could not be used. Instead, the standard K_c values as listed in Table 3 were used for every instance. Similar to citrus and dates, the NDVI values for olives have two patterns (Figure 11): the annual periodic pattern resulting from solar illumination angle and an inter-annual trend indicative of tree maturity. The arrow shown is conceptual to indicate how NDVI over time might be related to K_c and ET_c.

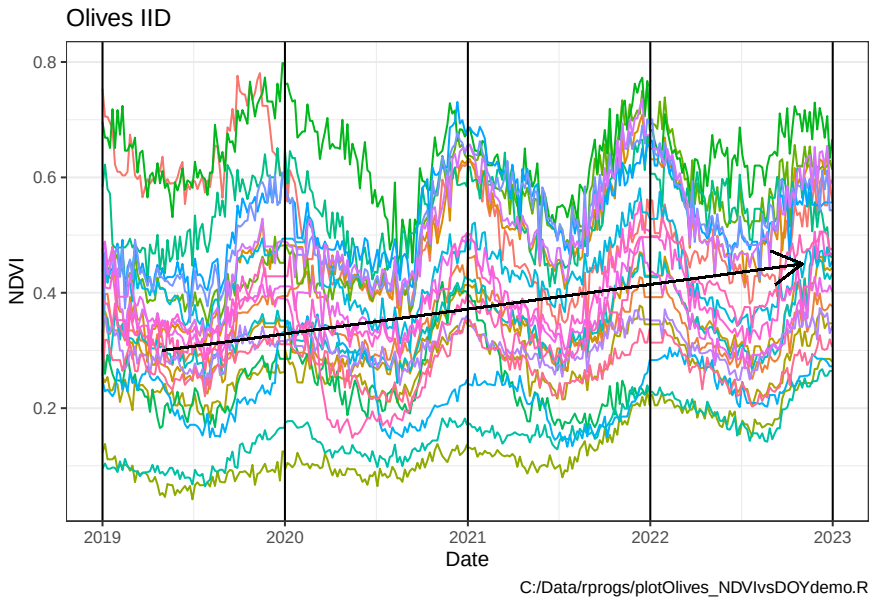

Figure 11. Olives vs. NDVI and Day of Year at IID. Colored lines represent distinct field averages. Vertical black lines delineate year boundaries. The arrow denotes the NDVI trend vs. year and is indicative of olive tree growth. At IID there were 22 verified sites.

4.11 Scripts for Carrot, Lettuce, Sugar beet and Wheat

The scripts for modeling carrot, lettuce, sugar beet, and wheat partition the NDVI time series into two parts representing the early and the late season growth stages, as illustrated by the white and gray boxes in Figure 4B (page 13). The division between these stages is made by locating the maximum NDVI. Using only the early stage NDVI values, the minimum NDVI is identified, the NDVI range computed, and the 10^{th}- and 90^{th}-percentile NDVI values determined. Using linear interpolation, the days corresponding to the INI/DEV and DEV/MID transitions are found. The start of the INI stage is found by offsetting backwards in time from the day at the INI/DEV transition. Offsets used are taken from Allen et al. (1998, page 104-108) and are 30, 25, 25, and 20 days, for carrot, lettuce, sugar beet, and wheat respectively. Late season stages are found in a similar way using 90^{th}- and 50^{th}-percentile NDVI thresholds and the previously computed NDVI range. The post-NDVI maximum value at the 90^{th}-percentile is used for the MID/END transition and the 50^{th}-percentile for the end of the END stage. A 50^{th}-percentile is used because it reliably detects end-of-season, while a 10^{th}-percentile often fails because late season NDVI range is often less than the early season range.

Seasons for these crops span two seasons, where planting may lie within fall months and harvest lies within winter or spring months. So the corresponding scripts require inputting NDVI data spanning two years.

To enable the remote sensing analysis, Reclamation's lettuce 'Fall Late' and 'Spring Early' K_c curves are combined into one new lettuce 'Winter' K_c curve. The lettuce 'Fall Early' and lettuce 'Spring Late' K_c curves are not changed.

Similarly, wheat K_c values are composited from small grains 'Fall' and small grains 'Spring' K_c curves.

Carrots are analyzed using LCRAS's small vegetables K_c curve sets, and they too are composited from fall and spring K_c curves.

Sugar beet is composited from fall and summer K_c curves.

4.12 Scripts for Cotton, Corn and Grapes

Scripts for cotton, corn, and grapes consider the growing seasons to be confined to one calendar year. Reclamation's LCRAS provides one set of K_c curves for each, and no compositing is needed for remote sensing analysis.

5 Objective 2: Application of Scripts

Project objective 2 is to apply the scripts- previously described in Section 4- to estimate crops growth stage lengths for the six or more of the significant crops in all of the Lower Colorado River irrigated areas for 2018-2021. In this section, ET_c results are grouped by crop type. Six or more crops reported are listed in Tables 8 and 9. Since crop counts depend upon observation year and month, determination of which crops were most signficant was done by finding the mean maximum field counts. Tables 8 and 9 show that the crops analyzed using NDVI growth stage determinations represent at least 77% of observations. Analyses for the Wellton-Mohawk valley were combined with the Yuma area, hence the listing of 6, instead of 7, irrigation areas. Henceforth, mention of the 'Yuma' area indicates inclusion of Wellton-Mohawk results. Note that study spans only the years where Sentinel 2 data were available: 2019-2022.

Table 8. Significant crops for LCRAS areas, 2019-2022, Part 1 of 2. $\overline{N}$ represents the average number of fields observed for the 4-year period. Percentage observed is relative to total number of fields with crops observed. Cum. is the cumulative percentage for each area, and indicates the relative abundance of crops analyzed.

Area	Crop	$\overline{N}$	Percentage	Cum.
Coachella	Dates	1204	39	39
	Grapes	551	18	57
	Citrus Mature	330	11	68
	Citrus Young	281	9	77
	Bermudagrass	190	6	83
	Carrot	40	1	84
	Citrus Declining	16	0.5	85
	Alfalfa	8	0.3	85
CRIT	Alfalfa	256	40	40
	Bermudagrass	154	24	64
	Wheat	39	6	70
	Cotton	31	5	75
	Sudangrass	27	4	79
	Kleingrass	14	2	81
IID	Bermudagrass	944	37	37
	Kleingrass	338	13	50
	Alfalfa	316	12	62
	Citrus Mature	158	6	68
	Sudangrass	94	4	72
	Citrus Young	78	3	75
	Sugar beet	51	2	77

Table 9. Significant crops for LCRAS areas, 2019-2022, Part 2 of 2.

Area	Crop	$\overline{N}$	Percentage	Cum.
Mohave	Alfalfa	136	42	42
	Bermudagrass	92	29	71
	Wheat	26	8	79
	Kleingrass	10	3	82
	Olives	1	0.3	82
	Corn	1	0.3	83
PVID	Alfalfa	289	39	39
	Bermudagrass	94	13	52
	Dates	68	9	61
	Kleingrass	59	8	69
	Cotton	57	8	77
	Wheat	31	4	81
	Citrus Mature	18	2	83
Yuma-Wellton	Bermudagrass	667	15	15
	Dates	590	14	29
	Citrus Mature	489	11	40
	Lettuce	485	11	51
	Wheat	338	8	59
	Citrus Young	296	7	66
	Sudangrass	220	5	71
	Alfalfa	211	5	76
	Kleingrass	136	3	79
	Citrus Declining	116	3	82
	Cotton	110	3	85

Table 10. Alfalfa Annual ET_c (mm/year).

	Year			
Area	2019	2020	2021	2022
Coachella	1558	1554	1578	1606
CRIT	1550	1655	1671	1603
IID	1554	1547	1571	1548
Mohave	1519	1634	1644	1659
PVID	1549	1640	1686	1620
Yuma	1558	1616	1601	1616

5.1 Alfalfa

Alfalfa is a perennial legume crop, predominantly raised for forage, with ∼1470 mm/year (Hanson et al., 2008). Alfalfa results show significant variability in ET_c across areas and years (Table 10). Examples of that variability are shown for Yuma in 2020 (Figure 12). Shown in gray are samples from 10 field sites for NDVI (top), K_c (middle), and daily ET_c (bottom). To better illustrate the patterns, dark blue lines represent K_c and ET_c from LCRAS. Daily ET_c ranges from 2-11 mm/day, where strong drops in daily ET_c are caused by cuttings.

Growth stage modeling results consistently show that total ET_c for all districts dominantly ranges between 1200 and 1500 mm/day. Histogram displays represent total ET_c distributions by irrigation area and year (Figure 13).

The y-axis (Frequency) denotes the number of ground-truthed fields. The vertical red lines indicate annual total ET_c as computed by the LCRAS methodology. The displacements between NDVI-based modal estimates (histogram peaks) and LCRAS represent the overall model differences. The dispersion shown by the histograms indicate the amount of within-field ET_c variability.

The number of cuttings per year has a major effect on total ET_c and, as illustrated, dominantly varies between 6 and 10 per year (Figure 14). Typical cuttings per year in LCRAS is 10.

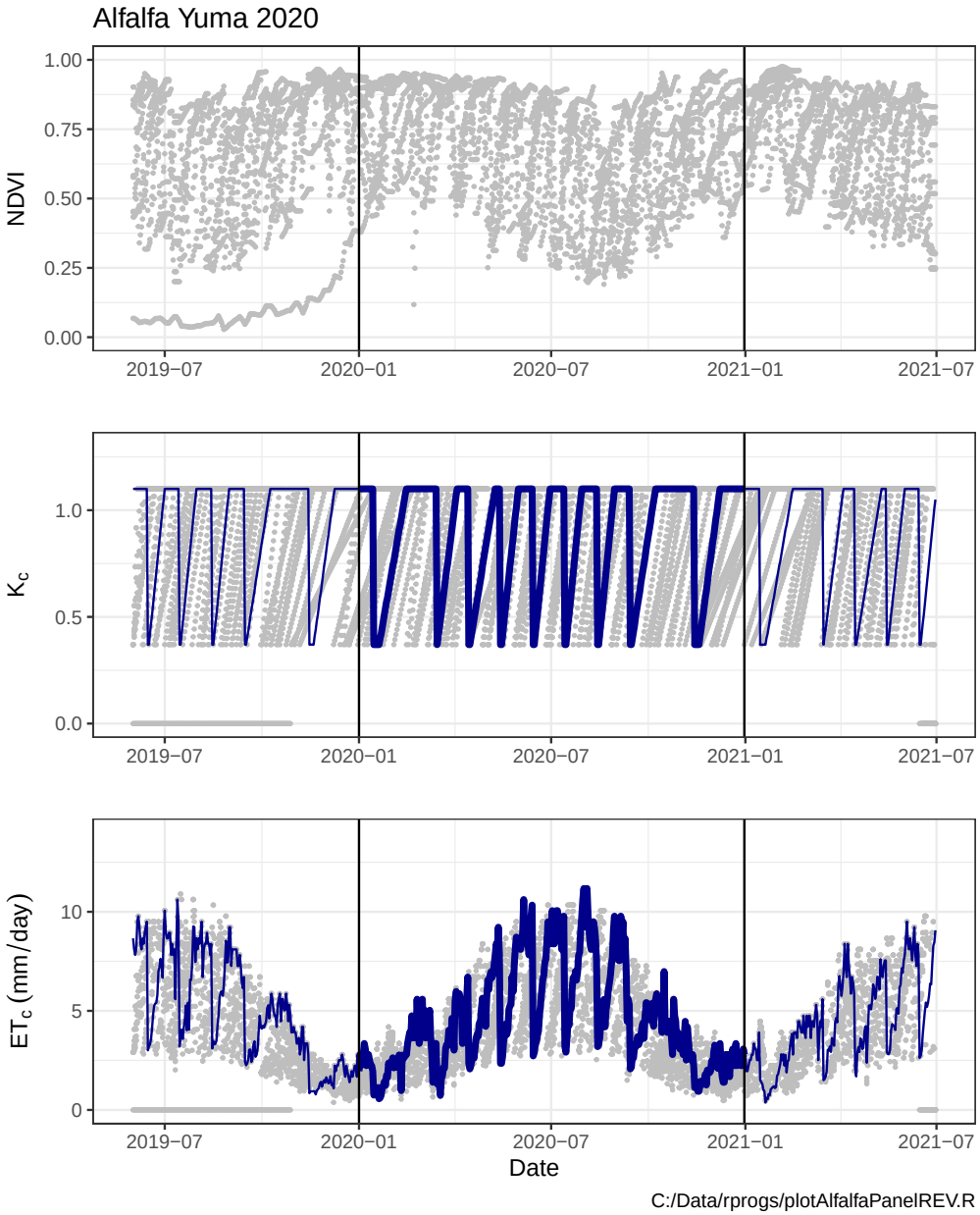

Figure 12. Alfalfa ET_c estimation from NDVI. Shown are examples of filtered and smoothed NDVI data over alfalfa fields in Yuma (top), conversion of NDVI to K_c curves (middle), and computation of daily ET_c from K_c and weather station based ET_{os} (bottom). Gray symbols illustrate NDVI-based modeling, blue lines show the corresponding LCRAS estimates.

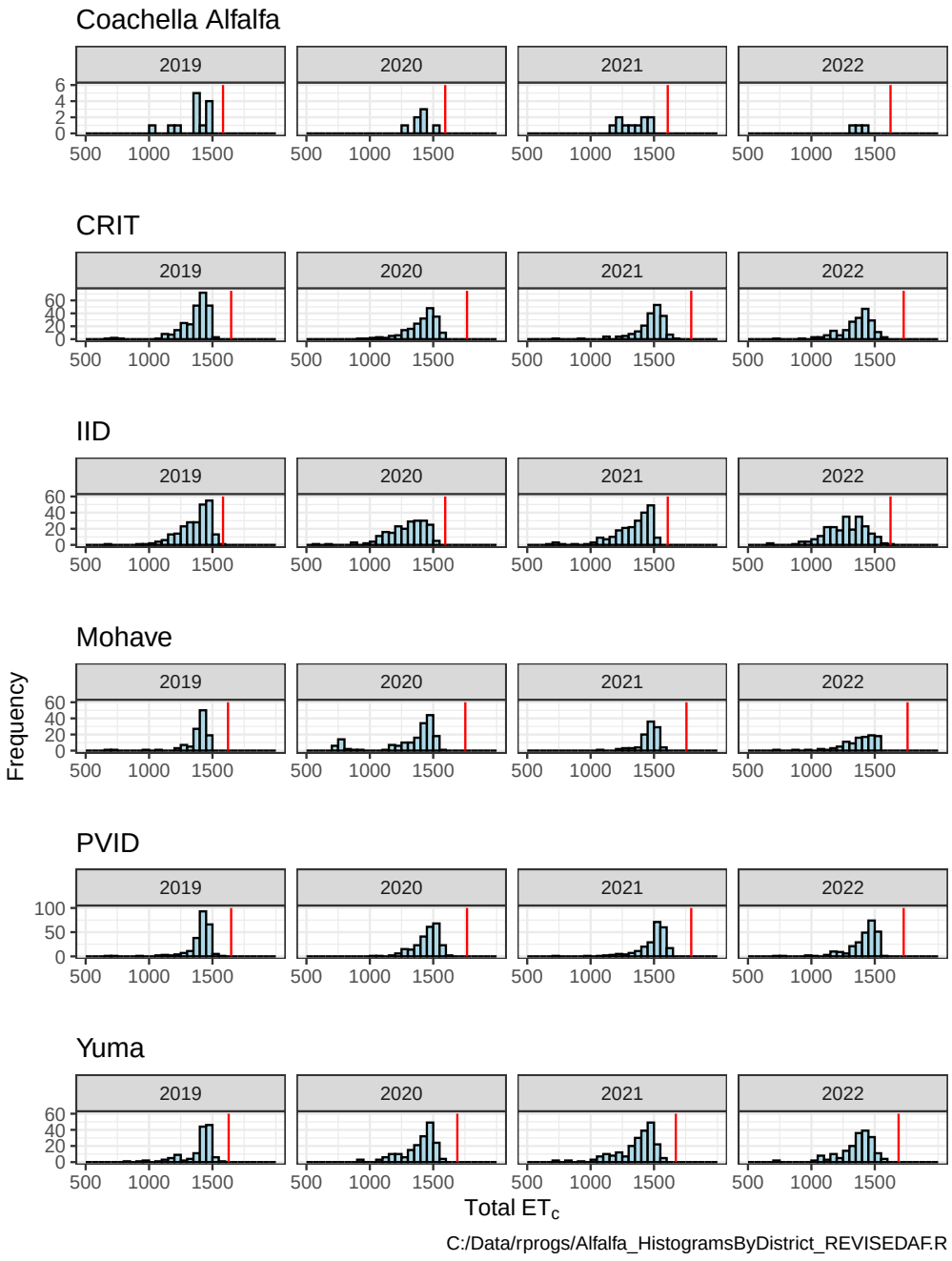

Figure 13. Total field-wise ET_c for alfalfa 2019-2022 from six irrigation areas (light blue) are compared with LCRAS estimates (red).

Satellite data for all years and districts show a mid-summer decrease in maximum NDVI (Figure 15), which is indicative of farm practice to reduce irrigation amounts during the highest temperatures. In accordance with the growth stage mapping protocol, alfalfa K_c values are not adjusted by NDVI magnitude in this study. Ground observations, however, would determine whether or not adjusted K_c values should be adopted.

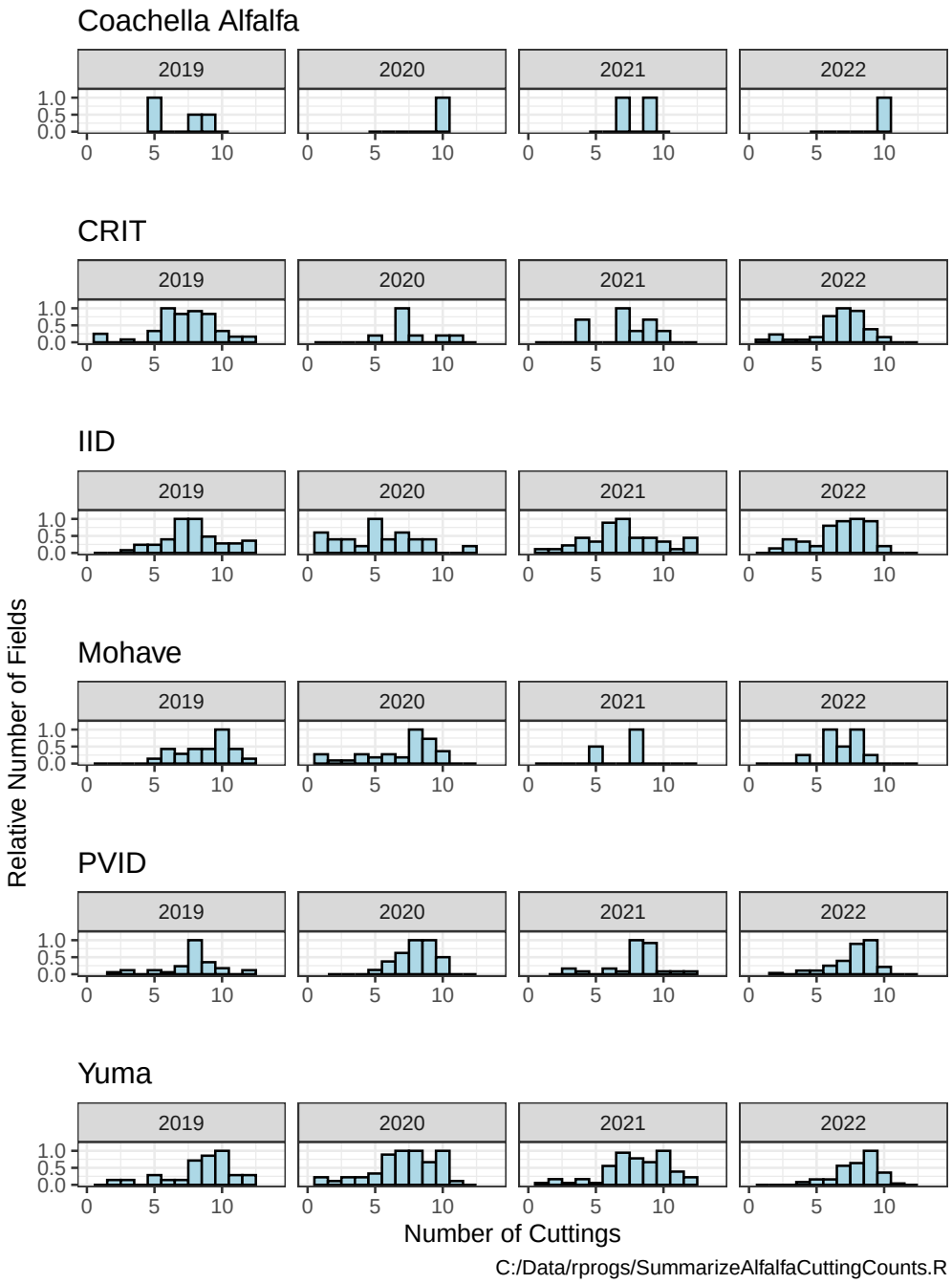

Figure 14. Number of alfalfa cuttings per year.

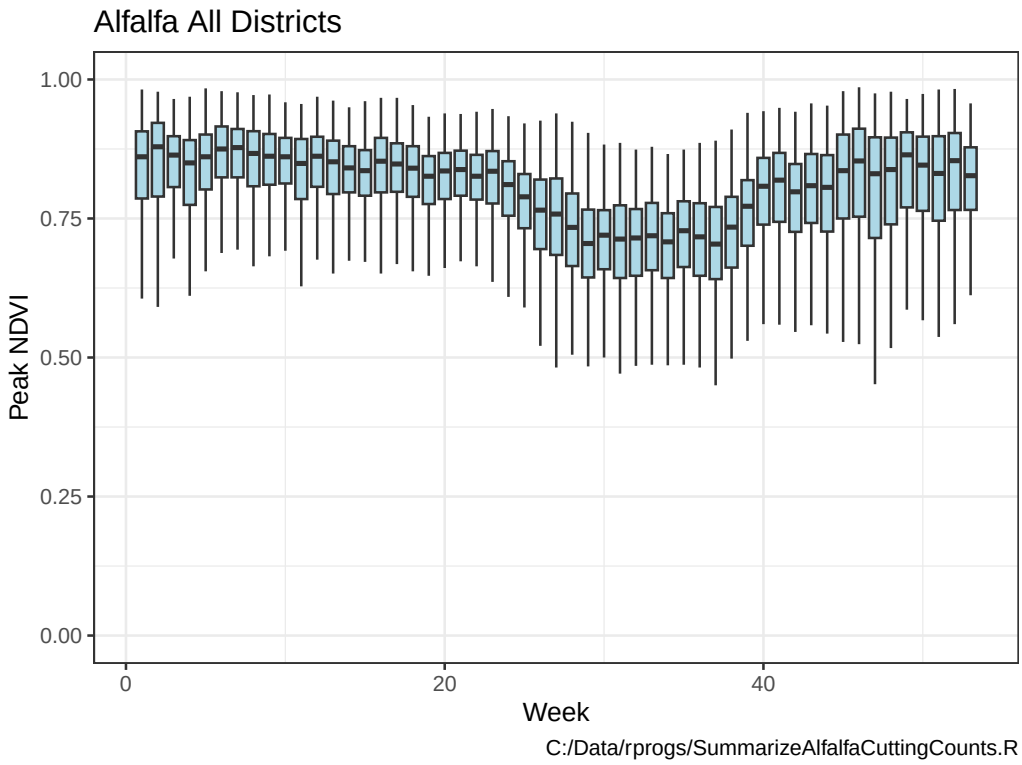

Figure 15. Maximum NDVI each week for alfalfa.

Table 11. NDVI results for combined Bermudagrass /Kleingrass Annual ET_c (mm/year).

	Year			
Area	2019	2020	2021	2022
Coachella	1600	1469	1507	1657
CRIT	1107	1175	1155	1020
IID	1329	1405	1426	1465
Mohave	984	1034	1068	937
PVID	1099	983	546	891
Yuma	1101	1113	768	1081

5.2 Bermudagrass and Kleingrass

Bermudagrass and Kleingrass are grown for turf or forage and are widespread across LCRAS areas. They are a major water consumer, requiring as much as 1600 mm per year (Meister, 2004a). Both are grown throughout the year and cut multiple times. As noted in Section 4, cutting patterns vary by irrigation area and are more irregular than found for alfalfa. These variable, and episodic, patterns make identification of growth stage difficult and error-prone.

Examples of different cutting practices are illustrated in Figures 16 and 17. At IID the NDVI patterns generally denote a single season with minor drops in cover, while at Yuma the cuttings are strongly bi-modal. Daily ET_c ranges from 2 mm/day in cooler months up to 8 mm/day in hotter months. Growth stage modeling indicated total annual ET_c values, with a few exceptions, range from approximately 1100 to 1800 mm/day for most irrigated areas (Table 11). Histograms for total ET_c over six irrigation areas in 2019-2022 emphasize the large variability in water use by Bermudagrass and Kleingrass : NDVI-based values are above and below LCRAS estimates (Figure 18).

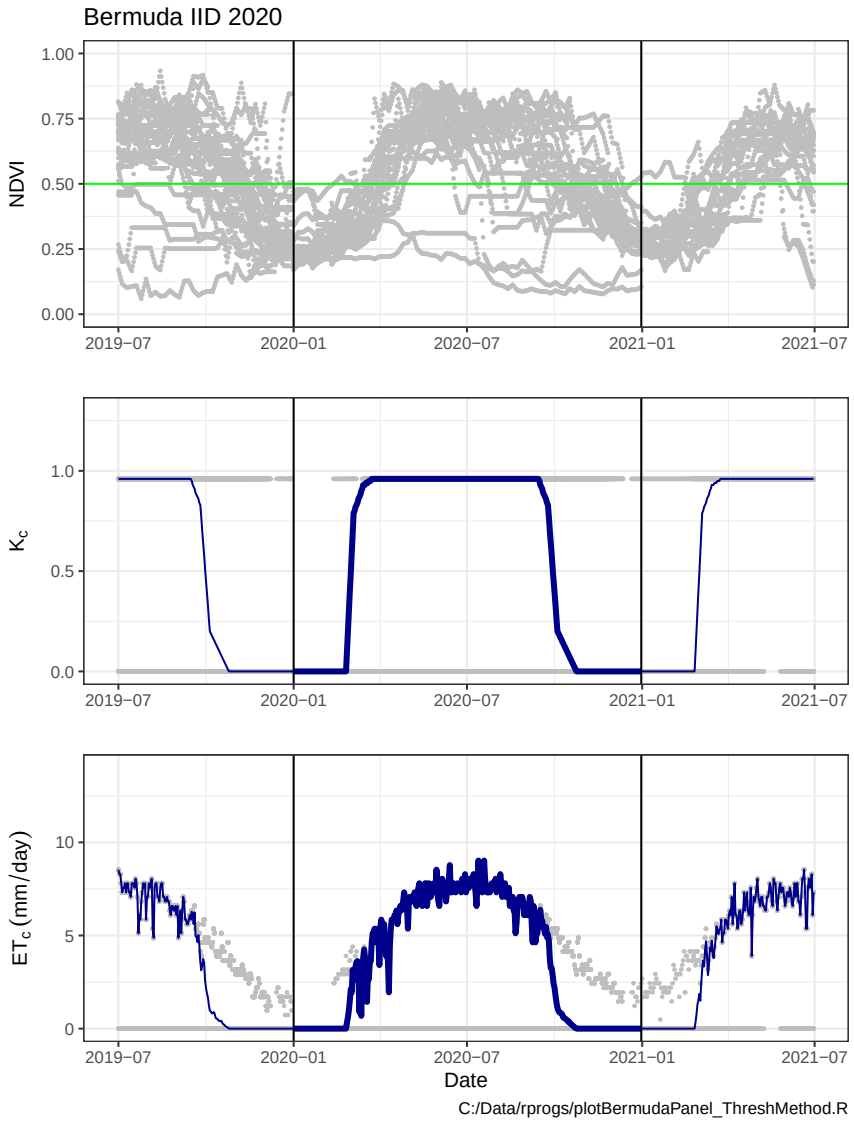

Figure 16. Example of the Bermudagrass /Kleingrass NDVI thresholding approach for IID sites. The minimal NDVI that discriminates crop from bare soil (green line, top) is intersected with field-averaged NDVI values. Wherever NDVI exceeds this threshold a MID K_c value is assigned, elsewhere it is set to zero (middle panel). The resulting K_c pattern is multiplied by the corresponding ET_{os} value to return daily ET_c (bottom panel). An example site is highlighted in blue.

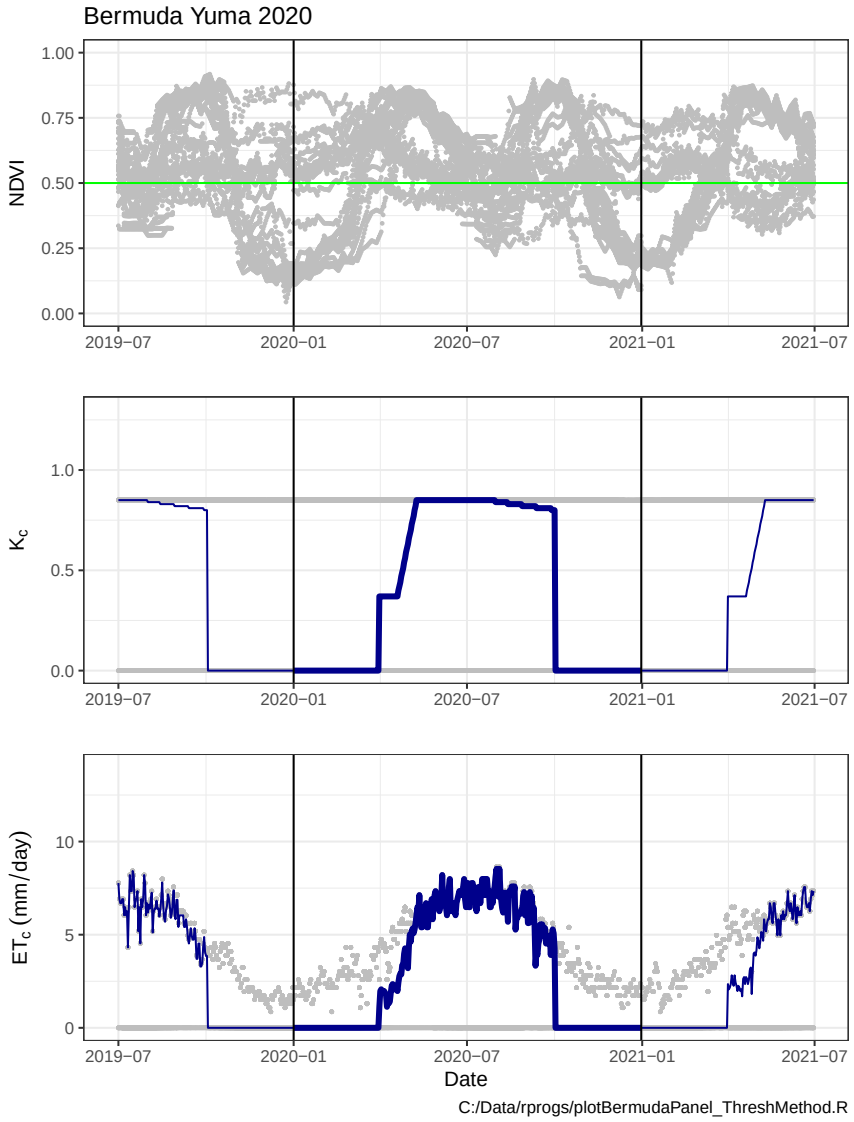

Figure 17. Example of Bermudagrass /Kleingrass thresholding for Yuma sites. The same procedure is applied as described in Figure 16. Note that unlike IID, the NDVI patterns are bi-modal.

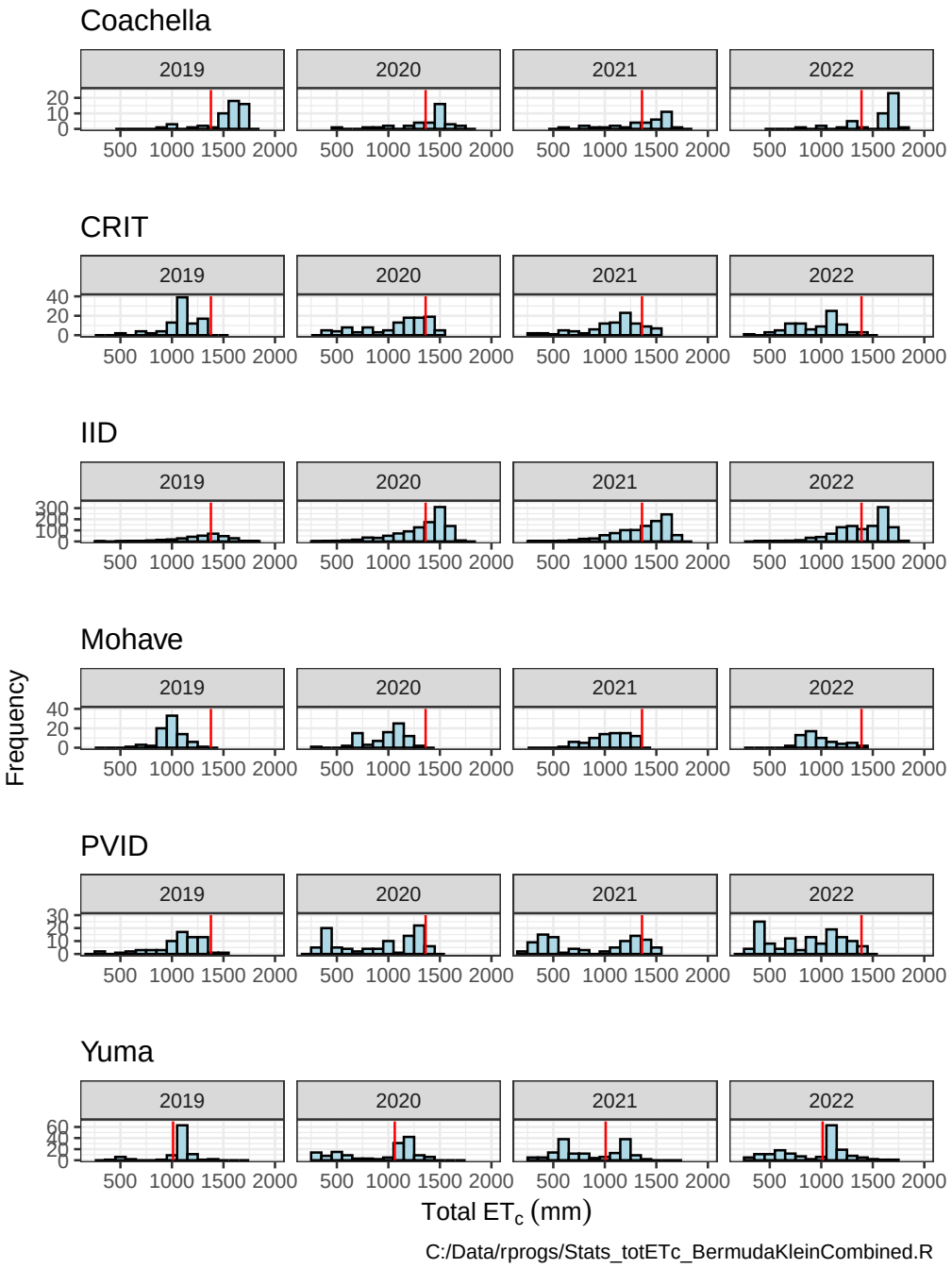

Figure 18. Total ET_c for combined Bermudagrass and Kleingrass sites for the 2019-2022 period compared with LCRAS.

Table 12. NDVI results for Citrus Annual ET_c (mm/year)

		Year			
Crop	Area	2019	2020	2021	2022
Citrus-Mature	Coachella	1103	1109	1122	1137
	IID	1102	1108	1121	1138
	PVID	1085	1026	707	689
	Yuma	1106	1147	1138	1153
Citrus-Young	Coachella	966	1031	999	1135
	IID	1095	1040	1059	1102
	Yuma	1101	1145	1133	1152
Citrus-Declining	Coachella	1098	1107	1120	1136
	IID	1103	1107	1120	939
	PVID	-	1171	-	-
	Yuma	1104	1147	1133	1152

5.3 Citrus

Citrus crops are significant for four irrigated areas: Coachella, IID, PVID, and Yuma-Wellton. They are perennial, thus are highly predictable for crop classifications. Reclamation categorizes citrus by tree height: mature ($>$ 3 m; Figure 19), young (1-3 m; Figure 20), declining (height not determinative; Figure 21). As noted in section 4, these categories have a strong correspondence to overall NDVI amplitudes and enable a K_c approach adaptive to tree height. The demonstrated examples shown for mature trees confirm the observation. That pattern is consistent with bidirectional reflection distribution function (BRDF) models that show the effect is a result of solar zenith angle changes and surface shading. The annual K_c pattern follows the NDVI shape and has low variability. It is possible that the K_c values need to be modified substantially. For example Jafari et al. (2021) report K_c values that have a convex upward shape instead of a concave pattern. The consequent result is that growth stage partitioning by day of year has a small effect on daily ET_c . Young trees, with 1-3 mm/day ET_c , often lack the parabolic pattern as illustrated in Figure 20. Declining citrus do show parabolic NDVI patterns where daily ET_c is $\sim$2-4 mm/day. Total ET_c ranges $\sim$1200 mm for California (Faber, 2015) and $\sim$1500 mm for Arizona (Wright, 2021).

The effect of the adaptive K_c approach for citrus is illustrated for Yuma (Figure 22), IID (Figure 23), and Coachella (Figure 24), where 'standard' indicates no adjustment of LCRAS K_c values. Generally the adjustment procedure has minimal effect on outcomes for mature trees, but significantly increases average ET_c values for young and declining citrus samples. Vertical red lines denote LCRAS estimates. In all 'adjusted' cases, NDVI values disperse total ET_c for mature trees to lesser amounts, ET_c for young trees to greater amounts, and ET_c for declining trees to both lesser and greater amounts.

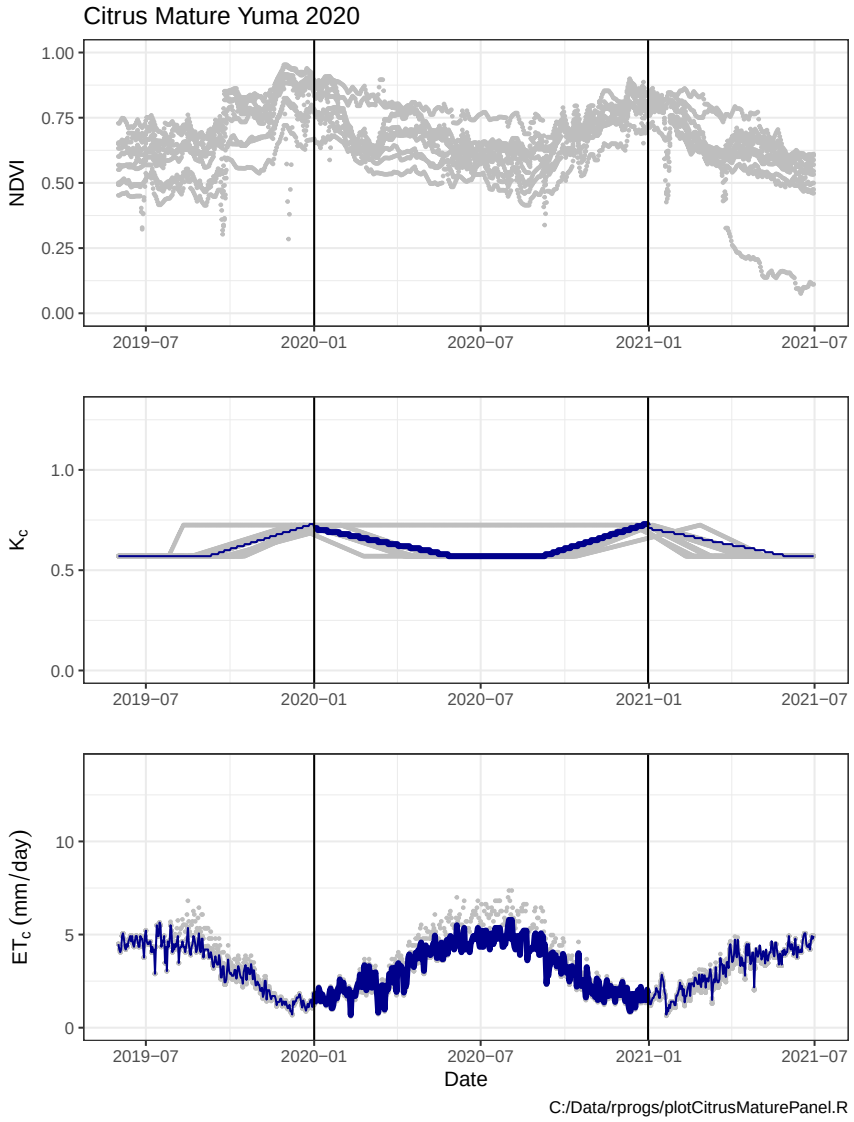

Figure 19. Mature citrus ET_c estimation from NDVI. Shown are examples of filtered and smoothed NDVI data over mature citrus fields in Yuma (top), conversion of NDVI to K_c curves (middle), and computation of daily ET_c from K_c and weather station based ET_{os} (bottom). Gray symbols illustrate NDVI-based modeling, blue lines show the corresponding LCRAS estimates.

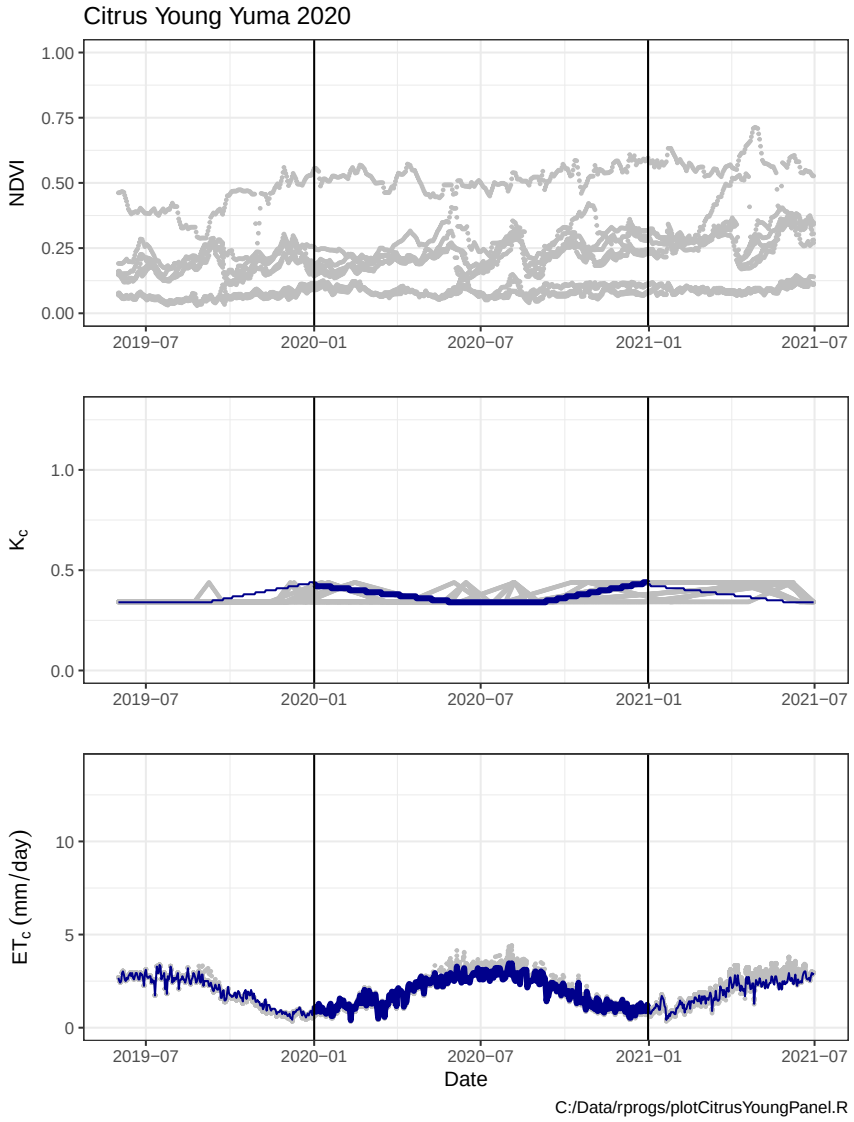

Figure 20. Young citrus ET_c estimation from NDVI. Shown are examples of filtered and smoothed NDVI data over young citrus fields in Yuma (top), conversion of NDVI to K_c curves (middle), and computation of daily ET_c from K_c and weather station based ET_{os} (bottom). Gray symbols illustrate NDVI-based modeling, blue lines show the corresponding LCRAS estimates.

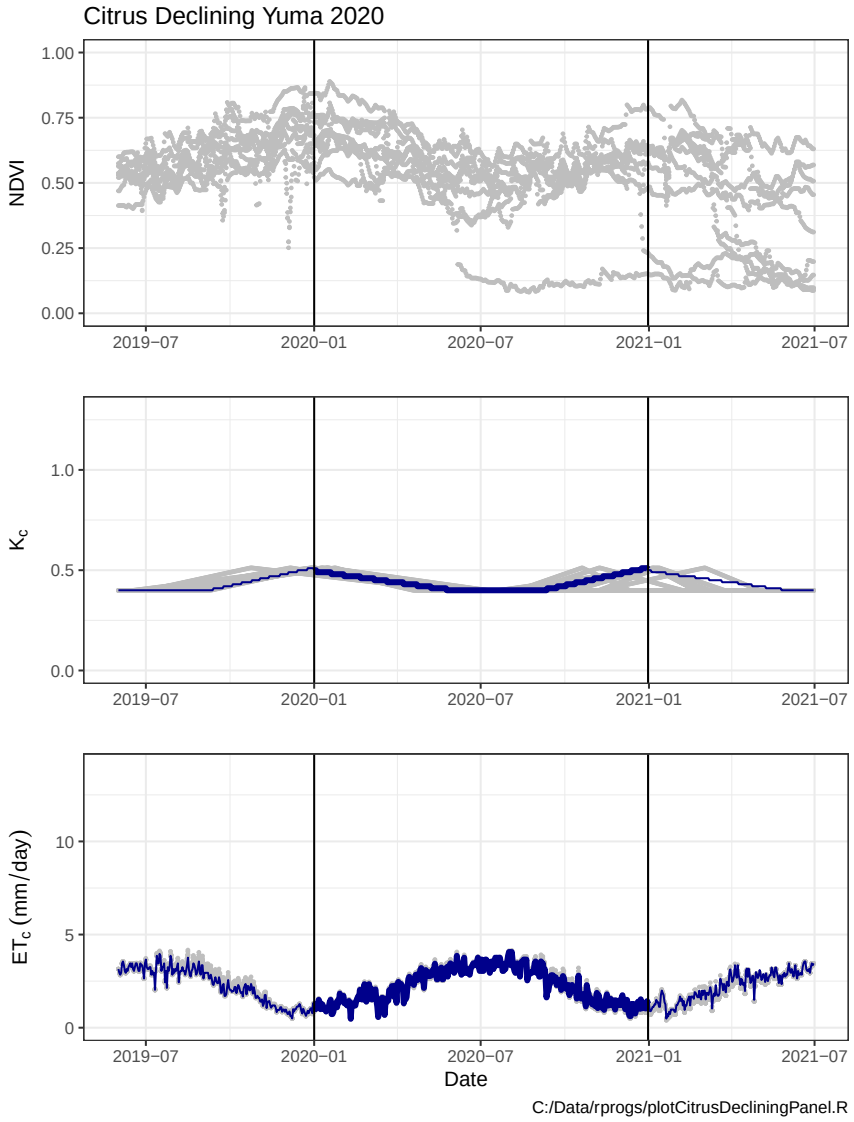

Figure 21. Declining citrus ET_c estimation from NDVI. Shown are examples of filtered and smoothed NDVI data over declining citrus fields in Yuma (top), conversion of NDVI to K_c curves (middle), and computation of daily ET_c from K_c and weather station based ET_{os} (bottom). Gray symbols illustrate NDVI-based modeling, blue lines show the corresponding LCRAS estimates.

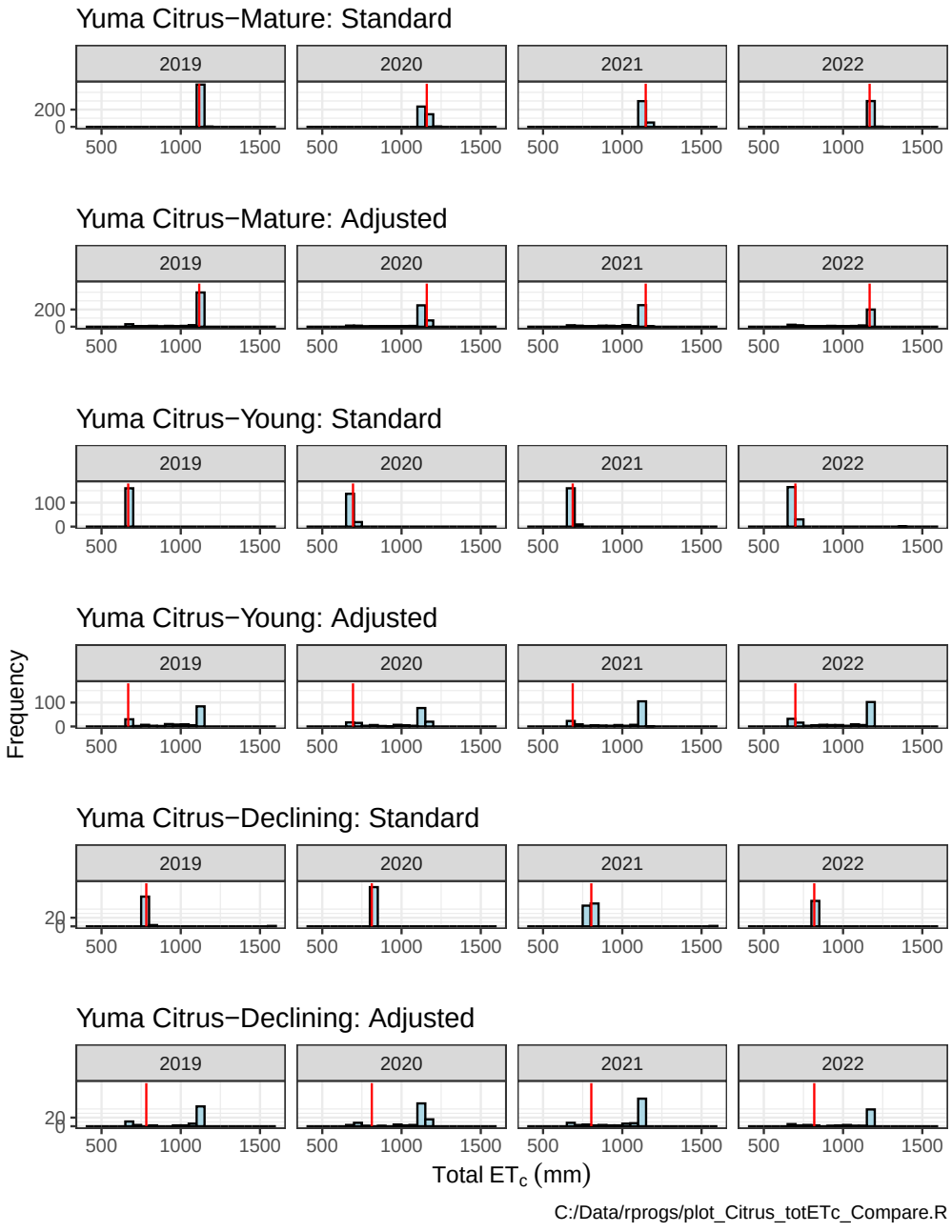

Figure 22. Total ET_c for Yuma citrus 2019-2022 computed for three tree maturities (Mature, Young, and Declining) in two ways: 'Standard' and 'Adjusted'. The 'Standard' histogram patterns represent ET_c results when using LCRAS K_c values, while the 'Adjusted' histograms show ET_c results when the linearly adjusted K_c values are applied.

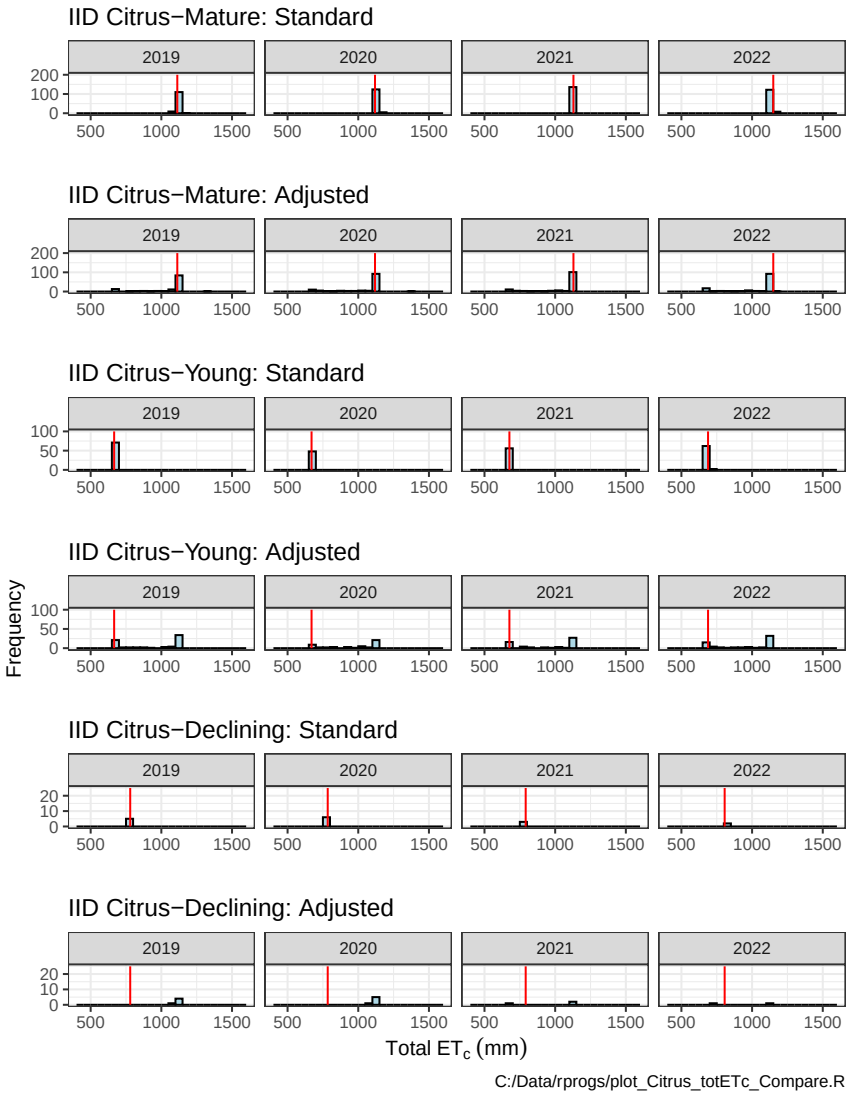

Figure 23. Total ET_c for IID citrus 2019-2022 computed for three tree maturities (Mature, Young, and Declining) in two ways: 'Standard' and 'Adjusted'. The 'Standard' histogram patterns represent ET_c results when using LCRAS K_c values, while the 'Adjusted' histograms show ET_c results when the linearly adjusted K_c values are applied. Vertical red lines denote LCRAS estimates.

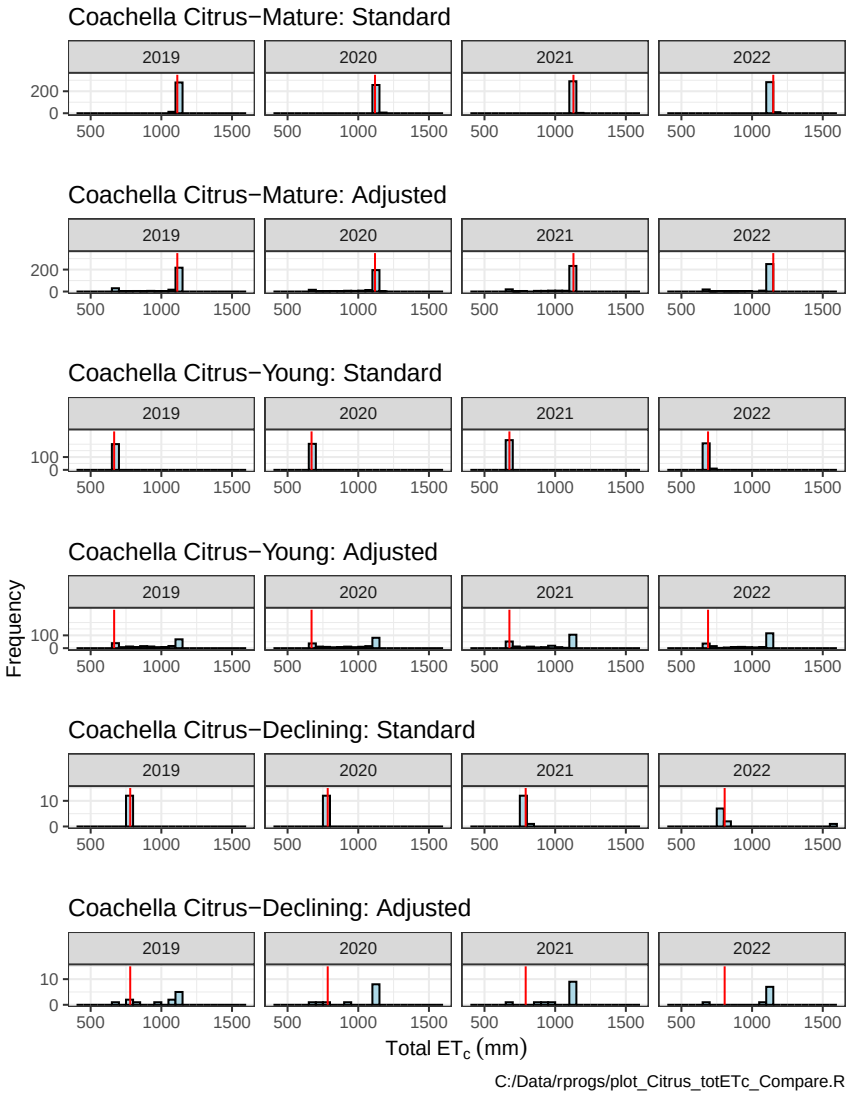

Figure 24. Total ET_c for Coachella citrus 2019-2022 computed for three tree maturities (Mature, Young, and Declining) in two ways: 'Standard' and 'Adjusted'. The 'Standard' histogram patterns represent ET_c results when using LCRAS K_c values, while the 'Adjusted' histograms show ET_c results when the linearly adjusted K_c values are applied. Vertical red lines denote LCRAS estimates.

Table 13. Carrots Annual ET_c (mm/day).

	Year			
District	2019	2020	2021	2022
Coachella	458	353	406	464

5.4 Carrots

Carrots are a biennial root vegetable observed at Coachella and IID; here we report results from Coachella (Table 13). They are planted starting late fall and harvested by late spring. Analysis of satellite NDVI data documents this practice (Figure 25). For growth stage modeling, K_c values for small vegetables were used and simplified from nearly curvilinear Reclamation K_c values (middle panel, Figure 25) and converted to the FAO-56 standard 3-parameter data set. Daily ET_c ranges 2-5 mm/day. Summation of winter and summer ET_c values resulted in total ET_c that ranges widely, 300-800 mm/year (Figure 26), and is almost always less than LCRAS ET_c. Future analysis of carrots should consider that crop durations are highly variable from field-to-field. Montazar et al. (2021) report values ranging 306-486 mm/year.

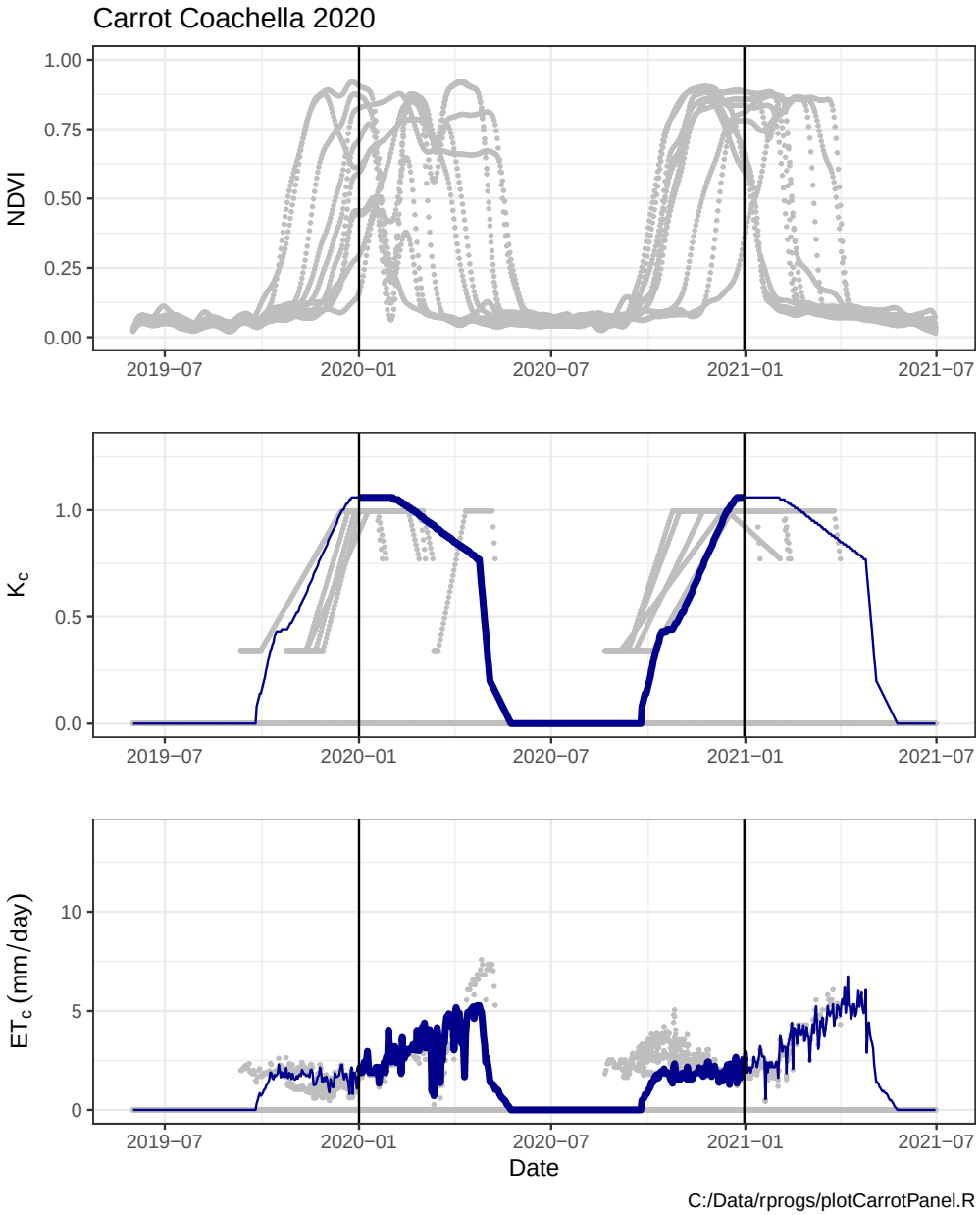

Figure 25. Carrot ET_c estimation from NDVI. Shown are examples of filtered and smoothed NDVI data over carrot fields in Coachella (top), conversion of NDVI to K_c curves (middle), and computation of daily ET_c from K_c and weather station based ET_{os} (bottom). Gray symbols illustrate NDVI-based modeling, blue lines show the corresponding LCRAS estimates.

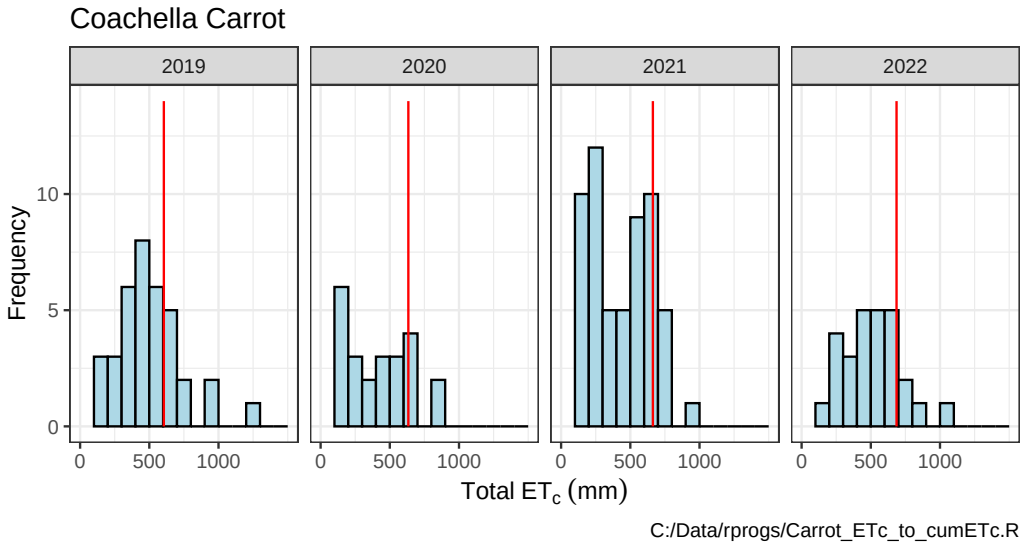

Figure 26. Distribution of NDVI-based total ET_c (blue) for carrots at Coachella 2019-2022 compared with LCRAS (red lines). ET_c values represent the summation of values from the fall months of the indicated year plus the early spring time periods from the subsequent year. For example,the 2019 data include ET_c values from fall of 2019 and spring of 2020.

Table 14. Corn Annual ET_c (mm/day).

	Year				
Area	2019	2020	2021	2022	2023
Yuma	857	812	832	763	737

5.5 Corn

Corn is observed throughout the different irrigated areas but is a relatively minor water consumer in all of the irrigation areas. Analysis of NDVI data shows that corn is planted early in the calendar year and harvested by mid-summer (Figure 27). The LCRAS K_c curve is consistent with this growing practice.

NDVI analyses of all verified corn fields (Figure 28), however, show a few differences from the LCRAS model, where actual day of planting is about 10-20 days later than modeled by LCRAS.

Daily ET_c ranges 1-10 mm/day. Total ET_c each year was generally 600-900 mm (Table 14), and agrees with LCRAS estimates (Figure 29). Total ET_c in California has been reported to be ∼680 mm (https://ucanr.edu/sites/Drought/files/167003.pdf) and ∼500 mm in Arizona (Erie et al., 1982).

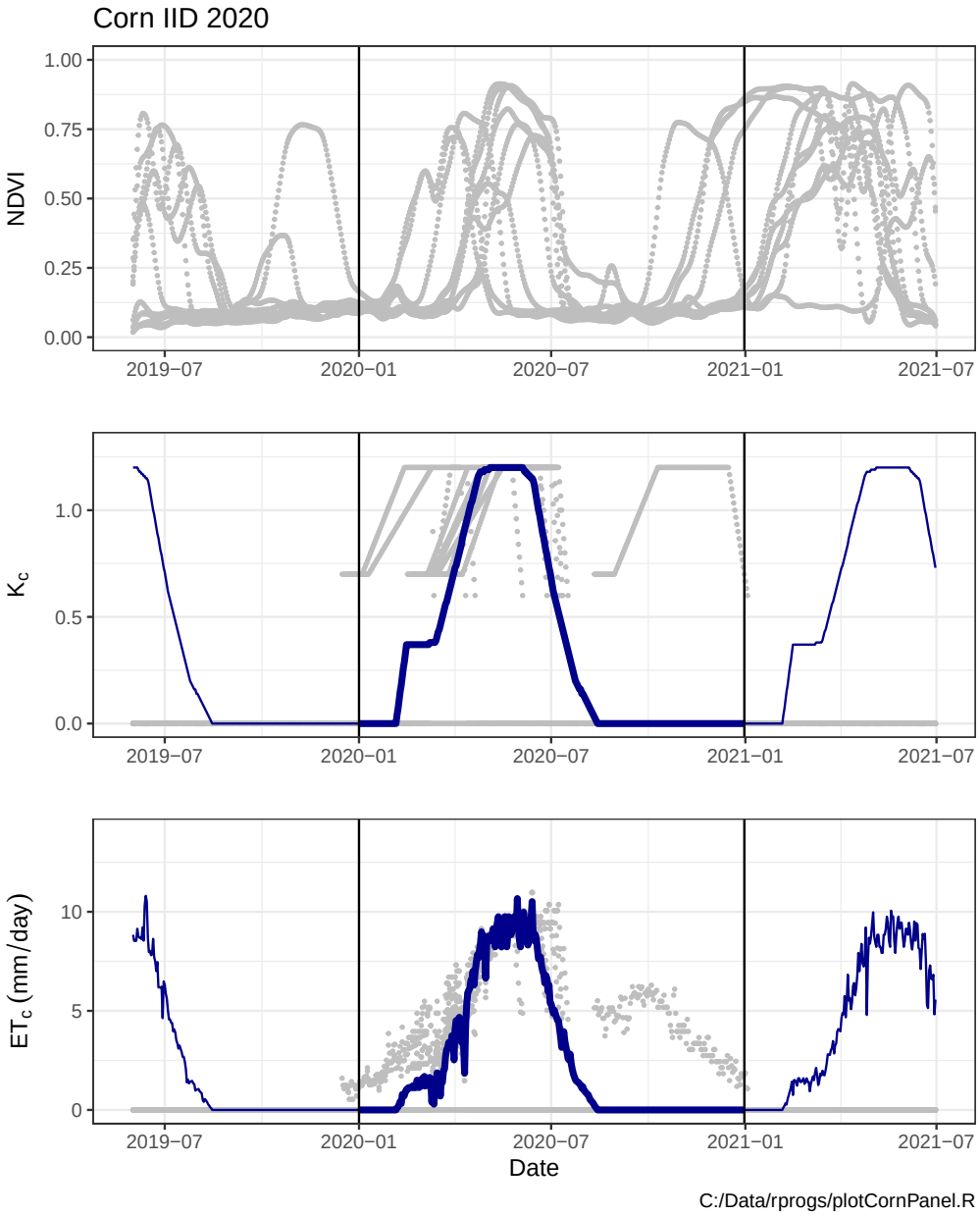

Figure 27. Corn ET_c estimation from NDVI. Shown are examples of filtered and smoothed NDVI data over corn fields in IID (top), conversion of NDVI to K_c curves (middle), and computation of daily ET_c from K_c and weather station based ET_{os} (bottom). Gray symbols illustrate NDVI-based modeling, blue lines show the corresponding LCRAS estimates.

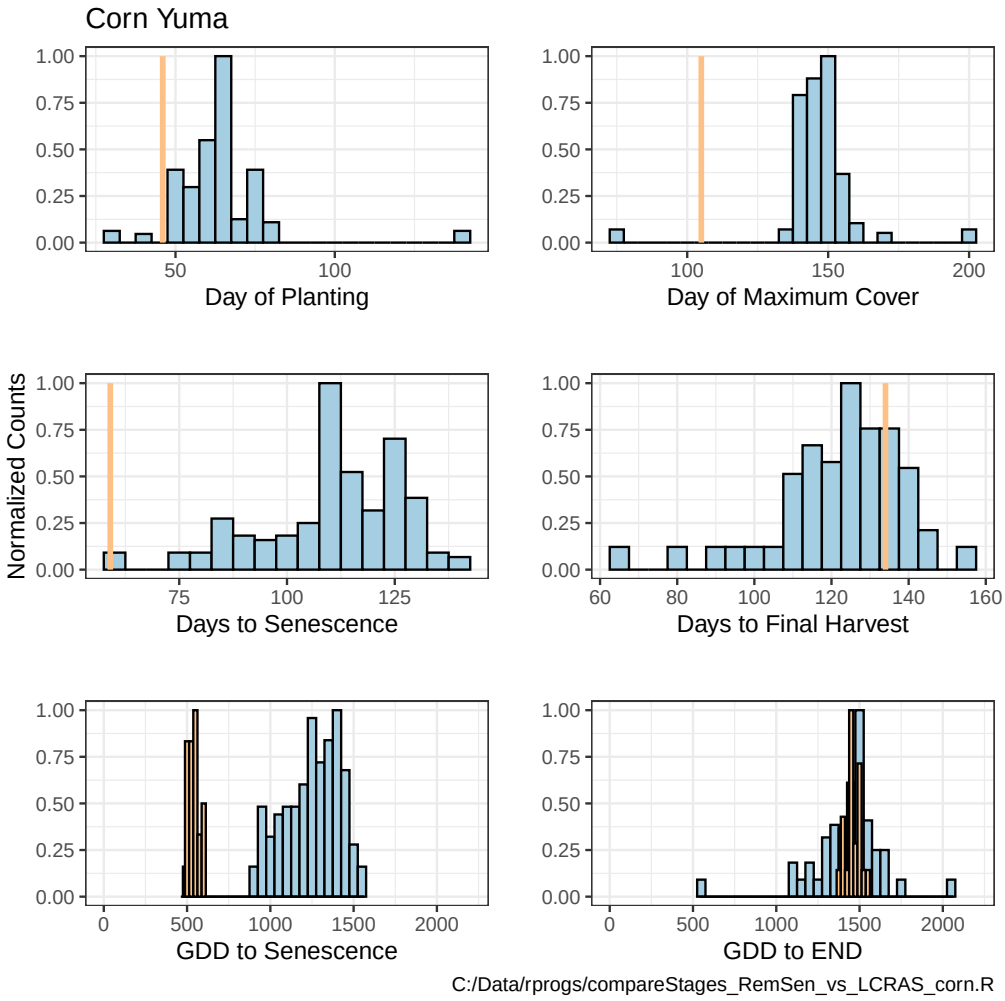

Figure 28. Growth stage estimation from NDVI and LCRAS for corn. The blue histograms represent estimates derived from NDVI data. Orange lines denote LCRAS events and orange histograms represent the distribution of Growing Degree Days (GDD) obtained using Yuma Valley weather data and GDD temperature limits of 10-30°C.

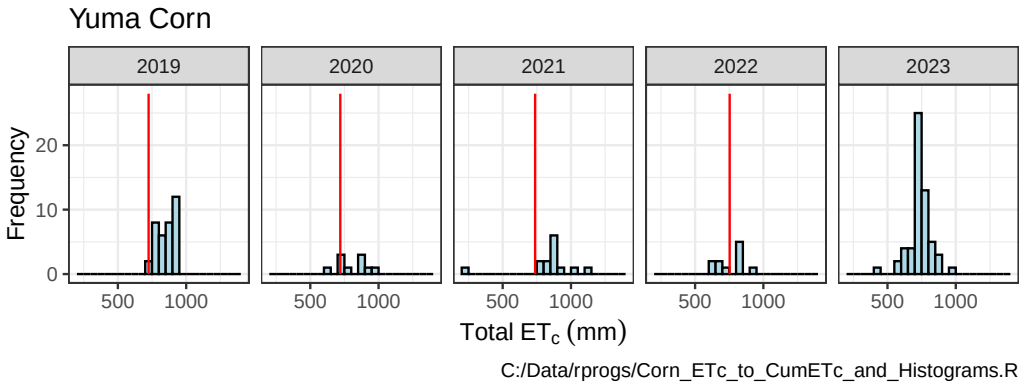

Figure 29. Total ET_c for corn at Yuma 2019-2023 compared with LCRAS. The additional year is included because many observations were made in 2023, but few in prior years due to COVID-related field restrictions.

Table 15. Cotton ET_c (mm/day).

	Year			
Area	2019	2020	2021	2022
CRIT	1055	1178	1041	1027
PVID	1112	1221	1146	1115
Yuma	984	962	907	920

5.6 Cotton

Cotton is a long-season crop grown in all districts. It is planted by April and harvested by end of calendar year. NDVI data show that cotton seasons are generally synchronous with well-defined growth patterns: rapid development, 3+ month mid-stage, followed by 3-month end-stage (Figure 30). NDVI data also show that cotton is planted earlier, and grown for longer times than modeled by LCRAS (Figure 31). Daily ET_c ranges 2-11 mm/day. Peak ET_c values are about 1 week earlier than LCRAS standard estimates. Total ET_c (Figure 32) ranges 800-1300 mm (Table 15), with values sometimes less than or greater than LCRAS models. Literature values are similar, with Hunsaker et al. (1994) reporting $\sim$1000 mm and Erie et al. (1982) $\sim$1050 mm.

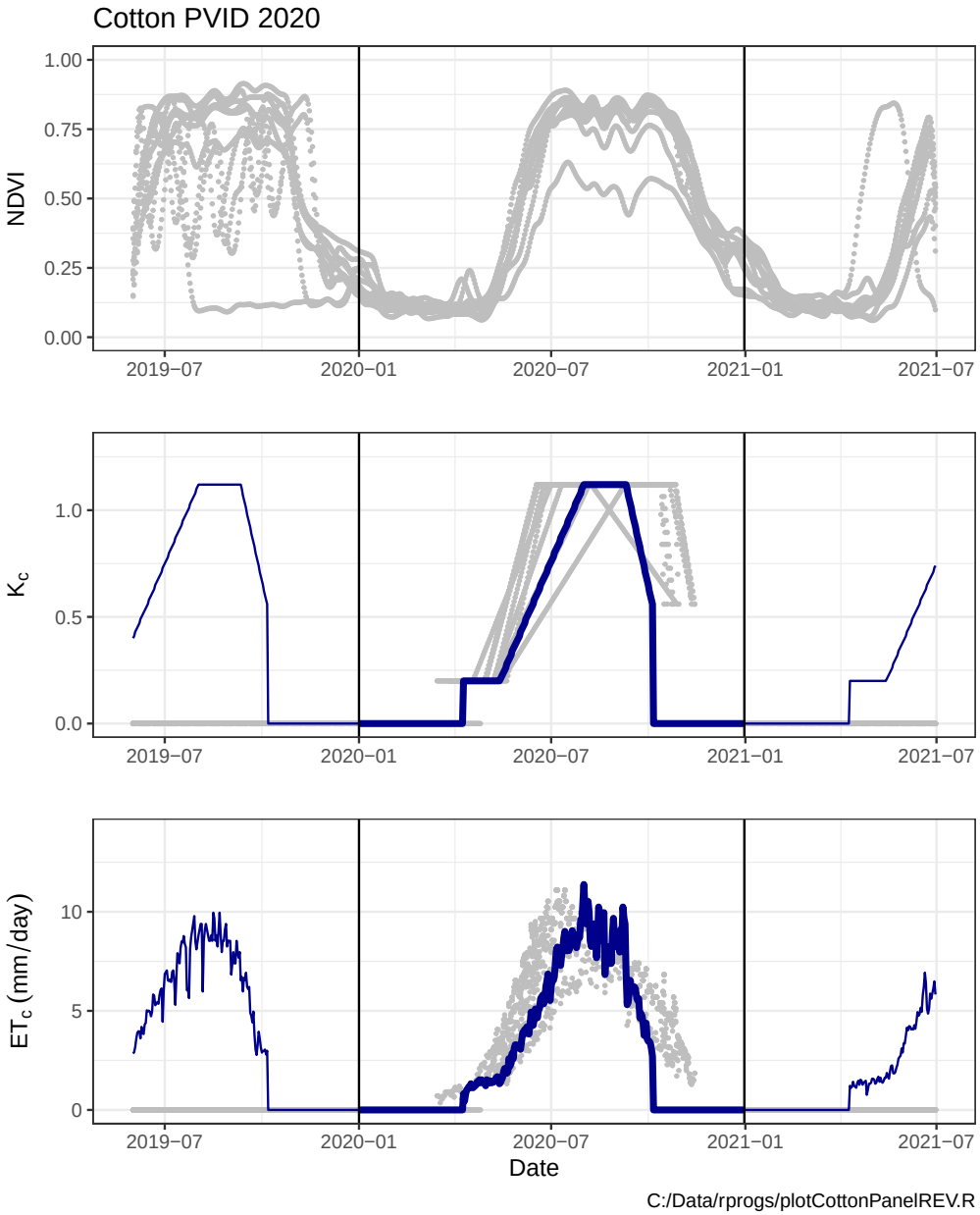

Figure 30. Cotton ET_c estimation from NDVI. Shown are examples of filtered and smoothed NDVI data over cotton fields in PVID (top), conversion of NDVI to K_c curves (middle), and computation of daily ET_c from K_c and weather station based ET_{os} (bottom). Gray symbols illustrate NDVI-based modeling, blue lines show the corresponding LCRAS estimates.

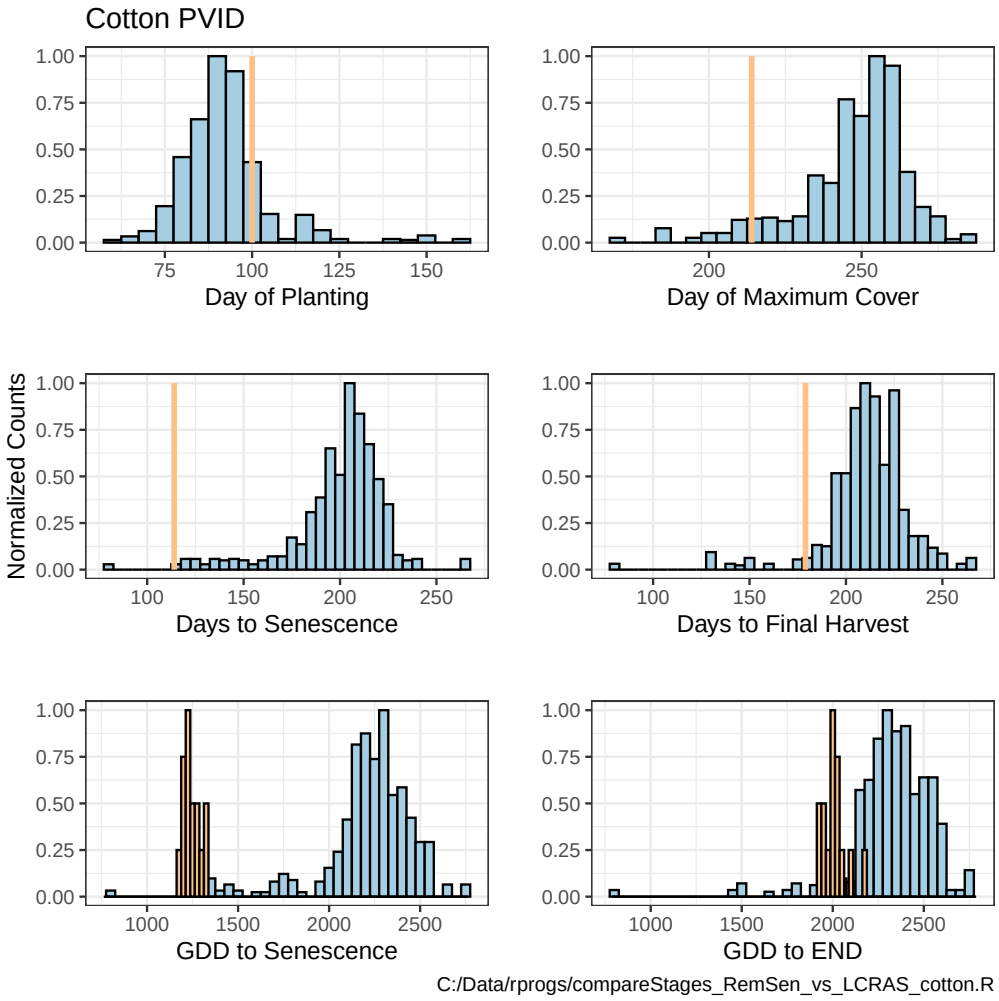

Figure 31. Growth stage estimation from NDVI and LCRAS for cotton. The blue histograms represent estimates derived from NDVI data. Orange lines denote LCRAS events and orange histograms represent the distribution of Growing Degree Days (GDD) obtained using Yuma Valley weather data and GDD temperature limits of 12.77-30°C.

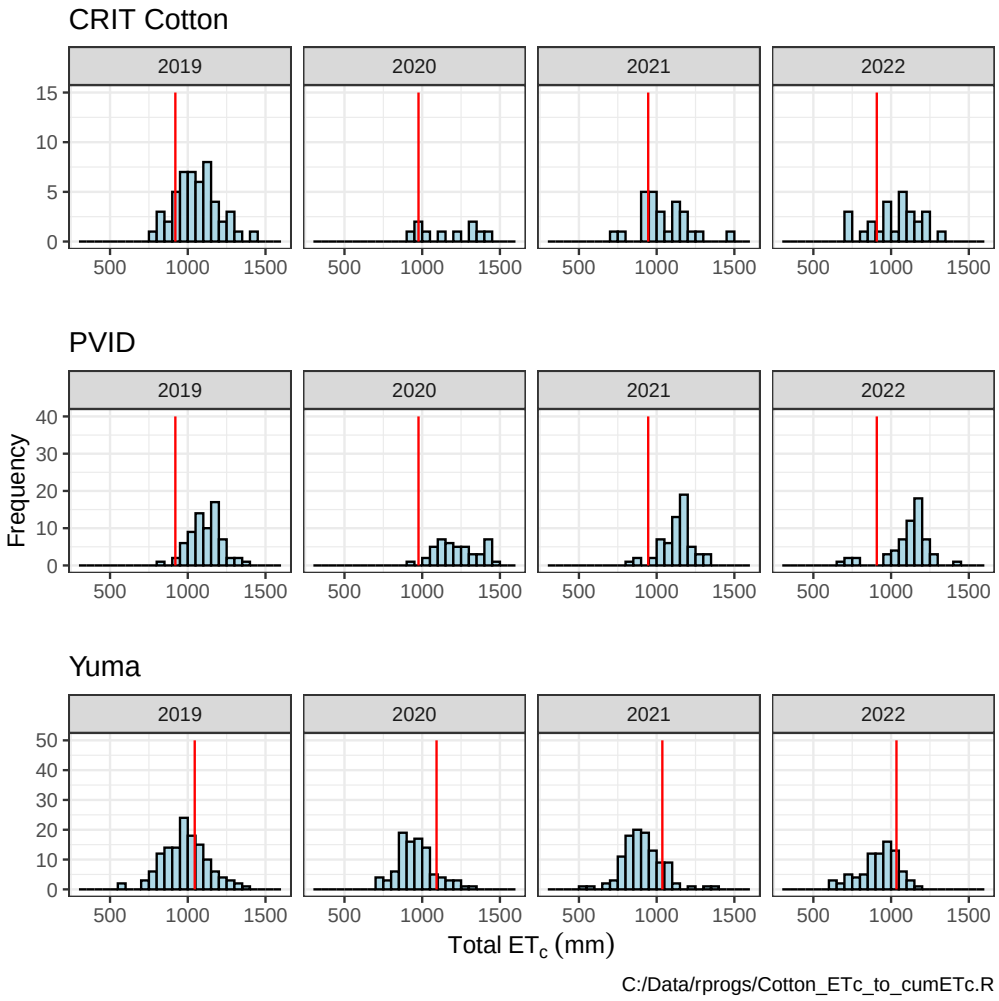

Figure 32. Total ET_c for cotton 2019-2022 (blue histograms) compared with LCRAS (red lines).

Table 16. Dates Annual ET_c (mm/year).

		Year			
Crop	Area	2019	2020	2021	2022
Dates-Mature	Coachella	1747	1813	1789	1814
	PVID	-	1906	1925	1869
	Yuma	1743	1813	1789	1814
Dates-Young	Coachella	1751	1761	1765	1790
	PVID	1788	1899	1924	1872
	Yuma	-	1814	1787	1826
Dates-Declining	Coachella	1735	1739	1760	1783
	PVID	1740	1901	1924	1869
	Yuma	1740	1811	1794	1812
Dates-Undifferentiated	Yuma	1746	1816	-	-

5.7 Dates

Dates are a perennial tree crop reported in all districts except for Mohave. Their NDVI exhibit a quadratic seasonal pattern similar to citrus, where maximal values are found in winter months and minimal values in mid-summer. K_c prescribed by LCRAS have little variability (0.82-1.01) with peak values in spring and with no clear correlation with NDVI data (Figure 33). Note that Montazar et al. (2020) report higher ($\sim$0.9) K_c values in the winter and lower ($\sim$0.6) in late fall. The growth stages are estimated in a similar way to citrus, where the 10^{th}-percentiles define the transitions between DEV and MID stages. Since Reclamation does not provide distinguishing K_c curves for different levels of tree maturity, the growth stage modeling did not use an adaptive K_c approach, i.e. only one set of K_c reference values are used to estimate ET_c. Accordingly, the daily ET_c values have low variability between fields, but have high seasonal variability of 2-10 mm/day. Results for total ET_c, 1700-1900 mm (Table 16), show a large divergence from LCRAS models (Figure 34) and are greater than values reported by Montazar et al. (2020): 1300-1500 mm.

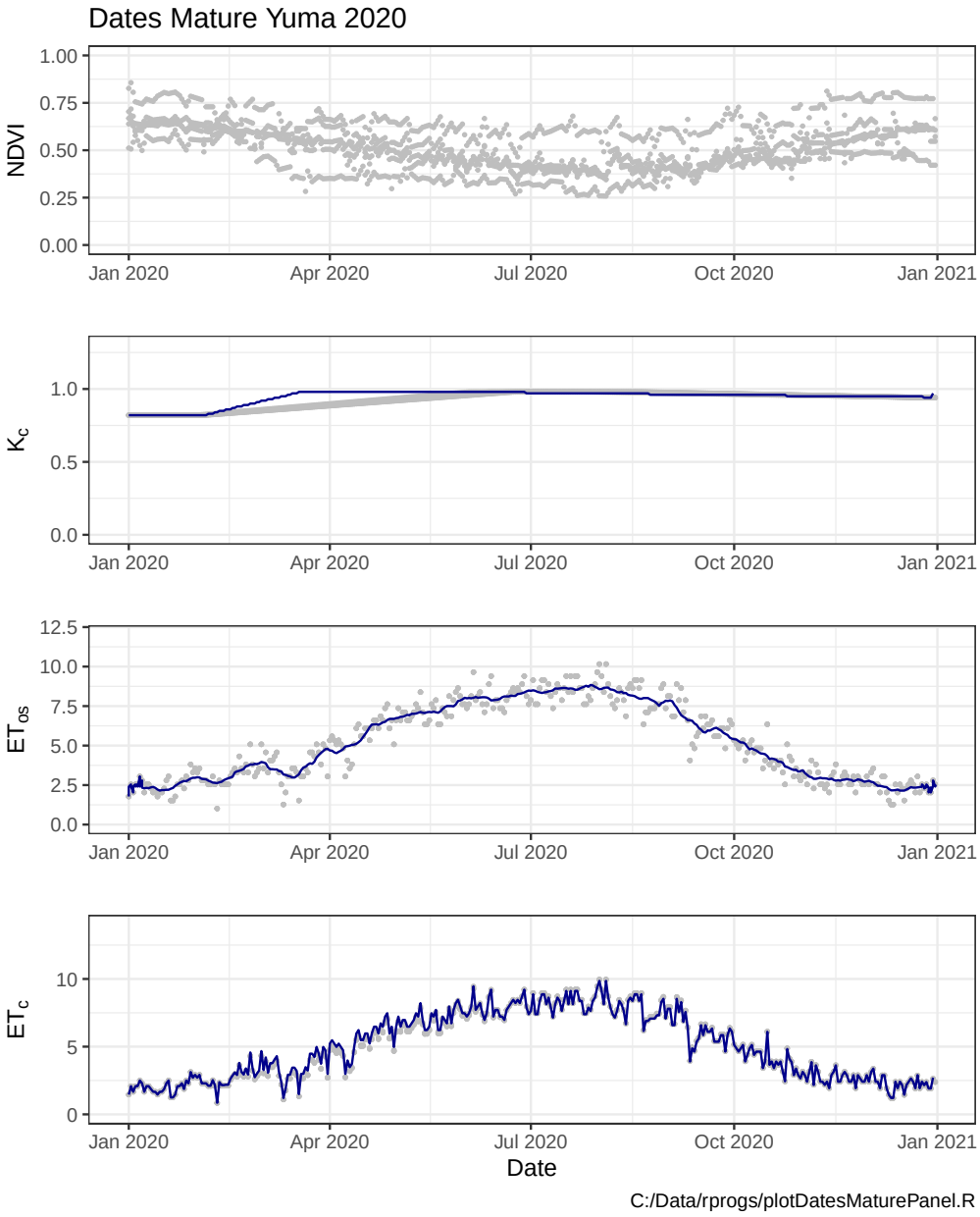

Figure 33. Mature dates ET_c estimation from NDVI. Shown are examples of filtered and smoothed NDVI data over mature date fields in Yuma (top), conversion of NDVI to K_c curves (second), collection of ET_{os} (third), and computation of daily ET_c from K_c and weather station based ET_{os} (bottom). Gray symbols illustrate NDVI-based modeling, blue lines show the corresponding LCRAS estimates and average ET_{os} .

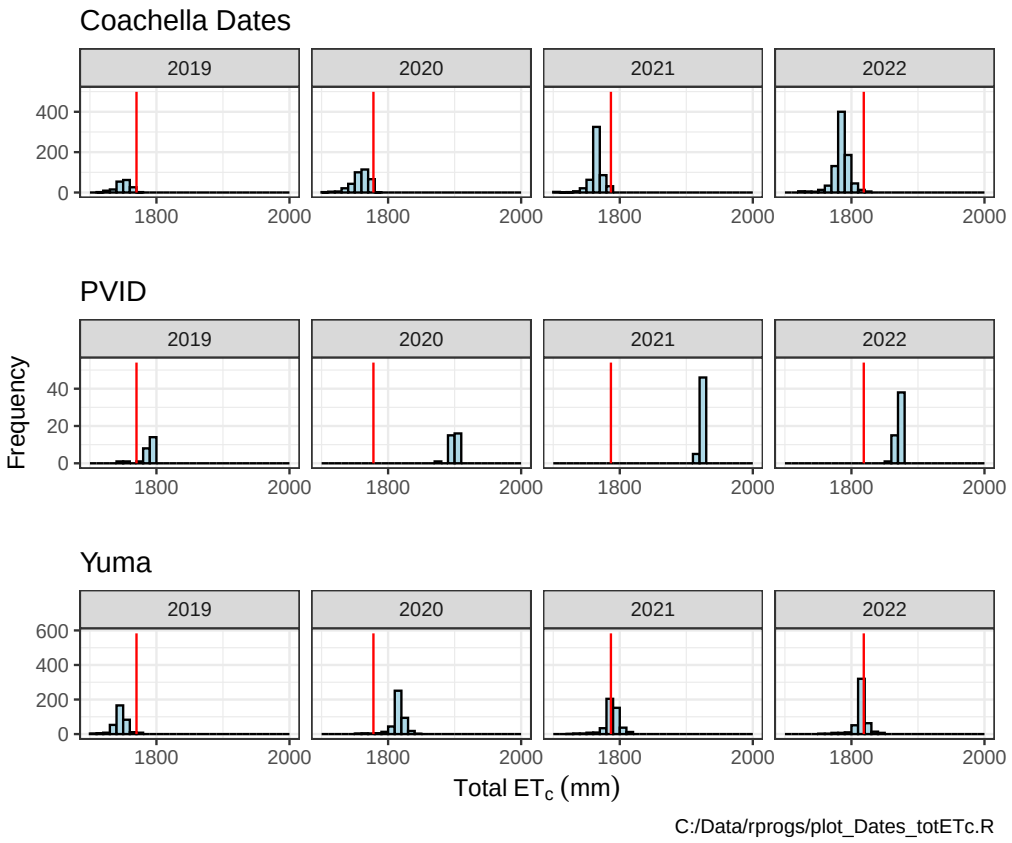

Figure 34. Total ET_c for dates (blue histograms, all maturities) 2019-2022 compared with LCRAS (red lines).

Table 17. Grapes ET_c .

	Year			
Area	2019	2020	2021	2022
Coachella	1144	1141	1086	1112

5.8 Grapes

Grapes are a long-season crop observed in a significant number of fields at Coachella and in fewer fields at Yuma. NDVI data indicate a several month variability between fields for growth: usually planted in January but sometimes planted early spring or fall (Figure 35). The Reclamation K_c pattern has nearly symmetric stages with equally long DEV and END durations and a MID period of about 6 weeks. Daily ET_c ranges $<$1 mm/day up to 7.5 mm/day. Peacock (1995) reports that mature vineyards used $\sim$550-700 mm/year, plus another 150-200 mm/year for leaching fraction. Considering just Coachella, total ET_c ranged 800-1300 mm/year (Figure 36),with an average total ET_c of $\sim$1100 mm/year (Table 17), and was consistently greater than LCRAS values, $\sim$900 mm/year.

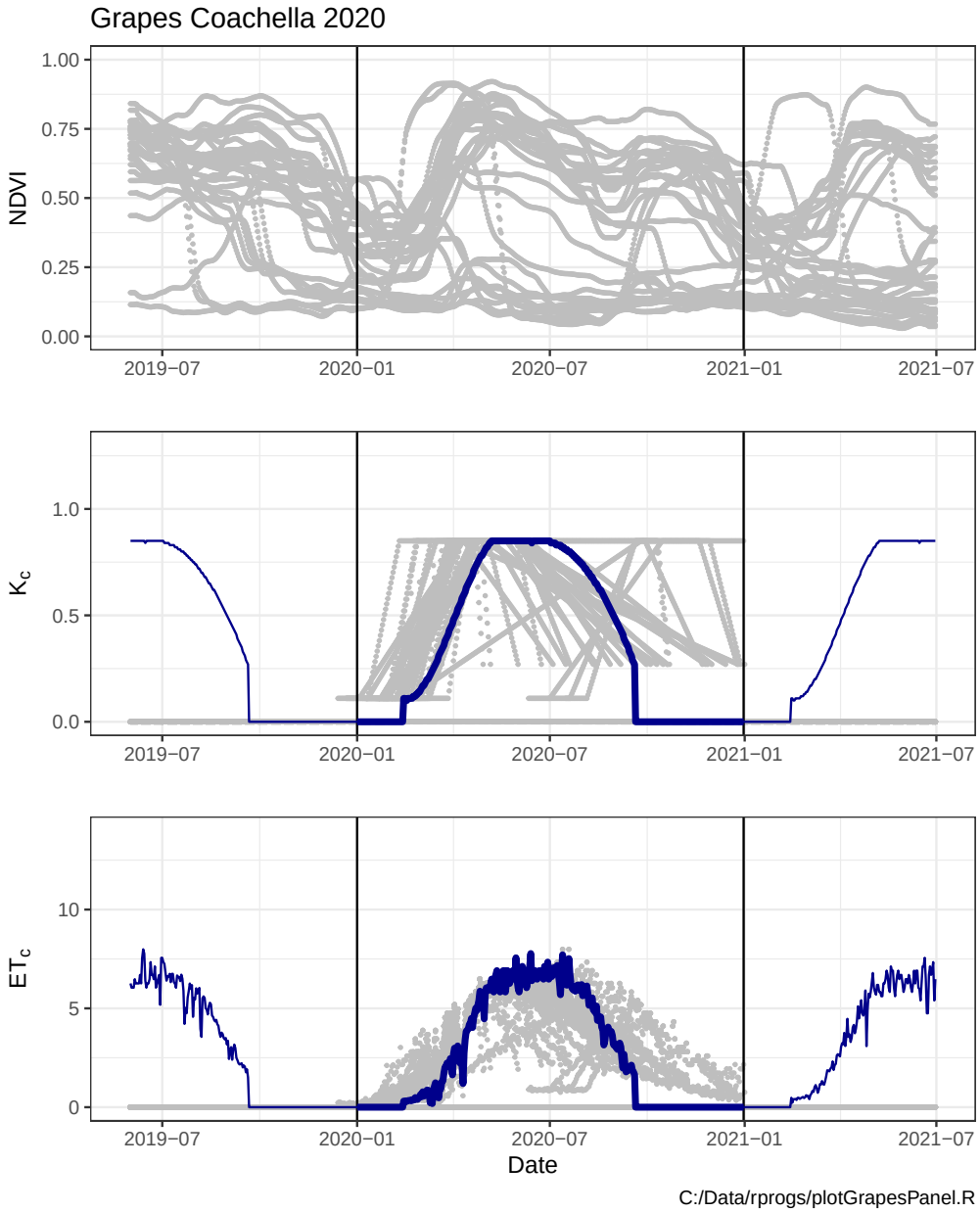

Figure 35. Grapes ET_c estimation from NDVI. Shown are examples of filtered and smoothed NDVI data over grape fields in Coachella (top), conversion of NDVI to K_c curves (middle), and computation of daily ET_c from K_c and weather station based ET_{os} (bottom). Gray symbols illustrate NDVI-based modeling, blue lines show the corresponding LCRAS estimates.

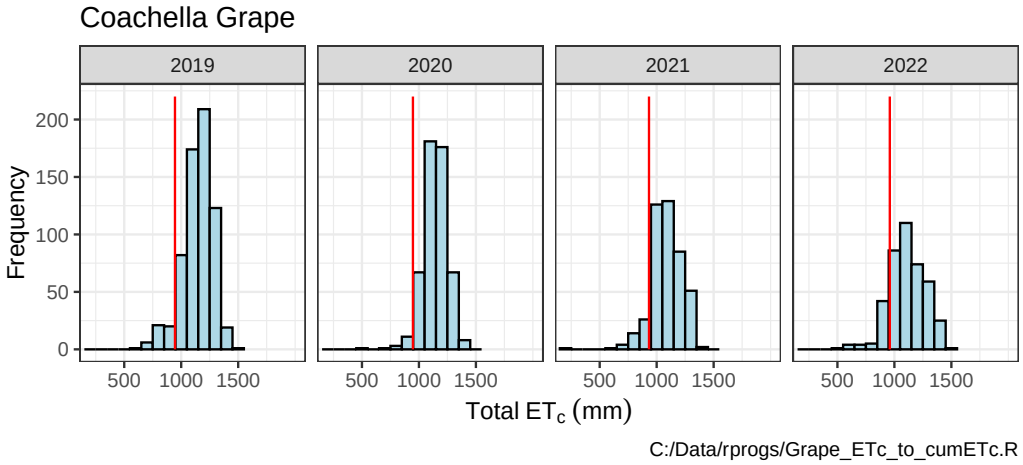

Figure 36. Total ET_c for grape 2019-2022 (blue histograms) compared with LCRAS (red lines).

Table 18. Kleingrass ET_c .

	Year			
Area	2019	2020	2021	2022
CRIT	1079	1200	1518	1333
IID	1737	1771	1928	1701
Mohave	1936	1375	1543	-
PVID	1301	1113	851	873

5.9 Kleingrass

Kleingrass is a perennial bunchgrass (https://plants.usda.gov/DocumentLibrary/plantguide/pdf/pg_paco2.pdf). Although this report analyzes Kleingrass in combination with Bermudagrass because it is believed that there is a high rate of crop misclassfication, this section reports the Kleingrass observations for completeness.

NDVI data shows that the crop is cut multiple times in spring-fall (Figure 37). Reclamation's LCRAS models the crop as a single season, while the growth stage approach considers each cutting separately (middle panel Figure 37). Daily Kleingrass ET_c ranges 2-8 mm/day with idle periods in winter months. Total ET_c from literature on Kleingrass ranges 450-760 mm/year (Mayberry and Meister, 2003), while values from remote sensing observations are highly variable, sometimes exceeding 1500 mm/year (Figure 38). LCRAS total ET_c was ∼1000 mm/year (Table 18).

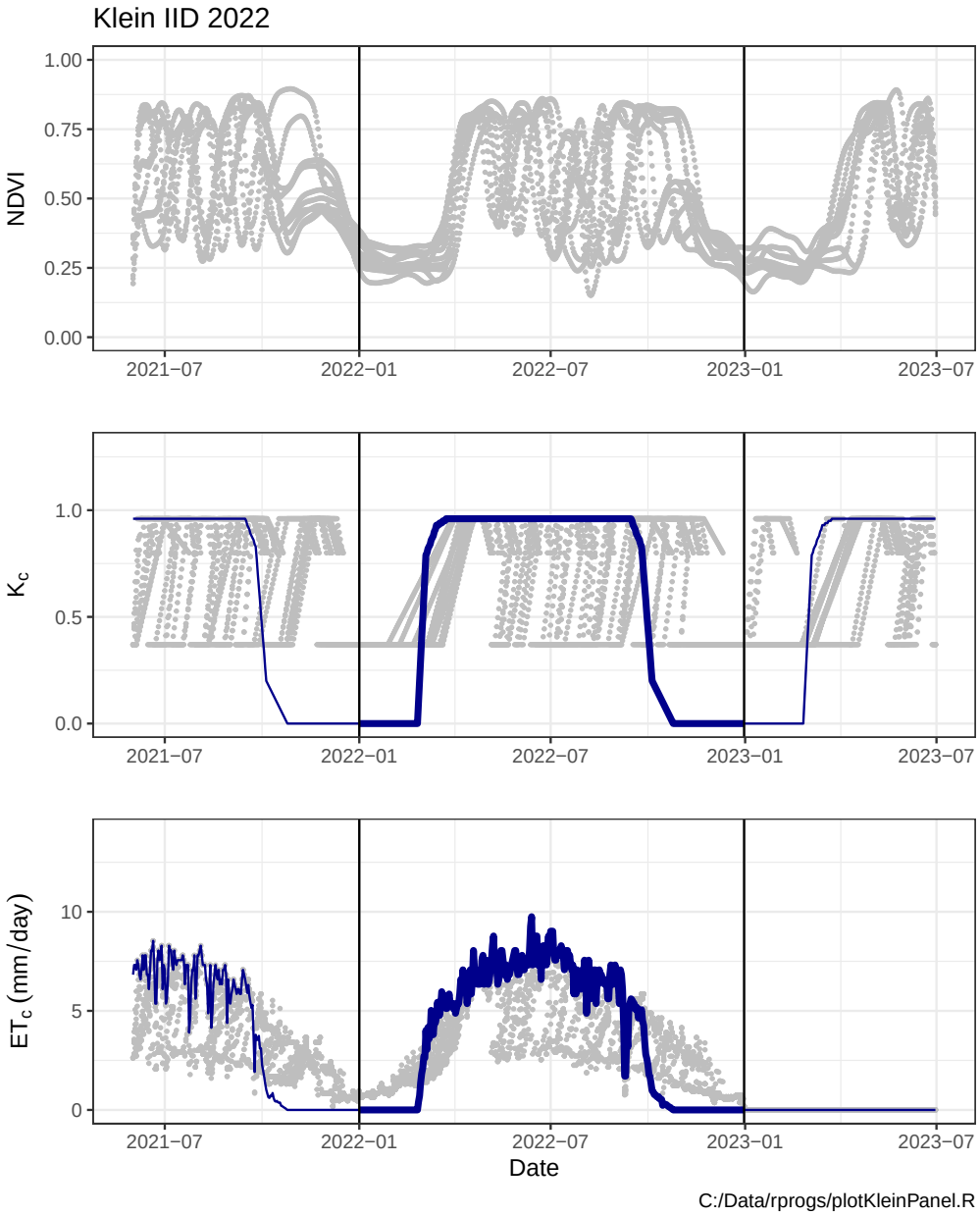

Figure 37. Kleingrass ET_c estimation from NDVI. Shown are examples of filtered and smoothed NDVI data over Kleingrass fields in IID (top), conversion of NDVI to K_c curves (middle), and computation of daily ET_c from K_c and weather station based ET_{os} (bottom). Gray symbols illustrate NDVI-based modeling, blue lines show the corresponding LCRAS estimates.

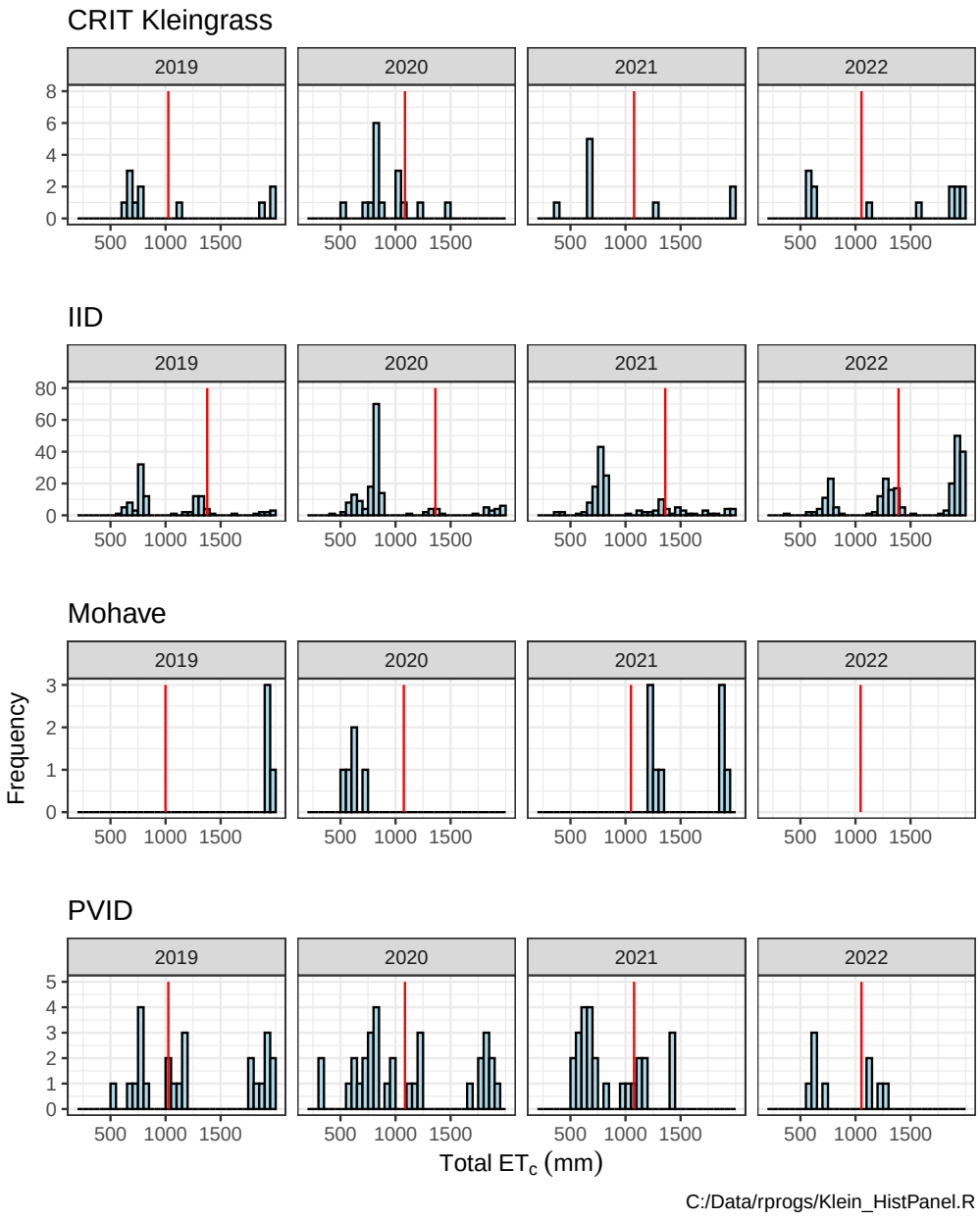

Figure 38. Total ET_c for Kleingrass 2019-2022 (blue histograms) compared with LCRAS (red lines).

Table 19. Lettuce ET_c (mm/year).

	Year			
Area	2019	2020	2021	2022
Yuma	-	240	294	246

5.10 Lettuce

Lettuce is an annual leafy green crop grown in all LCRAS districts except Mohave. However, Yuma was the only district with significant field validation visits. Note that NDVI for lettuce abuts spring-summer crops (commonly durum wheat). Because lettuce growth stages span year boundaries, assessment of ET_c normally includes two different plantings: the end of the prior season's planting and the initial part of the subsequent planting (Figure 39, middle panel). Daily ET_c ranges 1-4 mm/day. NDVI data confirm that lettuce is planted in fall to early winter, usually harvested by late winter, though sometimes as late as mid-spring (Figure 40). Total ET_c for lettuce is expected to be ∼280 mm (French et al., 2024), a value in agreement with modal values for fields observed in 2020-2022 (Table 19). Variability of total ET_c , however, is high, ranging 100-500 mm (Figure 41). LCRAS modeling estimates total ET_c to be ∼170 mm/year.

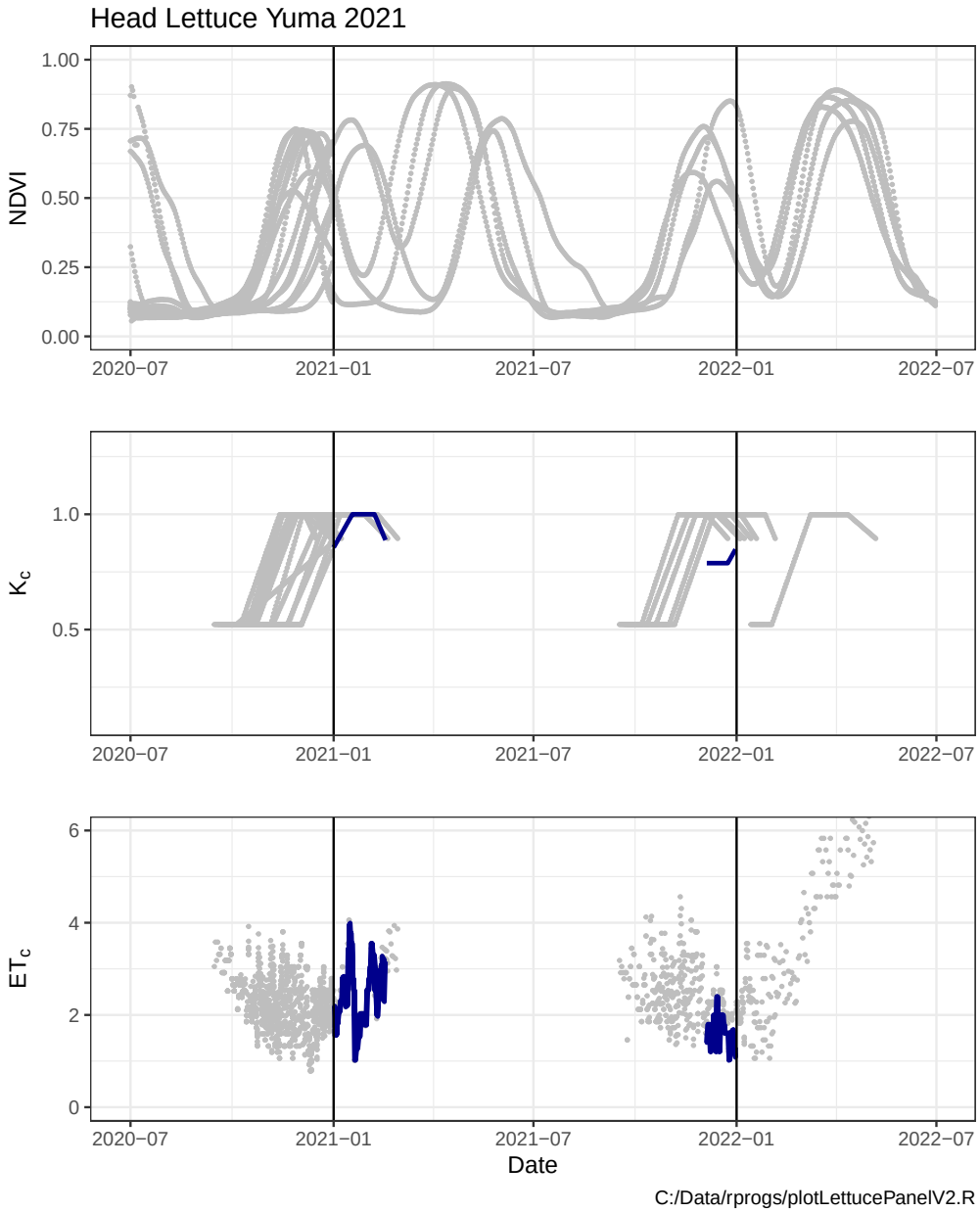

Figure 39. Lettuce ET_c estimation from NDVI. Shown are examples of filtered and smoothed NDVI data over lettuce fields in Yuma (top), conversion of NDVI to K_c curves (middle), and computation of daily ET_c from K_c and weather station based ET_{os} (bottom). Gray symbols illustrate NDVI-based modeling, blue lines show the corresponding LCRAS estimates.

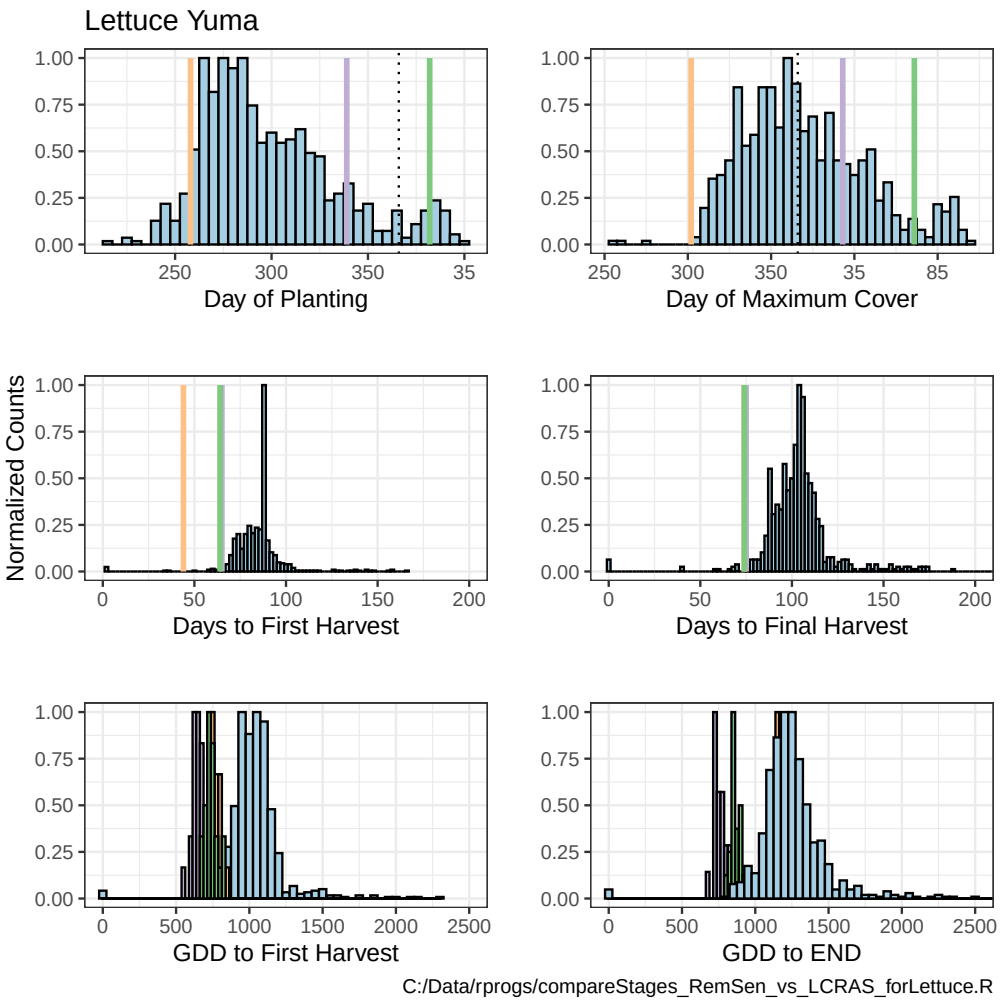

Figure 40. Growth stage estimation from NDVI and LCRAS for lettuce. The blue histograms represent estimates derived from NDVI data. Orange, blue, and green lines denote LCRAS events for three classes: Fall Early, Fall Late/Spring Early (combined here as 'Winter' from those listed in Table 4, page 18), and Spring Late. The same colors on the histograms represent the distribution of Growing Degree Days (GDD) obtained using Yuma Valley weather data and GDD temperature limits of 4.5-28°C.

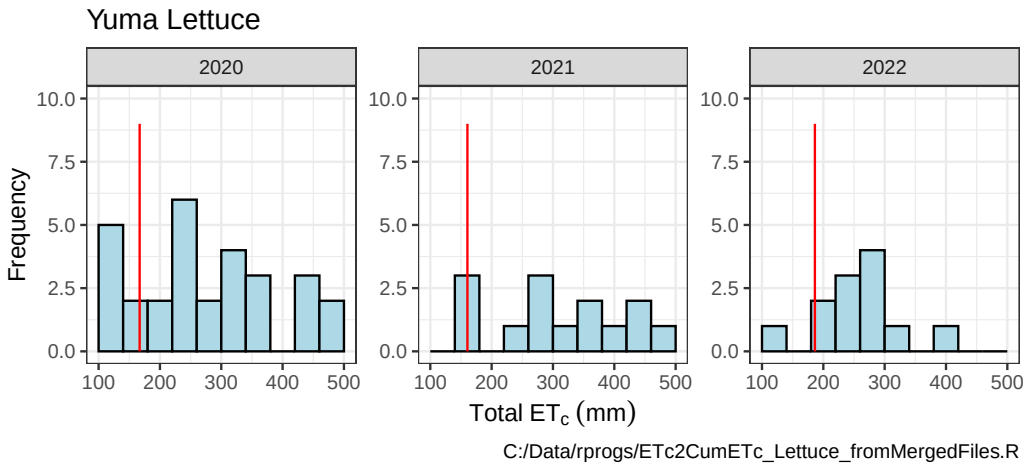

Figure 41. Total ET_c (mm/year) for lettuce at Yuma 2020-2022 compared with LCRAS. See 2019-2021 ET_c distributions modeled with Sentinel 1 radar in Figure 57.

Table 20. Olives ET_c (mm/year).

	Year			
Area	2019	2020	2021	2022
IID	1184	1194	1203	1234
Mohave	-	-	1339	1277
Yuma	1192	1239	1231	1245

5.11 Olives

Olives are a long-lived evergreen tree crop observed mostly in IID, and in lesser amounts in Coachella, Mohave, and Yuma. Water used is 1000-1100 mm, with about 700 mm representing transpiration (Beede and Goldhamer, 2005; Ramos and Santos, 2009). NDVI patterns, as for citrus and dates, have a seasonal quadratic pattern with maximum values in the winter and minimum values mid-summer (Figure 42). Crop coefficients have low annual variability, and are approximately half of ET_{os}. This means that daily ET_c patterns follow ET_{os} patterns and range 1-5 mm/-day. The high NDVI variability could be partitioned to differentiate and refine daily K_c values if relationships between tree maturity and condition were available. Growth stage modeling returned total ET_c values ranging ∼1200-1300 mm (Table 20), while LCRAS models returned ∼900 mm (Figure 43).

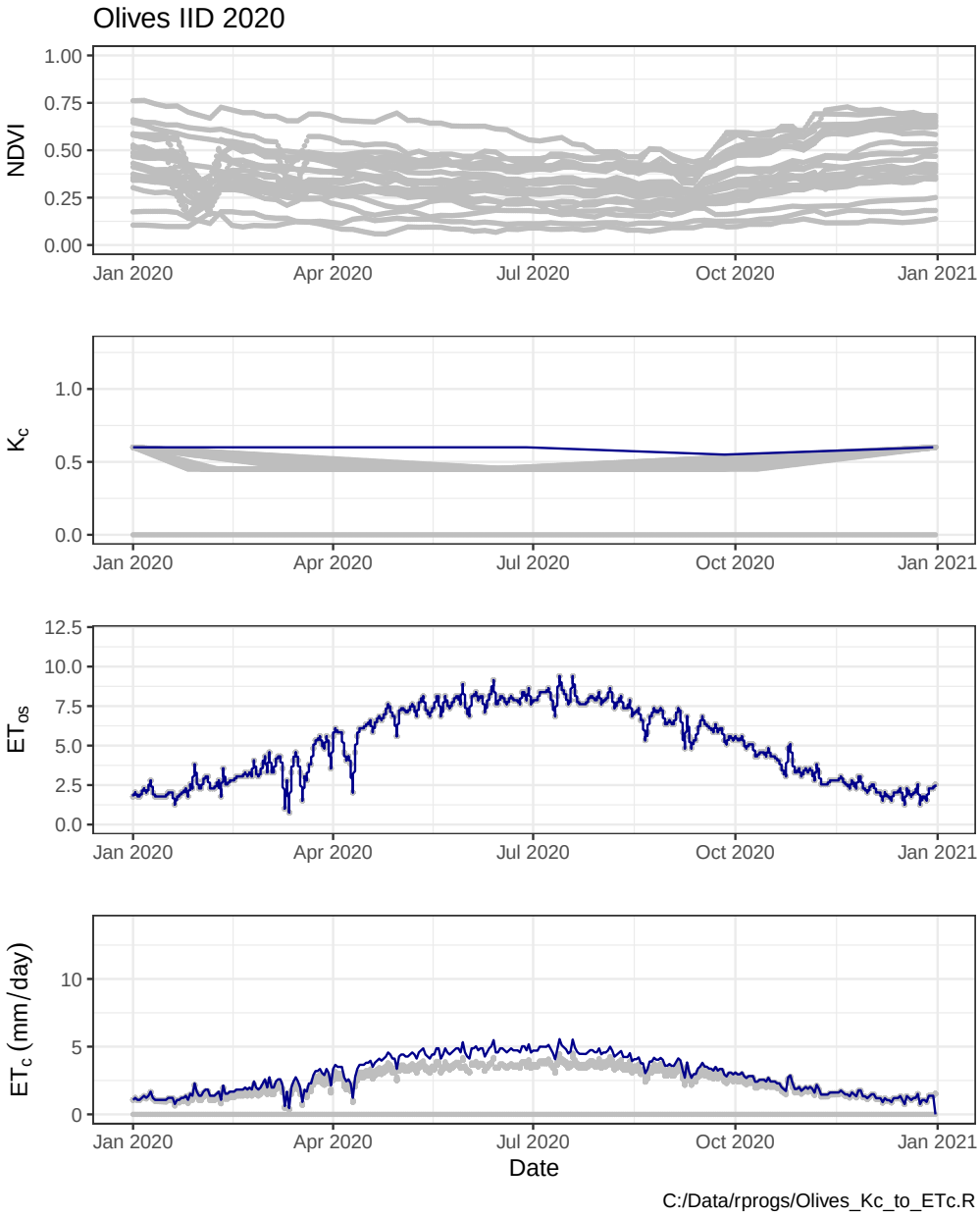

Figure 42. Olives ET_c estimation from NDVI. Shown are examples of filtered and smoothed NDVI data over olive fields in IID (top), conversion of NDVI to K_c curves (second), reference evapotranspiration (third), and computation of daily ET_c from K_c and weather station based ET_{os} (bottom). Gray symbols illustrate NDVI-based modeling, blue lines show the corresponding LCRAS estimates.

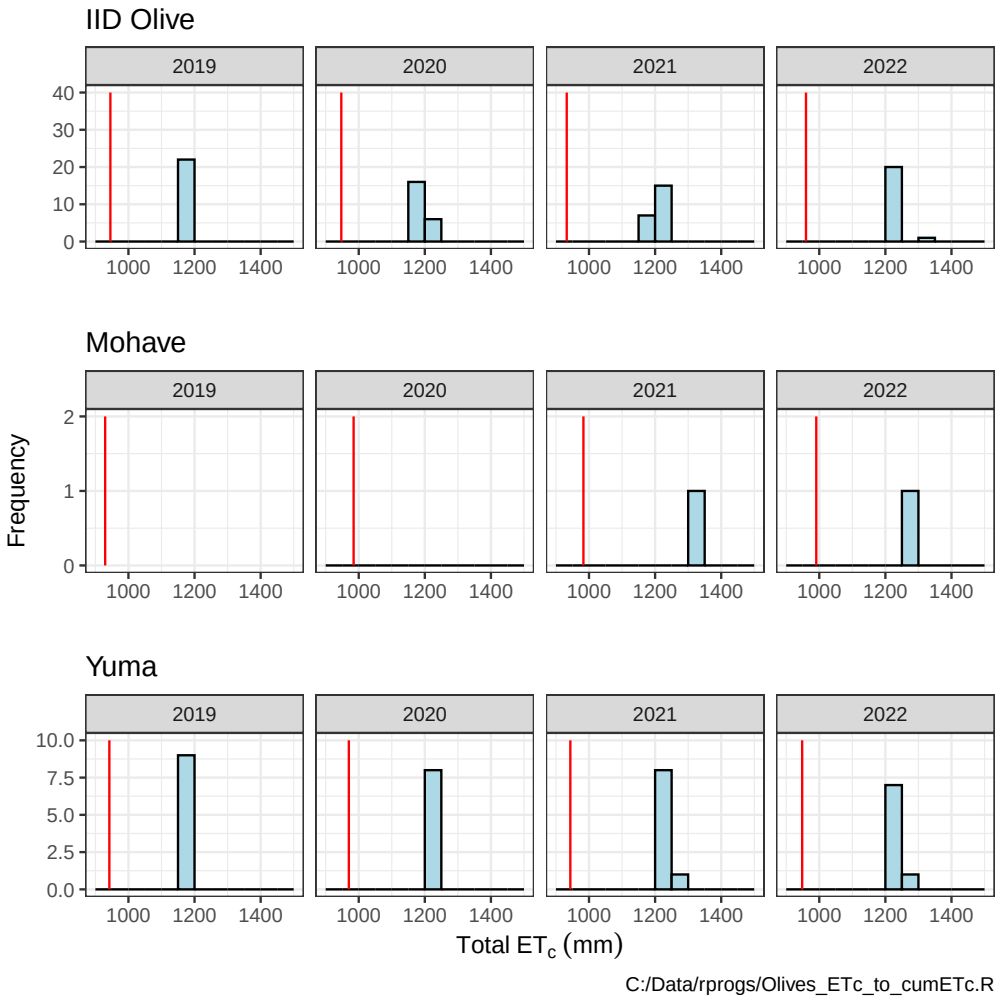

Figure 43. Total ET_c for olive 2019-2022 (blue histograms) compared with LCRAS (red lines). No observations were available at Mohave in 2019 and 2020.

Table 21. Sudangrass ET_c (mm/year).

	Year			
Area	2019	2020	2021	2022
CRIT	1438	1808	1738	1775
IID	1478	1586	1631	1626
Yuma	1379	1421	1335	1394

5.12 Sudangrass

Sudangrass is a summer annual crop, planted in spring. Water used is 700-1100 mm for four peak months (Meister, 2004b). Grown for pasture, green chop, silage, and hay (Knowles and Ottman, 2015), it is cut ∼4-5 times each season. Reclamation's K_c curve does not distinguish cutting events. This report follows Reclamation practice and develops growth stages assuming a single average growing season. A sample of NDVI data from CRIT (Figure 44) showed 2 main cutting events. Daily ET_c ranged 2-11 mm/day. There were few observations most years except for 2022. Generally total ET_c ranged 1500-2000 mm/year (Table 21), while LCRAS ET_c was ∼1000 mm/year (Figure 45).

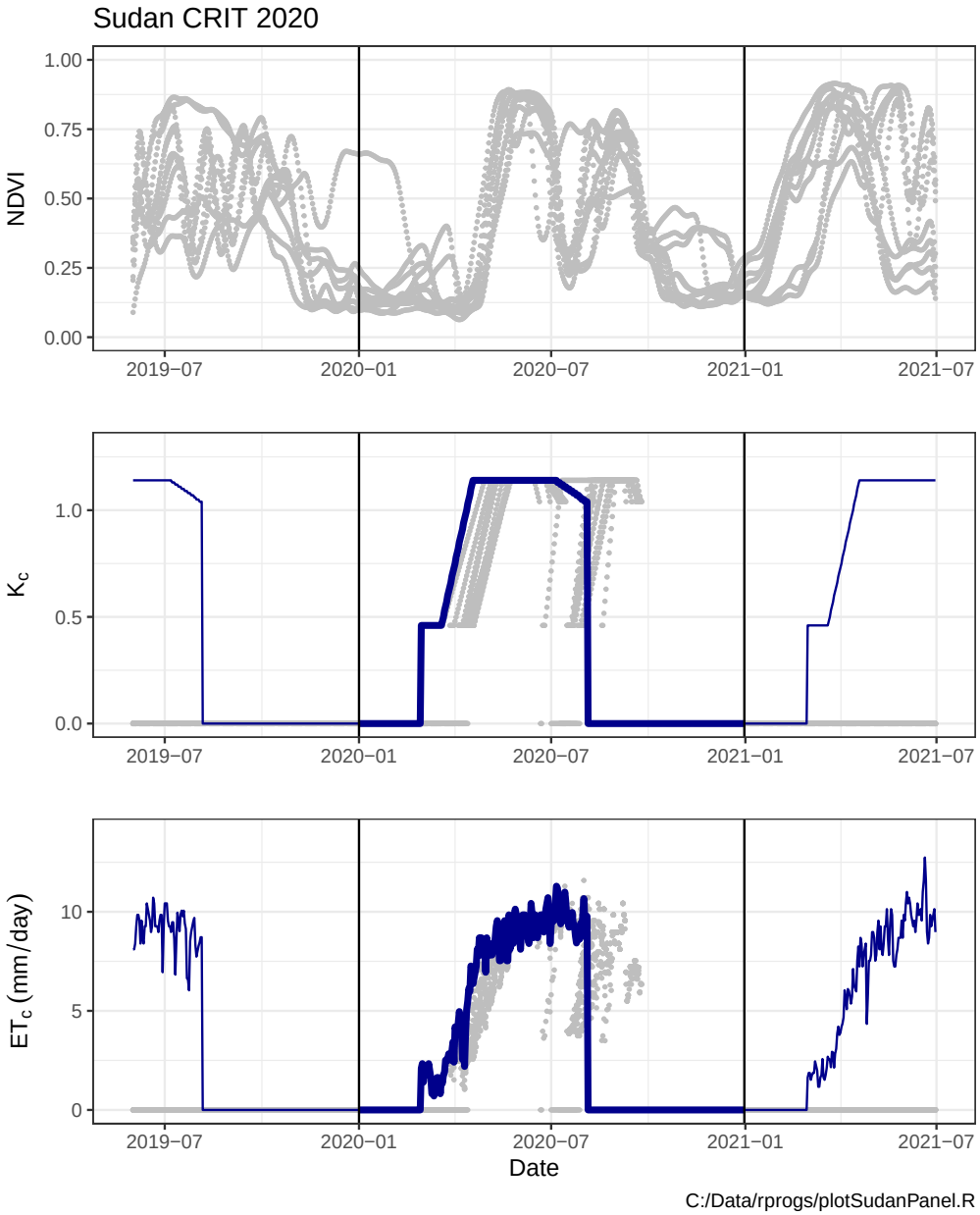

Figure 44. Sudangrass ET_c estimation from NDVI. Shown are examples of filtered and smoothed NDVI data over Sudangrass fields in CRIT (top), conversion of NDVI to K_c curves (middle), and computation of daily ET_c from K_c and weather station based ET_{os} (bottom). Gray symbols illustrate NDVI-based modeling, blue lines show the corresponding LCRAS estimates.

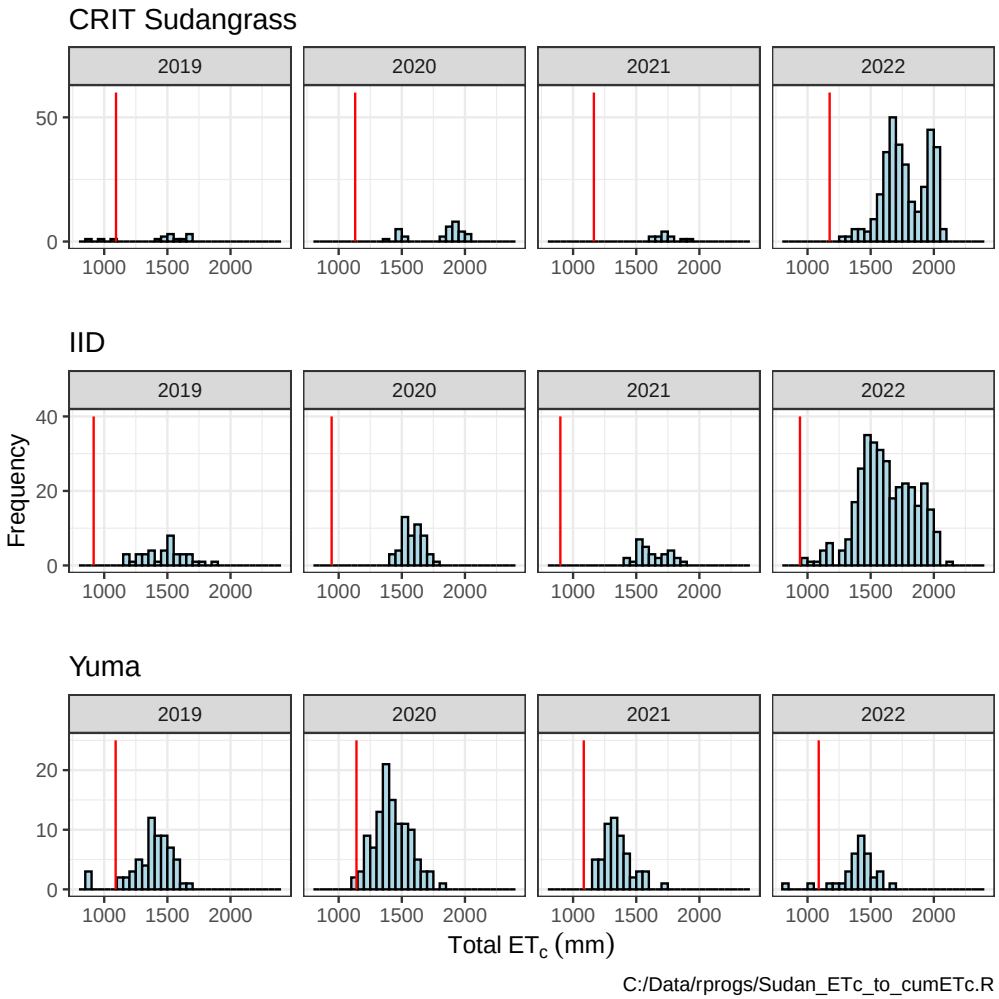

Figure 45. Total ET_c (mm/year) for Sudangrass 2019-2022 (blue histograms) compared with LCRAS (red lines). Observations were sparse in 2019-2021.

Table 22. Sugar beet ET_c (mm/year).

	Year			
Area	2019	2020	2021	2022
IID	940	816	929	847

5.13 Sugar beet

Sugar beet, solely observed in IID, is a long season crop, typically planted September-October and harvested in July (Kaffka and Tharp, 2013; Panella et al., 2014). NDVI data at IID indicate planting is a bit later, mainly October-November, while harvest is dominantly in June (Figure 46). Daily ET_c ranges 2.5-10 mm/day, with peak amounts just prior to harvest. Estimated total ET_c from growth stage modeling was highly variable, ranging from less than 500 mm/year up to 1900 mm/year (Figure 48). Total ET_c at IID for 2019-2022 averaged ∼900 mm/year (Table 22). LCRAS ET_c was estimated to be ∼1700 mm/year. Water required depends on yield and environment (Hills et al., 1990) with upper limits ranging from ∼1100 mm/year (Erie et al., 1982) to 1208 mm/year (Hills et al., 1990).

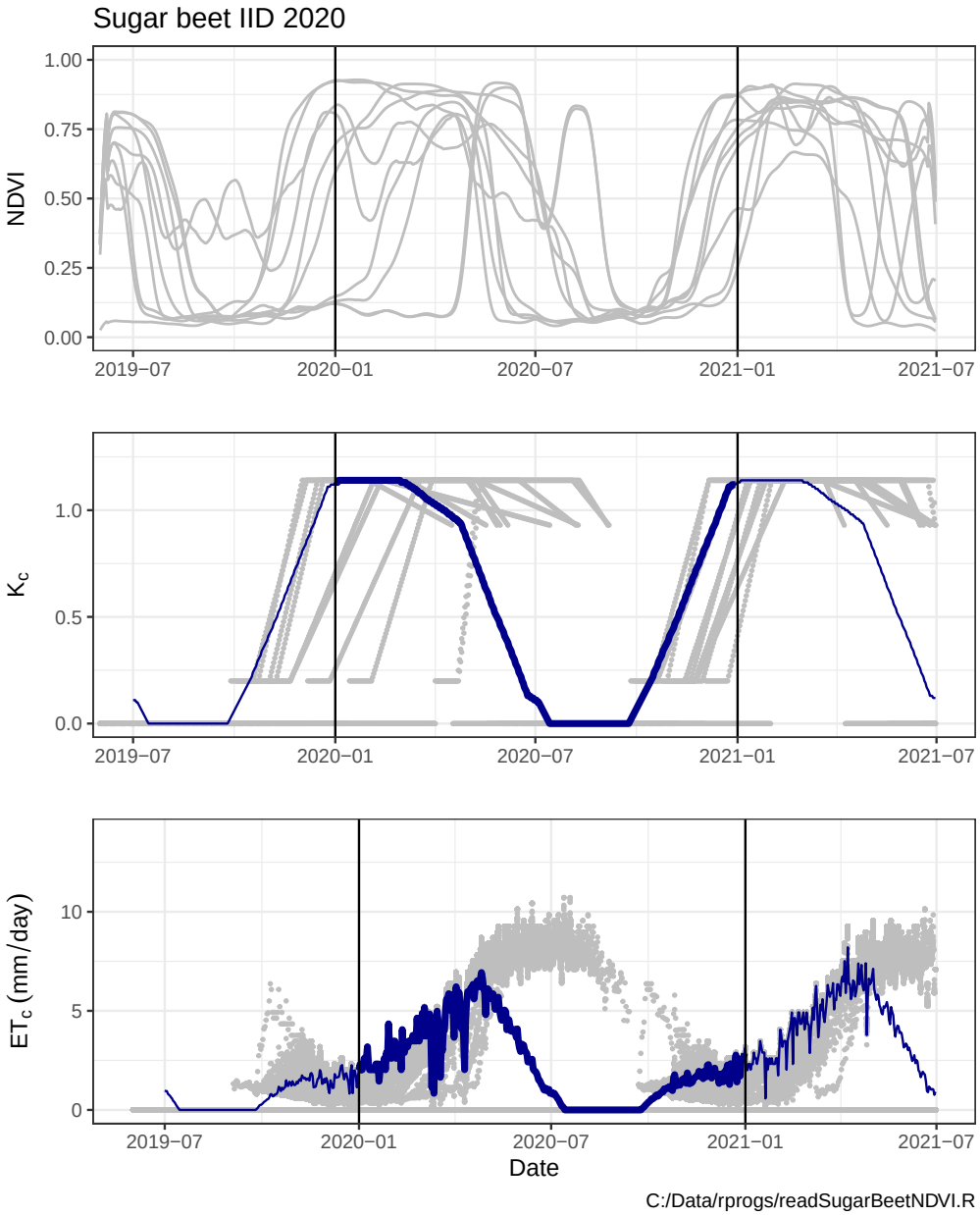

Figure 46. Sugar beet ET_c estimation from NDVI. Shown are examples of filtered and smoothed NDVI data over sugar beet fields in IID (top), conversion of NDVI to K_c curves (middle), and computation of daily ET_c from K_c and weather station based ET_{os} (bottom). Gray symbols illustrate NDVI-based modeling, blue lines show the corresponding LCRAS estimates.

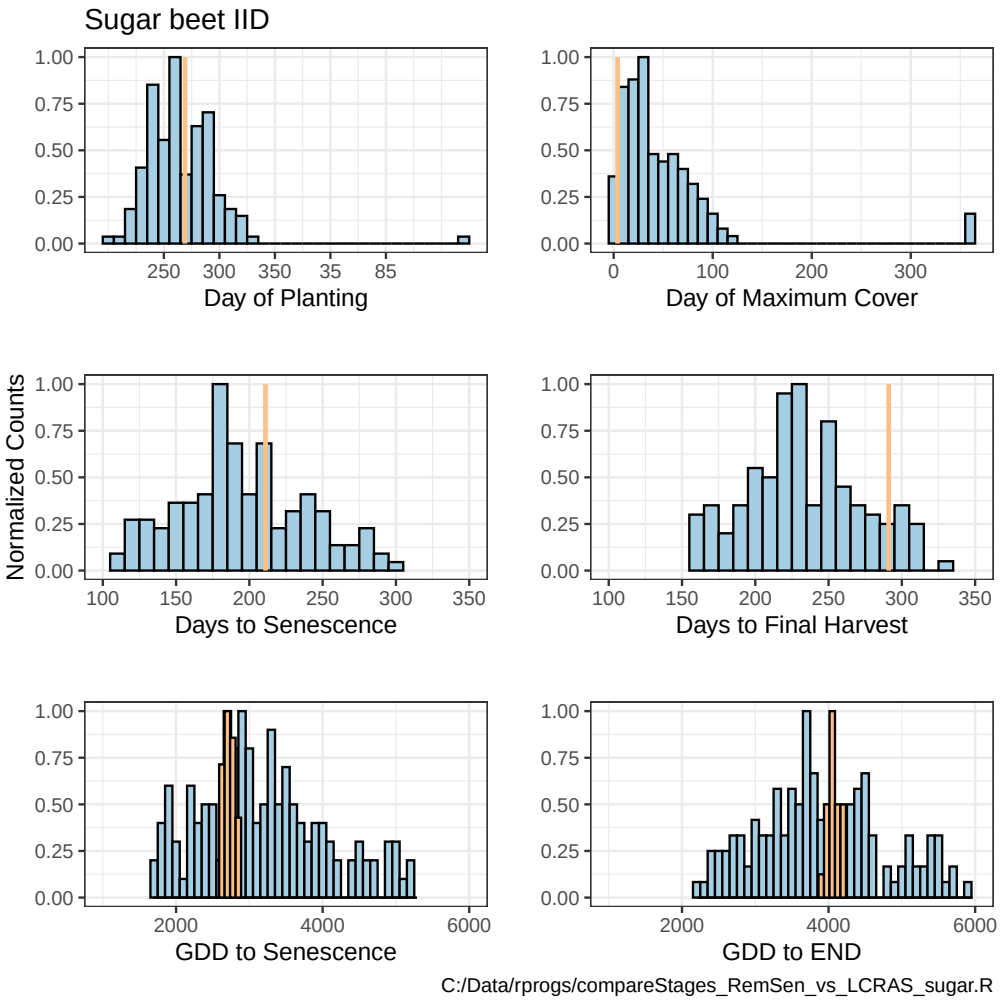

Figure 47. Growth stage estimation from NDVI and LCRAS for sugar beet. The blue histograms represent estimates derived from NDVI data. Orange lines denote LCRAS events and orange histograms represent the distribution of Growing Degree Days (GDD) obtained using the CIMIS Calipatria/Mulberry weather data and GDD temperature limits of 1.1-30°C.

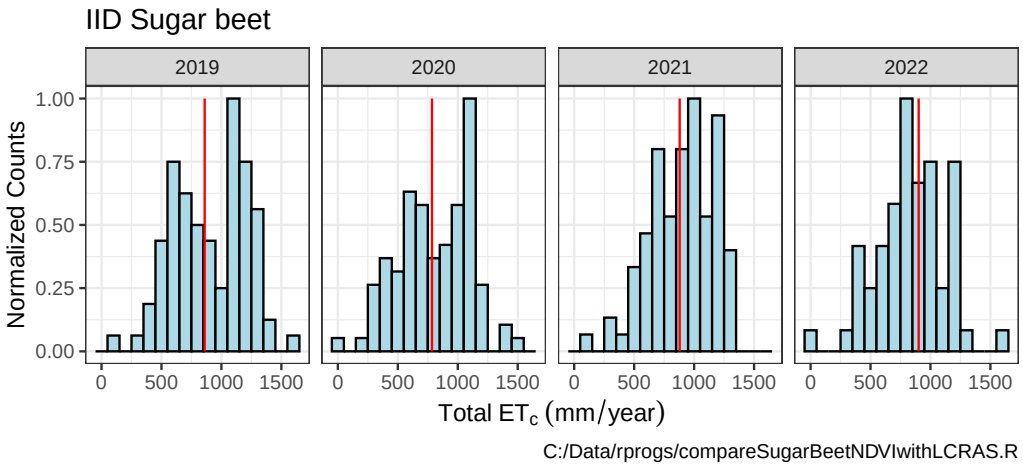

Figure 48. Total ET_c (mm/year) for sugar beet 2019-2022 (blue histograms) compared with LCRAS (red lines).

Table 23. Wheat Annual ET_c (mm/year).

	Year			
Area	2019	2020	2021	2022
CRIT	429	424	492	497
IID	437	491	496	509
Mohave	382	418	501	501
PVID	448	478	494	491
Yuma	472	438	499	485

5.14 Wheat

Wheat is an annual crop typically planted between December and early February (Meister, 2004b) and was observed for all irrigation districts. Consumptive water use by wheat is ∼600 mm a year (Husman and Ottman, 2015; French et al., 2020). Planting practice was confirmed by NDVI observations (Figure 49). Daily ET_c ranges 1-8 mm/day. Total ET_c was usually 400-600 mm/year (Table 23), compared with LCRAS estimates at 800 mm/year (Figure 51). Observations at Coachella were few and are not shown.

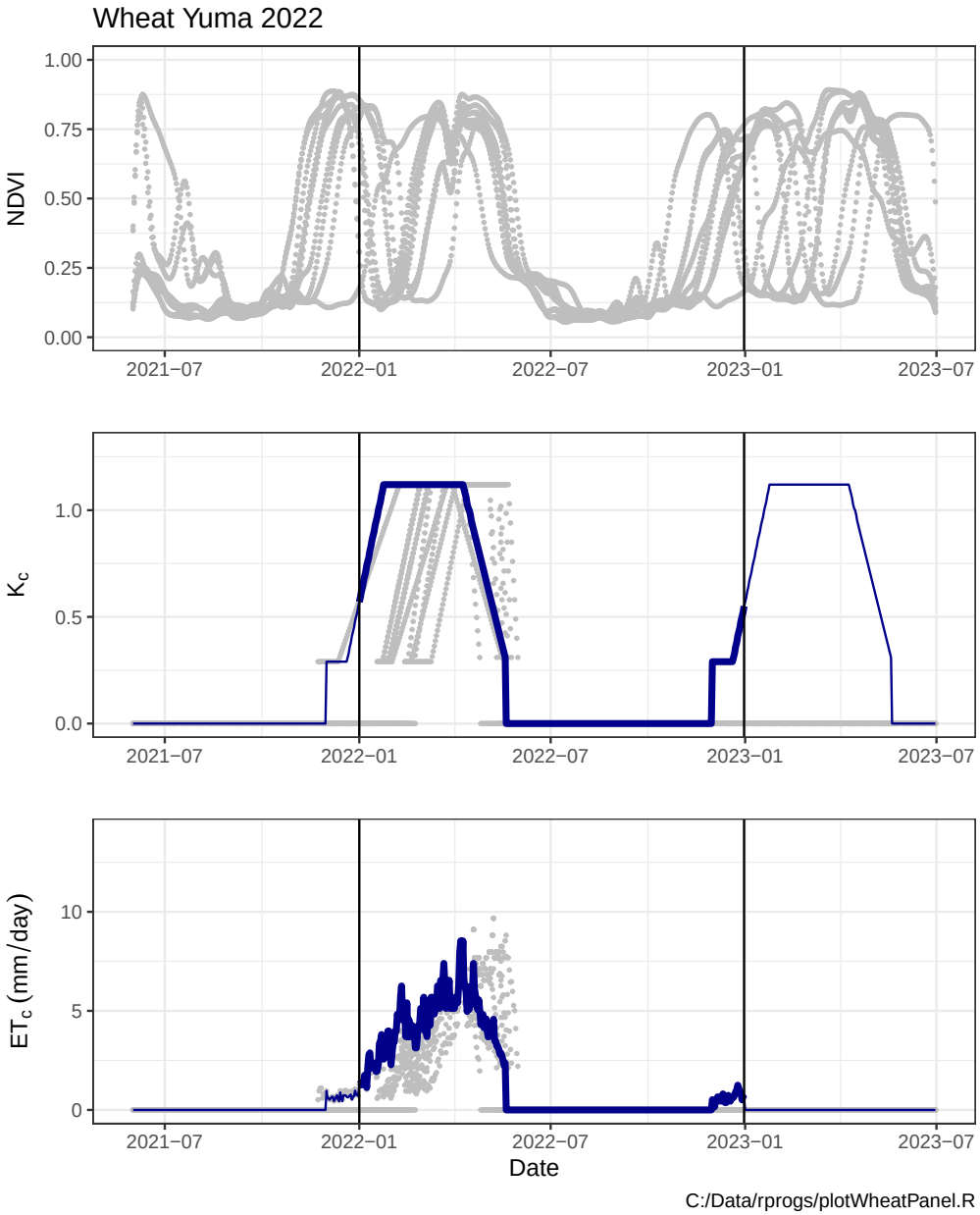

Figure 49. Wheat ET_c estimation from NDVI. Shown are examples of filtered and smoothed NDVI data over wheat fields in Yuma (top), conversion of NDVI to K_c curves (middle), and computation of daily ET_c from K_c and weather station based ET_{os} (bottom). Gray symbols illustrate NDVI-based modeling, blue lines show the corresponding LCRAS estimates.

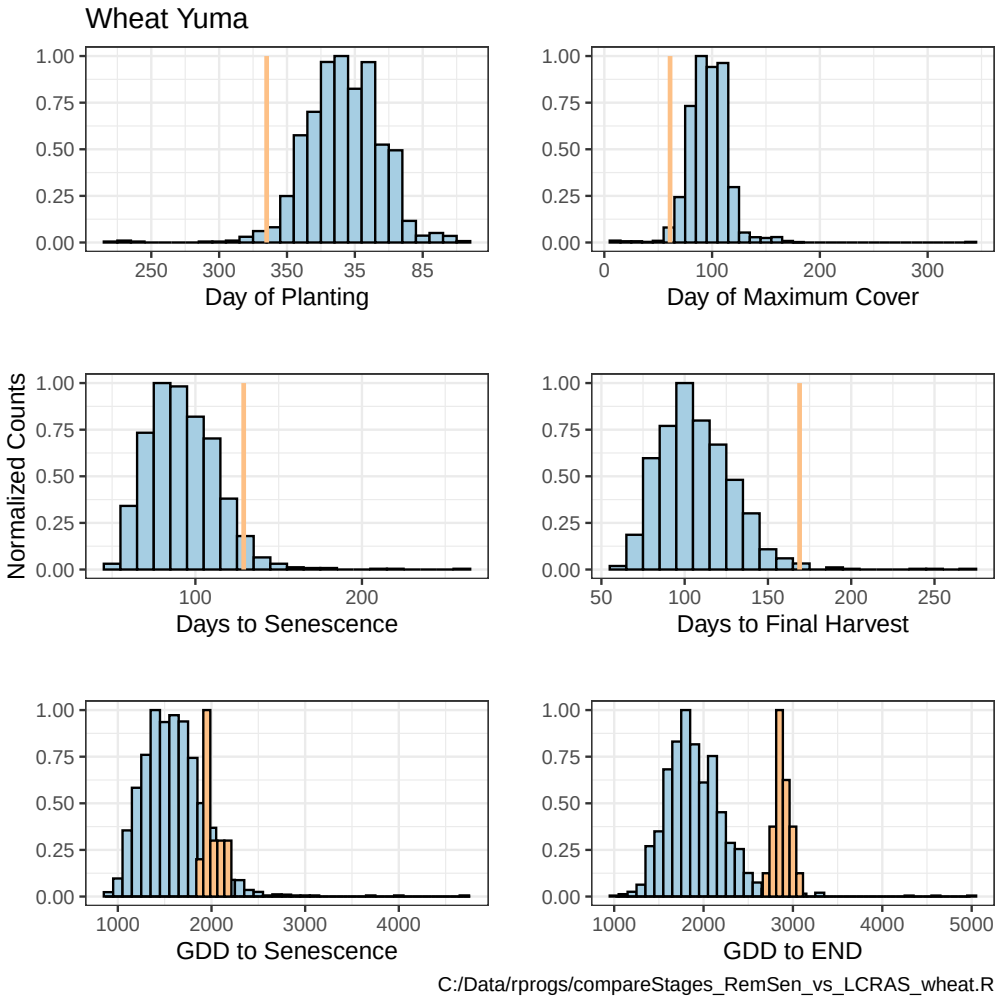

Figure 50. Growth stage estimation from NDVI and LCRAS for wheat at Yuma, 2019-2022. The blue histograms represent estimates derived from NDVI data. Orange lines denote LCRAS events and orange histograms represent the distribution of Growing Degree Days (GDD) obtained using Yuma Valley weather data and GDD temperature limits of 0-30°C

.

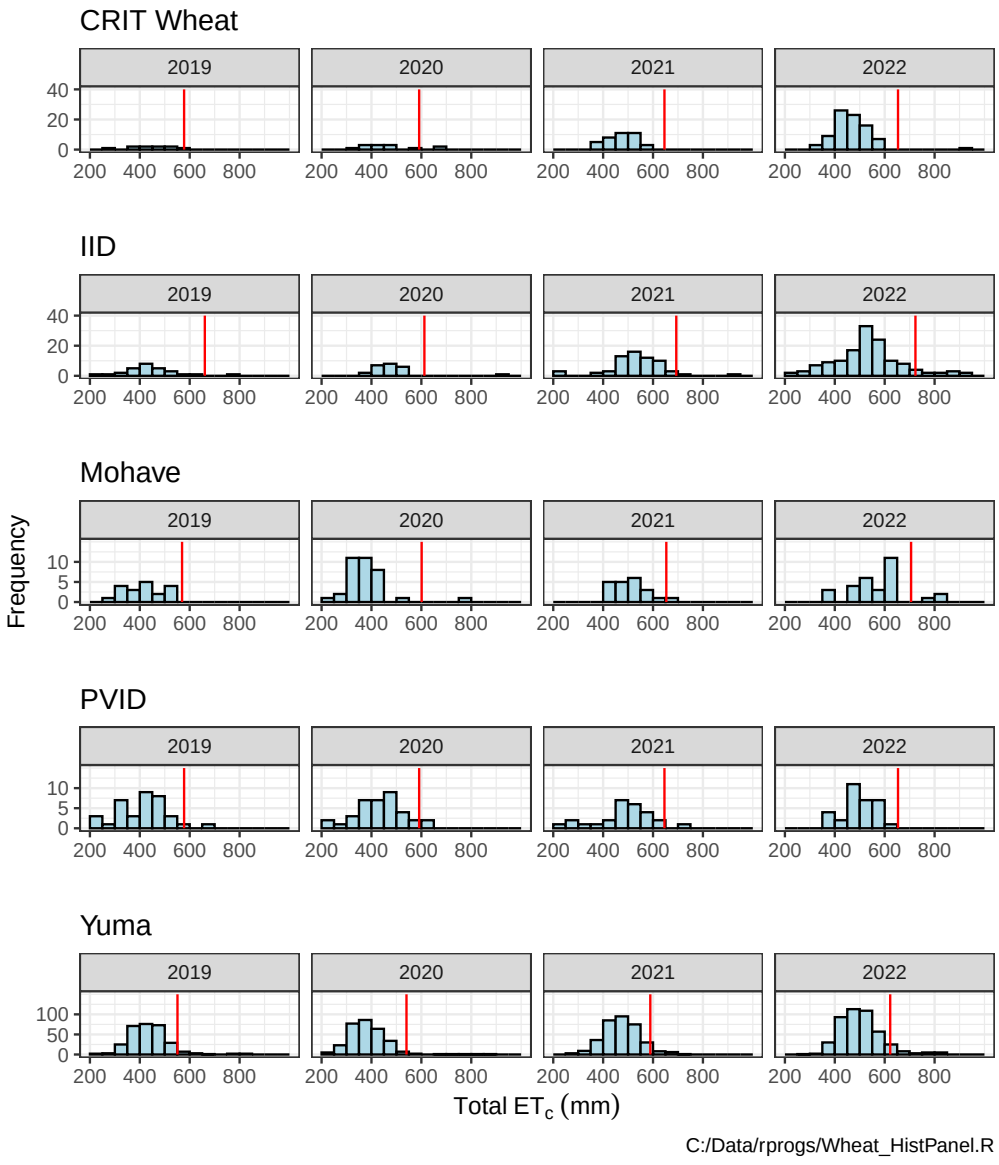

Figure 51. Total ET_c (mm/year) for wheat 2019-2022 (blue histograms) compared with LCRAS (red lines).

6 Objective 3: Compare ET_c Estimates

This section presents summary numerical results of crop ET_c estimates from NDVI models and LCRAS. Annual total ET_c values as provided by LCRAS are listed in Tables 32-34 (pages 108- 110).

Corresponding graphical displays are shown by crops in section 5.

6.1 Coachella

The Coachella area was analyzed for 6 main crops: dates, grapes, citrus, Bermudagrass /Kleingrass , carrots, and alfalfa. Dates, grapes, citrus, and Bermudagrass /Kleingrass are relatively important water consumers at Coachella, while carrots and alfalfa are less important.

Area annual ET_c values, by year, are listed in Tables 24 and 25. Shown are LCRAS estimates, followed by statistical ET_c values from NDVI modeling: first-quartile(Q1), median, third-quartile (Q3), number of fields (N), and the difference between the NDVI median (Δ) and the LCRAS value. Positive and negative Δ values respectively denote over- and under-estimated total ET_c relative to LCRAS ET_c .

Estimated ET_c for dates, mature citrus, and alfalfa are approximately the same for LCRAS and the NDVI-based model. Remote sensing modeling suggests that LCRAS under-estimates ET_c for grapes, young citrus, Bermudagrass /Kleingrass , but over-estimates carrot ET_c .

For dates, total ET_c values were $\sim$1700 mm/year and showed little variability. Regardless of tree maturity, NDVI-based estimates were about 10-30 mm less than LCRAS, a relative difference less than 1%. The low variability is a consequence of the minimal range of K_c values (0.82-0.98) that do not depend on tree maturity. Characterization of crop coefficients similar to what is done for citrus would increase field-to-field variability and potentially increase accuracy of consumptive water use.

Table grapes, dominant only at Coachella, appear to use $\sim$1100 mm per year based on NDVI-based estimates. LCRAS ET_c estimates $\sim$950 mm, an under-estimation difference of $\sim$20%. The greater amount from NDVI modeling is due to the longer peak growing season than set nominally by LCRAS. To illustrate, examples from 30 Coachella grape fields (Figure 52) show that the duration and dominant growth period modeled by the LCRAS K_c curve (red line) is shorter and earlier in each year than observed by satellites.

NDVI modeling of citrus at Coachella shows minimal differences for mature trees, where total ET_c is $\sim$1100 mm/year. However, LCRAS ET_c is significantly less

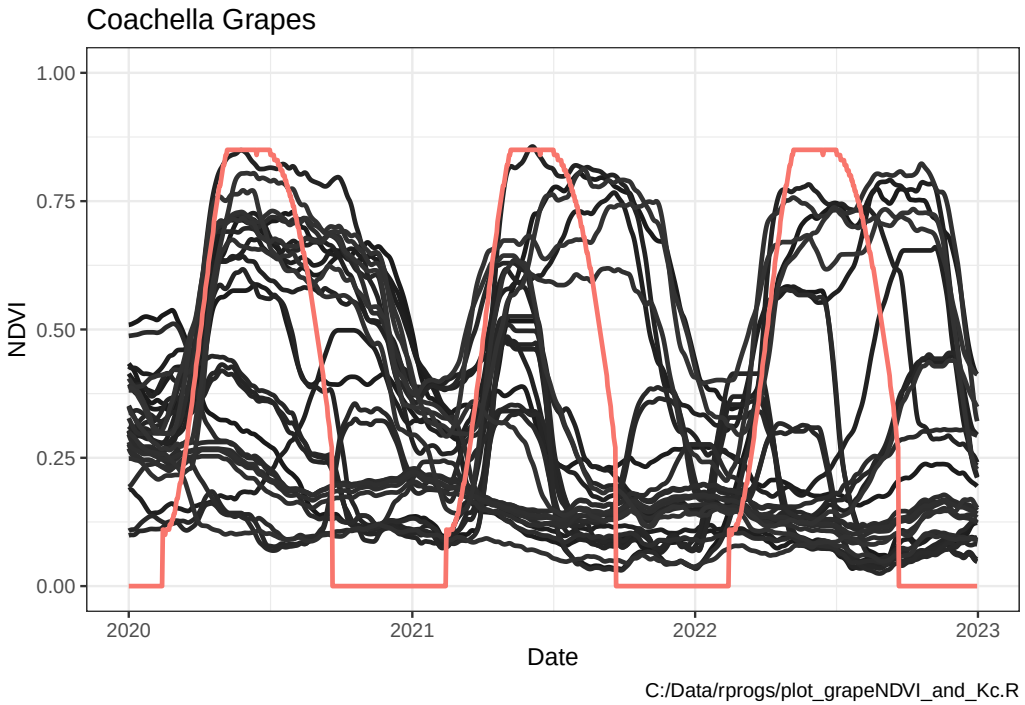

Figure 52. NDVI for grapes at Coachella (gray lines). Red line denotes LCRAS K_c curve. Generally the observed growing season for grapes is longer and ends later than modeled by LCRAS.

than NDVI-based ET_c, by $\sim$300 mm. This modeling difference is due to the adaptive K_c approach, where early winter NDVI values are used to adjust K_c curves.

NDVI modeling of Bermudagrass and Kleingrass using the NDVI-threshold of 0.5 indicates total ET_c is $\sim$1500-1600 mm/year in contrast to LCRAS estimates of $\sim$1375 mm/year. Because the NDVI signatures over these fields are highly variable, this modeling difference is tentative.

LCRAS modeling of carrots was $\sim$1200 mm/year, a value derived using a spring small vegetable K_c curve. Analysis of growth stages by NDVI indicates total ET_c is likely closer to 300-400 mm/year.

LCRAS and NDVI-based models for alfalfa are usually in close agreement, with total ET_c $\sim$1600 mm/year.

Table 24. Coachella ET_c Results Part 1

Crop	Year	LCRAS	NDVI				Δ
			Q1	Median	Q3	N	
Dates-Mature	2019	1770	1745	1746	1749	15	-24
	2020	1778	1749	1758	1765	164	-20
	2021	1787	1762	1765	1767	317	-22
	2022	1819	1780	1785	1789	629	-34
Dates-Young	2019	1770	1746	1752	1759	149	-18
	2020	1778	1756	1765	1771	177	-13
	2021	1787	1762	1767	1773	207	-20
	2022	1819	1784	1792	1799	190	-26
Dates-Declining	2019	1770	1729	1734	1741	7	-36
	2020	1778	1727	1737	1755	17	-41
	2021	1787	1755	1760	1769	16	-26
	2022	1819	1776	1787	1793	23	-32
Grapes	2019	945	1069	1158	1239	656	213
	2020	947	1080	1146	1207	515	199
	2021	933	1009	1082	1181	439	149
	2022	960	1006	1111	1227	411	151
Citrus-Mature	2019	1113	1099	1103	1105	294	-10
	2020	1119	1101	1109	1114	263	-10
	2021	1129	1117	1122	1124	294	-8
	2022	1150	1136	1137	1138	217	-15
Citrus-Young	2019	666	771	966	1103	201	299
	2020	670	760	1031	1108	203	361
	2021	676	719	999	1122	232	323
	2022	688	800	1135	1138	217	446
Citrus-Declining	2019	780	807	1098	1104	12	319
	2020	784	877	1107	1109	12	323
	2021	791	991	1120	1122	13	328
	2022	806	1135	1136	1138	10	330

Table 25. Coachella ET_c Results Part 2

Crop	Year	LCRAS	NDVI				Δ
			Q1	Median	Q3	N	
Bermudagrass /Kleingrass	2019	1378	1516	1600	1656	52	222
	2020	1361	1295	1469	1523	36	108
	2021	1361	1282	1507	1607	34	147
	2022	1391	1589	1657	1684	44	266
Carrot	2019	682	291	458	600	40	-224
	2020	715	135	353	531	29	-362
	2021	743	207	406	613	61	-337
	2022	766	285	464	621	31	-302
Alfalfa	2019	1583	1512	1558	1600	10	-25
	2020	1595	1546	1554	1566	11	-41
	2021	1608	1560	1578	1635	8	-30
	2022	1624	1600	1606	1626	11	-18

6.2 CRIT

The CRIT area was analyzed for five crops: alfalfa, Bermudagrass /Kleingrass , wheat, cotton, and Sudangrass . Outcomes from the study showed that ET_c estimates for alfalfa and wheat were significantly less with NDVI-based modeling than with LCRAS, while remote sensing of cotton and Sudangrass indicated higher ET_c values (Table 26). The Bermudagrass /Kleingrass aggregate estimates were about the same with either approach.

The most notable disagreement lies with Sudangrass , caused by LCRAS' growth duration being too short and by its planting date being too early (Figure 53). This exemplifies that planting practices change year-to-year, and those changes are resolved with remote sensing.

Similar discrepancies between actual and presumed LCRAS field management explain ET_c differences with cotton and wheat. For cotton the growing periods start earlier and last longer than LCRAS models (Figure 31). For wheat, the opposite applies: actual plantings are later, and growing periods are shorter than for LCRAS (Figure 50).

Lower total ET_c NDVI-based estimates for alfalfa are an outcome from the number of actual cuttings, which mostly range 5-10 cuttings per year (Figure 14) vs. the LCRAS standard of 9 cuttings per year.

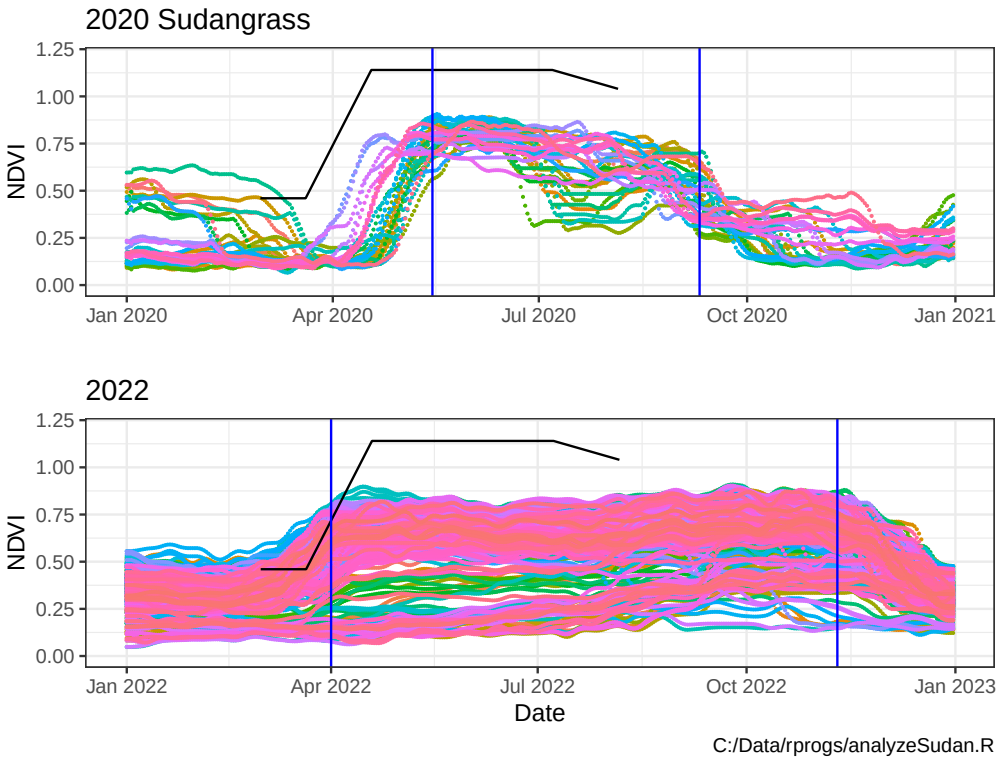

Figure 53. Comparing Sudangrass growth at CRIT in 2020 and 2022. Shown are NDVI traces for all sites (340 in 2022). The approximate duration of the MID stage from NDVI dates were 118 and 223 days for 2020 and 2022 (vertical blue lines), respectively. The black line denotes the LCRAS K_c curve. Sudangrass growth duration with the LCRAS model are 80 days for MID and 158 days total season.

Table 26. CRIT ET_c Results

Crop	Year	LCRAS	NDVI				Δ
			Q1	Median	Q3	N	
Alfalfa	2019	1647	1519	1550	1563	80	-97
	2020	1767	1618	1655	1673	83	-112
	2021	1794	1632	1671	1701	127	-123
	2022	1728	1553	1603	1633	165	-125
Bermudagrass /Kleingrass	2019	1025	1039	1107	1174	93	82
	2020	1085	832	1175	1340	110	90
	2021	1077	1017	1155	1262	100	78
	2022	1054	755	1020	1122	91	-34
Wheat	2019	578	383	429	497	17	-149
	2020	591	387	424	460	34	-167
	2021	646	446	492	520	92	-154
	2022	653	459	497	544	104	-156
Cotton	2019	920	974	1046	1124	50	126
	2020	976	1004	1180	1338	10	204
	2021	946	949	1006	1145	26	61
	2022	908	920	1069	1140	26	161
Sudangrass	2019	1093	1427	1524	1622	14	430
	2020	1131	1689	1888	1941	31	757
	2021	1165	1681	1724	1782	12	559
	2022	1175	1653	1744	1954	340	569

6.3 IID

The IID area was analyzed for five crops: combined Bermudagrass /Kleingrass , alfalfa, citrus (mature and young), Sudangrass and sugar beet. Outcomes from the study showed polarized results where total ET_c were sometimes less than LCRAS and other time significantly greater than LCRAS (Table 27). Generally Bermudagrass /Kleingrass , alfalfa, mature citrus, and sugar beet crop ET_c estimates were about the same for either the NDVI or LCRAS approach. Assessment of the growth stage identification for sugar beet showed no large bias (Figure 47). Young citrus, Sudangrass , and sugar beet ET_c estimates, however, differed by large amounts.

Increased ET_c for young citrus results from the use of the adaptive K_c approach. For these sites, the mean winter-time NDVI values often indicated that the fields were more mature.

Increased ET_c for Sudangrass occurred for the same reasons as noted previously for the CRIT area: growing seasons were longer than modeled by LCRAS.

Table 27. IID ET_c Results

Crop	Year	LCRAS	NDVI				Δ
			Q1	Median	Q3	N	
Bermudagrass /Kleingrass	2019	1378	1153	1329	1450	327	-49
	2020	1361	1191	1405	1512	1083	44
	2021	1361	1194	1426	1566	1045	65
	2022	1391	1232	1465	1609	1139	74
Alfalfa	2019	1583	1523	1554	1573	146	-29
	2020	1595	1389	1547	1579	197	-48
	2021	1608	1492	1571	1596	207	-37
	2022	1624	1374	1548	1603	204	-76
Citrus-Mature	2019	1113	1098	1102	1105	121	-10
	2020	1119	1050	1108	1111	130	-10
	2021	1129	1072	1121	1124	137	-9
	2022	1150	1008	1138	1141	131	-12
Citrus-Young	2019	666	1101	1103	1103	5	436
	2020	670	1106	1107	1109	6	437
	2021	676	894	1120	1122	3	444
	2022	688	800	1135	1138	217	446
Sudangrass	2019	916	1354	1500	1581	39	584
	2020	944	1520	1586	1645	51	642
	2021	899	1527	1606	1736	30	707
	2022	940	1482	1608	1791	340	668
Sugar beet	2019	860	641	940	1160	93	80
	2020	785	592	816	1057	96	31
	2021	880	708	929	1130	91	50
	2022	902	686	847	1041	65	-55

Table 28. Mohave ET_c Results

Crop	Year	LCRAS	NDVI				Δ
			Q1	Median	Q3	N	
Alfalfa	2019	1623	1506	1519	1538	106	-104
	2020	1753	1593	1634	1651	88	-119
	2021	1756	1625	1644	1658	87	-112
	2022	1759	1623	1659	1687	81	-100
Bermudagrass /Kleingrass	2019	999	906	984	1051	80	-15
	2020	1075	855	1034	1128	83	-41
	2021	1049	932	1068	1220	78	19
	2022	1046	848	937	1066	59	-109
Wheat	2019	569	322	382	471	31	-187
	2020	601	318	418	447	45	-183
	2021	653	140	501	556	40	-152
	2022	706	376	501	577	48	-205

6.4 Mohave

Three crops were evaluated at Mohave: alfalfa, combined Bermudagrass /Kleingrass , and wheat. NDVI modeling of alfalfa and wheat returned lower ET_c estimates than LCRAS (Table 28). Reasons for these results were described previously in the CRIT and IID sections. Generally there were fewer cuttings of alfalfa than the LCRAS standard of 9, thus lowering the crop water use estimates. Wheat plantings were later, had shorter durations than LCRAS, and also had lower ET_c estimates. The ET_c estimates for Bermudagrass /Kleingrass were about the same for either modeling approach except in 2022. More detailed analysis of modeling growth stages for these grasses would be needed to understand the 2022 results.

6.5 PVID

Six crops were evaluated at PVID: alfalfa, combined Bermudagrass /Kleingrass , mature citrus, cotton, dates (declining, mature, young), and wheat. Alfalfa and wheat ET_c results were less than LCRAS for reasons described above in the CRIT section (Table 29). Cotton ET_c were greater than LCRAS results. Bermudagrass /Kleingrass ET_c results were significantly lower than LCRAS for two years, and much less (by 530 mm) for 2021. Reasons for these differences may lie with the erratic and unpredictable cropping practices. Unlike results from alfalfa and Sudangrass sites, the Bermudagrass /Kleingrass NDVI patterns often do not allow discrimination of full cover from partial cuts. Differences in ET_c results for dates for all maturity levels are minimal but are probably not representative of actual ET_c values because there is only one set of LCRAS K_c values. This means that an adaptive approach, as done for citrus, could not be done.

Table 29. PVID ET_c Results

Crop	Year	LCRAS	NDVI				Δ
			Q1	Median	Q3	N	
Alfalfa	2019	1647	1536	1549	1564	123	-98
	2020	1767	1617	1640	1665	148	-127
	2021	1794	1670	1686	1704	223	-108
	2022	1728	1595	1620	1642	180	-108
Bermudagrass /Kleingrass	2019	1025	978	1099	1219	73	74
	2020	1085	419	983	1262	100	-102
	2021	1077	341	546	1260	113	-531
	2022	1054	450	891	1128	128	-163
Citrus-Mature	2019	774	983	1085	1093	17	311
	2020	826	817	1026	1170	12	200
	2021	837	706	707	1186	18	-131
	2022	814	687	689	1147	16	-125
Cotton	2019	920	1043	1126	1172	71	206
	2020	976	1112	1205	1339	45	229
	2021	946	1079	1148	1188	62	203
	2022	908	1077	1143	1192	60	235
Dates-Declining	2019	1782	1740	1740	1740	1	-42
	2020	1892	1898	1898	1902	3	6
	2021	1917	1924	1924	1925	3	8
	2022	1866	1867	1868	1870	4	2
Dates-Mature	2020	1892	1905	1906	1906	4	14
	2021	1917	1925	1925	1925	19	9
	2022	1866	1867	1870	1871	20	4
Dates-Young	2019	1782	1789	1790	1791	24	8
	2020	1892	1896	1899	1902	25	7
	2021	1917	1925	1925	1926	29	9
	2022	1866	1872	1873	1873	30	7
Wheat	2019	578	388	448	471	61	-130
	2020	591	421	478	500	57	-113
	2021	646	410	494	548	52	-152
	2022	653	439	491	517	38	-162

6.6 Yuma

ET_c results for eight crops were analyzed at Yuma: combined Bermudagrass /Kleingrass , dates (mature, young, declining), citrus (mature, young, declining), lettuce, wheat, Sudangrass , alfalfa, and cotton (Tables 30 and 31). Differences between the NDVI-derived and LCRAS ET_c results, for crops other than lettuce, and the reasons for them, have been described previously and are not repeated.

NDVI analysis of ET_c for lettuce showed significant increases in consumptive crop water use above those from LCRAS by 100-250 mm. This result comes from the difference in modeled growth stages. Generally, it appears that most lettuce sites were planted in early fall and had longer growing seasons ($\sim$10-20 days) than LCRAS. However, some of the ET_c differences might be less than analyzed because of complexities reflected in LCRAS. For example, lettuce can be evaluated under four different scenarios- Fall Early, Fall Late, Spring Early, and Spring Late (Figure 40). How the fields are classified has a major effect on modeled ET_c . Fall Early lettuce plantings might use significantly more water than Fall Late or Spring Early plantings, or they might use about the same if the season durations were correspondingly decreased. The fixed durations and timings for the LCRAS approach do not accommodate actual growing practice.

Table 30. Yuma ET_c Results Part 1.

Crop	Year	LCRAS	NDVI				Δ
			Q1	Median	Q3	N	
Bermudagrass /Kleingrass	2019	1014	1067	1101	1132	96	87
	2020	1064	531	1113	1182	150	49
	2021	1011	597	768	1165	163	-242
	2022	1016	642	1081	1137	172	65
Dates-Mature	2019	1776	1738	1745	1748	51	-31
	2020	1839	1812	1815	1818	103	-24
	2021	1816	1785	1788	1791	299	-28
	2022	1842	1811	1814	1816	311	-29
Dates-Young	2020	1839	1812	1819	1826	94	-20
	2021	1816	1780	1791	1797	161	-25
	2022	1842	1812	1817	1823	170	-25
Dates-Undifferentiated	2019	1776	1742	1746	1752	282	-30
	2020	1839	1812	1815	1819	235	-24
Citrus-Mature	2019	1117	1102	1106	1109	494	-10
	2020	1159	1145	1147	1150	386	-12
	2021	1148	1057	1138	1142	348	-10
	2022	1168	1038	1153	1157	301	-15
Citrus-Young	2019	668	812	1101	1107	160	433
	2020	694	836	1145	1149	156	451
	2021	687	870	1133	1141	169	446
	2022	699	774	1152	1155	196	453
Citrus-Declining	2019	782	1034	1104	1107	73	322
	2020	812	1113	1147	1149	91	335
	2021	804	1013	1133	1140	102	328
	2022	818	1000	1152	1154	59	334
Lettuce	2019	143	158	235	313	179	92
	2020	167	228	277	365	142	110
	2021	161	261	320	424	201	159
	2022	186	389	451	545	5	265

Table 31. Yuma ET_c Results Part 2.

Crop	Year	LCRAS	NDVI				Δ
			Q1	Median	Q3	N	
Wheat	2019	551	416	472	507	306	-79
	2020	540	407	438	463	330	-102
	2021	589	440	499	546	415	-91
	2022	622	437	485	528	475	-137
Sudangrass	2019	1090	1312	1400	1482	63	310
	2020	1141	1339	1410	1517	114	269
	2021	1085	1259	1332	1400	58	247
	2022	1089	1372	1416	1475	35	327
Alfalfa	2019	1628	1546	1558	1573	180	-70
	2020	1690	1568	1616	1633	504	-74
	2021	1672	1558	1601	1618	447	-71
	2022	1688	1571	1616	1632	221	-72
Cotton	2019	1045	885	978	1066	134	-66
	2020	1092	890	949	1013	96	-143
	2021	1037	834	897	974	111	-140
	2022	1035	859	946	1004	82	-89

Table 32. LCRAS Annual ET_c (mm/year): Coachella, CRIT

Area	Crop	2019	2020	2021	2022	Mean	SD
Coachella	Alfalfa	1583	1595	1608	1624	1603	18
	Bermudagrass	1378	1361	1361	1391	1373	14
	Carrot	682	715	743	766	727	36
	Citrus-Dec	780	784	791	806	790	11
	Citrus-Mat	1113	1119	1129	1150	1128	16
	Citrus-Yng	666	670	676	689	675	10
	Corn	902	888	902	944	909	24
	Cotton	977	997	955	976	977	17
	Dates	1770	1778	1787	1819	1788	21
	Decid Orch	1408	1424	1411	1432	1419	11
	Grape	945	947	933	960	946	11
	Kleingrass	1378	1361	1361	1391	1373	14
	Lettuce	217	242	247	249	239	15
	Olive	1083	1088	1095	1117	1096	15
	Sudangrass	916	945	899	940	925	21
	Wheat	661	612	693	723	672	48
CRIT	Alfalfa	1647	1767	1794	1728	1734	64
	Bermudagrass	1025	1085	1077	1054	1060	27
	Carrot	857	976	1010	972	954	67
	Citrus-Dec	774	826	838	814	813	28
	Citrus-Mat	1105	1179	1195	1161	1160	39
	Citrus-Yng	661	706	715	695	694	24
	Corn	757	773	817	835	796	37
	Cotton	920	976	946	908	938	30
	Dates	1782	1892	1917	1866	1864	59
	Decid Orch	1462	1552	1560	1513	1522	45
	Grape	954	991	1007	997	987	23
	Kleingrass	1025	1085	1077	1054	1060	27
	Lettuce	154	168	165	147	158	10
	Olive	1077	1146	1161	1131	1129	37
	Sudangrass	1094	1131	1165	1175	1141	37
	Wheat	578	591	646	653	617	38

Table 33. LCRAS Annual ET_c (mm/year): IID, Mohave

Area	Crop	2019	2020	2021	2022	Mean	SD
IID	Alfalfa	1583	1595	1608	1624	1603	18
	Bermudagrass	1378	1361	1361	1391	1373	14
	Carrot	693	629	715	727	691	44
	Citrus-Dec	780	784	791	806	790	11
	Citrus-Mat	1113	1119	1129	1150	1128	16
	Citrus-Yng	666	670	676	689	675	10
	Corn	902	888	902	944	909	24
	Cotton	977	997	955	976	977	17
	Dates	1770	1778	1787	1819	1788	21
	Decid Orch	1408	1424	1411	1432	1419	11
	Grape	945	947	933	960	946	11
	Kleingrass	1378	1361	1361	1391	1373	14
	Lettuce	217	242	247	249	239	15
	Olive	1083	1088	1095	1117	1096	15
	Sudangrass	916	945	899	940	925	21
	Sugar beet	860	785	880	902	857	51
	Wheat	661	612	693	723	672	48
Mohave	Alfalfa	1623	1753	1756	1759	1723	67
	Bermudagrass	999	1075	1049	1046	1042	32
	Carrot	678	741	778	829	757	64
	Citrus-Dec	763	823	823	834	811	32
	Citrus-Mat	1089	1174	1175	1191	1157	46
	Citrus-Yng	652	703	703	713	693	28
	Corn	744	789	797	839	792	39
	Cotton	893	949	917	896	914	26
	Dates	1754	1882	1882	1904	1855	68
	Decid Orch	1439	1539	1528	1532	1509	47
	Grape	930	985	983	991	972	29
	Kleingrass	999	1075	1049	1046	1042	32
	Lettuce	160	161	162	157	169	2
	Olive	1061	1140	1141	1156	1124	43
	Sudangrass	1071	1133	1141	1171	1129	42
	Wheat	569	601	653	706	632	60

Table 34. LCRAS Annual ET_c (mm/year): PVID, Yuma.

Area	Crop	2019	2020	2021	2022	Mean	SD
PVID	Alfalfa	1647	1767	1794	1728	1734	64
	Bermudagrass	1025	1085	1077	1054	1060	27
	Carrot	639	661	678	730	677	39
	Citrus-Dec	774	826	838	814	813	28
	Citrus-Mat	1105	1179	1195	1161	1160	39
	Citrus-Yng	661	706	715	695	694	24
	Corn	757	773	817	835	796	37
	Cotton	920	976	946	908	938	30
	Dates	1782	1892	1917	1866	1864	59
	Decid Orch	1462	1552	1560	1513	1522	45
	Grape	954	991	1007	997	987	23
	Kleingrass	1025	1085	1077	1054	1060	27
	Lettuce	154	168	165	147	158	10
	Olive	1077	1146	1161	1131	1129	37
	Sudangrass	1094	1131	1165	1175	1141	37
	Wheat	578	591	646	653	617	38
Yuma	Alfalfa	1628	1690	1672	1688	1670	29
	Bermudagrass	1014	1064	1011	1016	1026	25
	Carrot	678	692	743	774	722	45
	Citrus-Dec	783	812	804	818	804	16
	Citrus-Mat	1117	1159	1148	1168	1148	22
	Citrus-Yng	668	694	687	699	687	13
	Corn	725	720	738	753	734	15
	Cotton	1045	1092	1037	1035	1052	27
	Dates	1776	1839	1816	1842	1818	31
	Decid Orch	1418	1472	1440	1453	1446	23
	Grape	942	970	944	948	951	13
	Kleingrass	1014	1064	1011	1016	1026	25
	Lettuce	143	167	161	186	164	18
	Olive	1086	1126	1113	1131	1114	20
	Sudangrass	1090	1141	1085	1089	1101	27
	Wheat	551	540	589	622	576	37

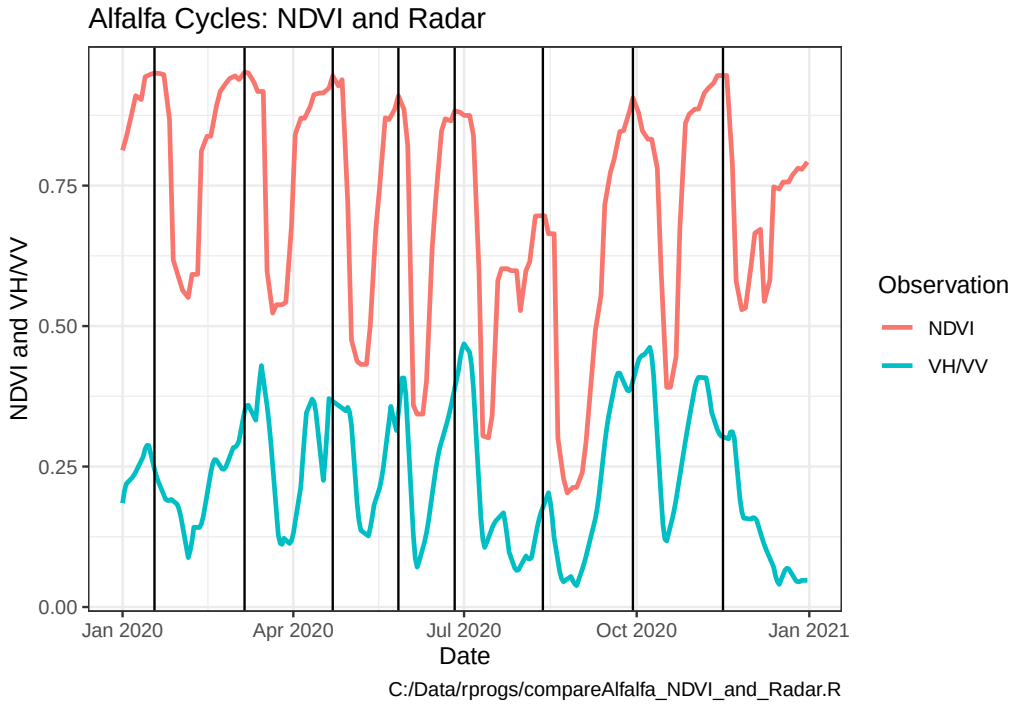

Figure 54. Tracking alfalfa cuttings with NDVI (red) and VH/VV from active radar (blue). Shown are interpolated field-averaged daily values over a single site in the Yuma Area in 2020. Vertical black lines denote dates with peak NDVI. Cutting intervals range 30-48 days.

7 Extending ET_c estimation with Radar Remote Sensing

The growth stage approach works well for the LCRAS region and is applicable for any other irrigated region. However, practicality of the technique is limited when skies are cloudy. Even in the Lower Colorado River region there are times when clouds interfere with NDVI-retrieval. In these instances, growth stages for short-season crops would be unresolved, despite daily satellite overpasses.

An alternative that can fill these data gaps lies with satellite-based active C-band radar data sets. Radar data provide a surrogate for crop cover. Using vertical (V) and horizontal (H) polarization measurements, irrigation events and crop biomass changes can be detected (McNairn and Brisco, 2004; Jiao et al., 2011; Guillevic et al., 2024). The measurements are denoted in letter-pairs: the first indicates the transmitted po-

larization and the second the received polarization. Vertical-transmitted/Vertical-received (VV) measurements are sensitive to early irrigation events. The ratio of Vertical-transmitted/Horizontal-received measurement to VV measurements (VH/VV) can be used as a biomass indicator and a surrogate for NDVI. The Sentinel-1 satellites (Sentinel-1 Satellites) are one source of these: they provide ∼15 m resolution images every 6-12 days. Another possible source will be from the NISAR satellite, a joint NASA-ISRO microwave mission (NISAR) that will increase overpass frequencies to five days and increase spatial resolution up to 5 m. At the time of this report, NISAR is expected to be launched in spring 2025.

Demonstrations of radar capabilities are shown for three crops: alfalfa, citrus, and lettuce.

Full cover of alfalfa is seen by peak NDVI values and by peak VH/VV polarization ratio values. For estimating ET_c over alfalfa, it is important to track cutting cycles, a task that requires frequent observations. These are obtained with Sentinel-1 and Sentinel-2. Using 6 day periodicity for Sentinel-1 radar data and 3-5 day periodicity for Sentinel-2 NDVI data over the Yuma site in 2020 identifies 8 major cuttings (Figure 54).

Evaluation of citrus maturity can be done using NDVI or the VH/VV radar values (Figure 55). Day-to-day values are noisy, but weekly to annual trends for NDVI and VH/VV are the same: low values for young citrus (1-3 m heights) and higher values for mature citrus (>3 m tree height). Discrimination between mature and declining trees is not realized with NDVI. Current results suggest that radar will also not be able to reliably discriminate between these citrus tree classes.

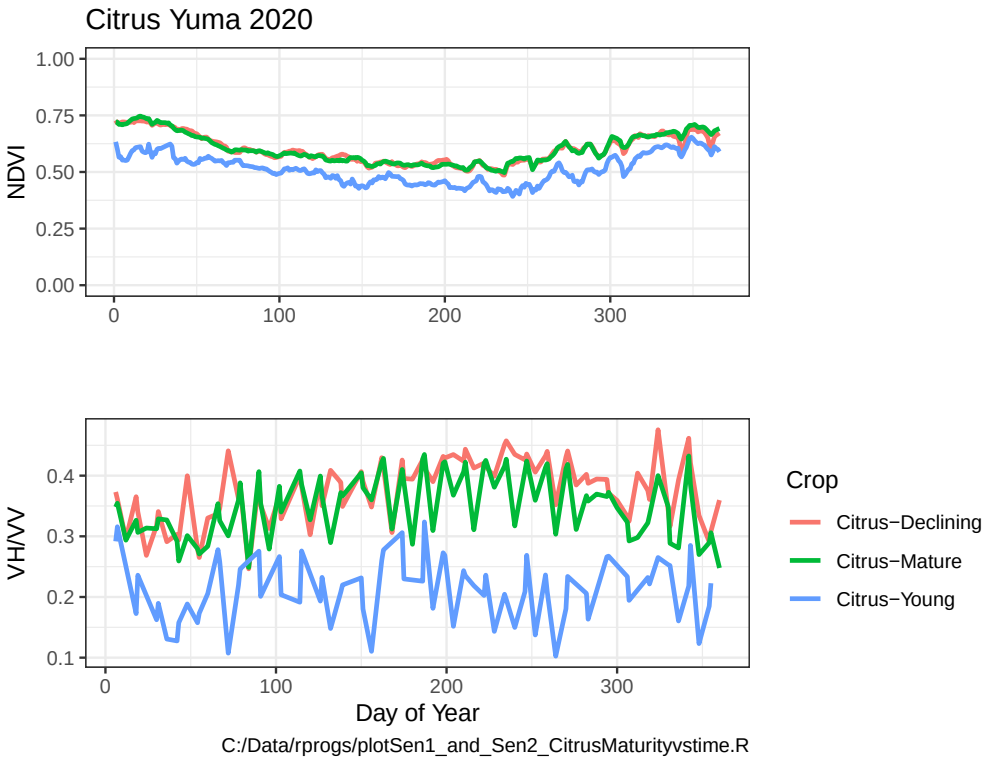

Figure 55. Citrus maturity vs. day of year using NDVI (top) and radar VH/VV (bottom). Note that radar data discriminate young and mature citrus in the same way- average VH/VV and NDVI are both greater for mature trees than for young trees.

Table 35. Lettuce ET_c (mm/year) from radar observations.

Year	ET_c			
	VH/VV	NDVI	LCRAS	N
2019-2020	185	240	143	23
2020-2021	238	294	167	17
2021-2022	251	246	161	52

The VH/VV metric can also track growth stages for vegetable crops. As illustrated for four head-lettuce fields (Figure 56), crop development, mid-season, and end-season stages are all resolved at the same times, whether by radar or by NDVI. An additional capability with VV radar is detection of the start of initial stages (data not shown). Using the same quantile selection approach with VH/VV as was done with NDVI results in similar ET_c estimates (Table 35), with values in between LCRAS and NDVI-based results. Fields sampled with Sentinel-1 also show similar ET_c distributions: compare 2020 and 2021 radar-derived results (Figure 57) with those from Sentinel-2 NDVI (Figure 41, page 78).

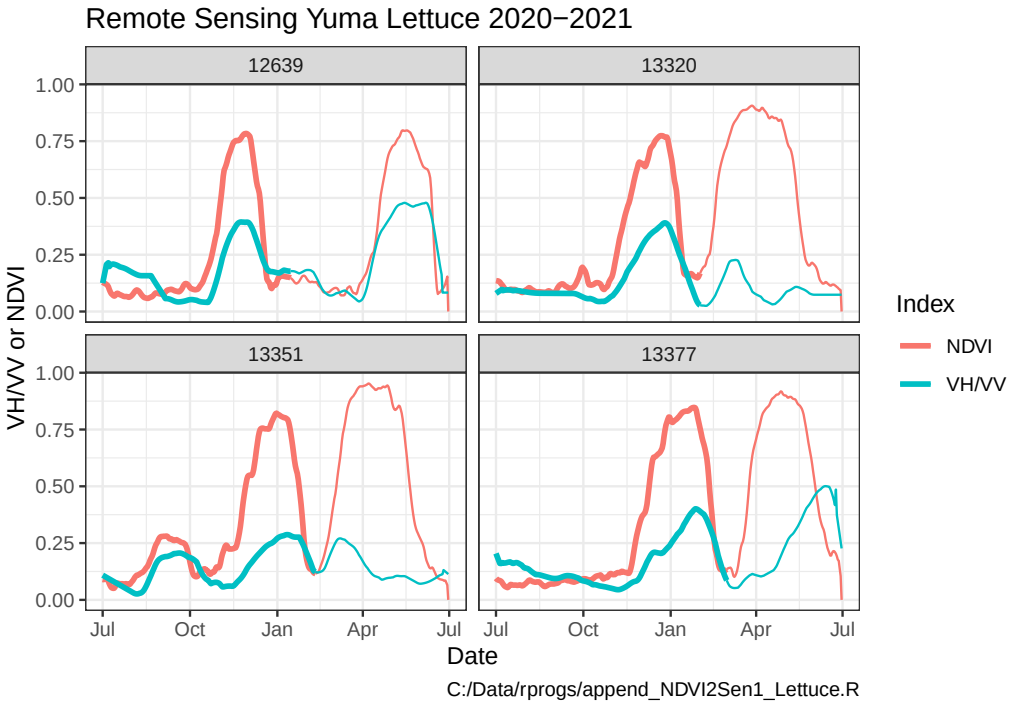

Figure 56. Lettuce time series at Yuma showing similar patterns for vegetation and soil as represented by NDVI (thick red) and VH/VV (thick blue). Both time series were smoothed and interpolated to daily time steps. The thin red and thin blue lines represent an unidentified crop; at Yuma this would commonly be durum wheat.

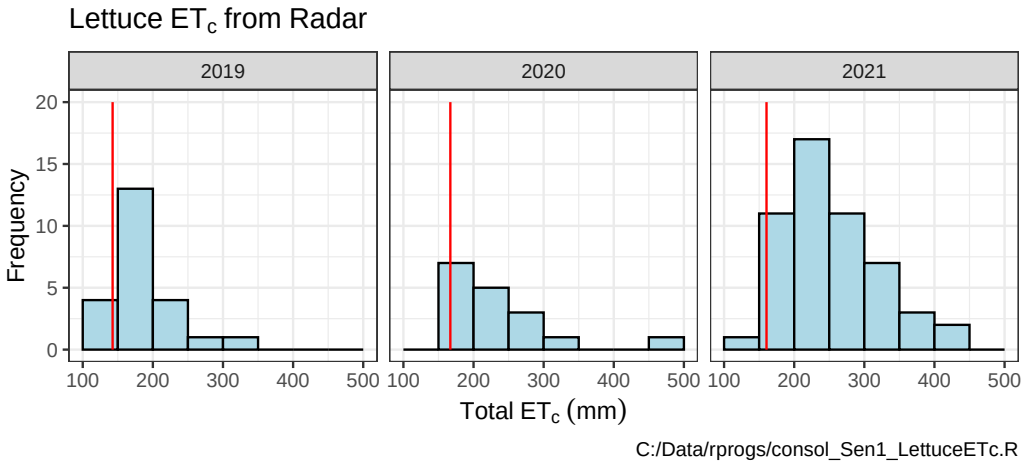

Figure 57. Total ET_c (mm/year) for lettuce (blue histograms) at Yuma using radar observations. Corresponding LCRAS ET_c values are shown as red lines.

8 Implications, Comments, and Recommendations

Reclamation recognized that the FAO-56 crop coefficients, not having been calibrated for the extreme heat environments in the five LCRAS irrigation areas, needed adjustment. Accordingly, the Bureau revised the coefficients for all significant crops (Jensen, 1998, 2003). The result was an improved representation of ET_c by area and year because the updates specified and incorporated knowledge of local cropping practices and weather.

However, the updates use fixed planting dates and crop durations, and so can not adapt to actual field management. The NDVI methodology introduced in this report provides an additional level of refinement to LCRAS that produces more accurate and more comprehensive understanding of actual growth stages. The refinement uses readily available satellite remote sensing images, web-based software processing, and locally developed scripts to return estimates of daily and annual ET_c for all irrigated crops grown in the lower Colorado River Basin.

The following sections summarize the implications of these findings, provide comments on the inputs and outputs from the NDVI approach, and make general and specific recommendations for Reclamation action.

8.1 Implications

This study shows that remote sensing technology can enable a more comprehensive and more representative set of ET_c estimates than possible with the current LCRAS methodology. The scripts and documentation provided by this report enable adoption of the technology by Reclamation. Its implementation includes simple and complex components that require skilled and knowledgeable staff. The data sets and software required are readily available, frequently at no cost. If adopted, the technique could enhance reliability of its Evapotranspiration Report.

8.2 Comments on the NDVI growth stage methodology

This project proposed, tested, and evaluated a methodology to improve ET_c estimation accuracy by tracking crop growth stages using satellite-based NDVI. Multiple scripts written in the R language and GEE javascript were written to handle processing (Table 1). This section comments on three components of the project: remote sensing data quality and data availability, processing of the data, and results from the processing.

8.2.1 Remote Sensing Data

The methodology relied upon availability of high quality visible/near infrared remote sensing data. Observations from Sentinel 2 (Sentinel 2 Products) met this need: overpass images were available routinely for North America every 3-5 days at 10 m resolution. Prior to 2018 these data were not available. Observations from two other sensors were considered: Landsat (Landsat Products) and Planet (Planet Products). Landsat, a very high quality, well-calibrated sensor, available for decades, collects observations at longer intervals (8-16 days) and poorer spatial resolution (30 m), than Sentinel-2. The longer intervals make tracking of short season crops inaccurate and especially difficult when cloudy skies intervene. Planet sensors, a more recent option, are available nearly daily at 4 m resolution- and so exceed Sentinel-2 sampling. Planet data, however, are not free and calibration quality is not as good as Sentinel 2 or Landsat.

8.2.2 NDVI Processing

Initial processing steps were routine and encountered few obstacles. They included assembling shapefiles describing the locations of fields and crop types in all irrigation areas, compiling associated weather station data, and using the GEE API to deliver the NDVI time-series by time and location.

Subsequent processing steps, described in Section 4, were also generally routine. Some intervention was required to identify and remove bad or excessively noisy NDVI values. The steps included time-series filtering, interpolation, and smoothing needed to create the crop growth stages.

Script development (Section 4) to identify the crop growth stages was more problematic. While prototype scripts existed at project start, these scripts had not been tested for all crops and irrigation areas. Because of differences in NDVI signals among crops– some change smoothly with time, others rapidly, and still others erratically– two questions soon arose: 1) should there be individual, customized scripts for each crop, or should there be one?, and 2) how should the growth stage approach be configured to handle tree crops?

The decision was made to develop two sets of scripts and provide Reclamation the opportunity to evaluate benefits and drawbacks of each.

For the first set, scripts were revised and created to partition growth stages for 14 specific crops. This approach kept program lengths short, facilitated programming debugging, and enabled rapid processing. Each script was customized to accommodate single or multiple cropping cycles, differences in growing season duration, and

Table 36. NDVI Growth Stage Tracking Outcome Groups.

Group	Crops	Outcome
1	alfalfa, lettuce, wheat, cotton, corn, sugar beet	Fully successful
2	citrus, dates, olives	Alternative identified
3	Bermudagrass , Kleingrass , Sudangrass , carrots	Undetermined

whether or not crops spanned calendar year boundaries.

The second programming path created a unified package that considers all crops. This approach simplifies model runs– users do not have to selectively implement scripts by crop type– but its run-times are lengthy (sometimes ∼30 minutes). The script is large (22,500 lines) and complex, making maintenance more difficult than for the first set.

Handling the second question– modeling of tree crops– was resolved in an exploratory fashion. Initially growth stage partitioning was done in a similar way to annual crops, and finally partitioning became a hybrid approach where the resulting quantiles were adjusted for tree maturity. By using NDVI quantiles, we assumed that K_c patterns for citrus were representative, both of which decrease in the spring and increase in the fall. With processing experience, two facts became apparent. One was that the NDVI decrease/increase patterns occurs for all tree crops and is largely a remote sensing artifact from season changes in solar zenith angles. The other was that tree maturity, Reclamation K_c curves, and corresponding NDVI values were closely correlated. These two realizations led to a modification for modeling. Quantile selections were used for growth stage delineation, while seasonal NDVI averages were used to adjust K_c values.

8.2.3 Growth Stage Modeling Outcomes

The success of the NDVI growth stage tracking methodology was demonstrated by different groups of crops assessed. These outcomes fell into three groups: 1- Fully successful, 2- Alternative Identified, and 3- Undetermined (Table 36).

The ‘Fully successful’ crops (group 1), consisted of annual crops in large fields (10+ acres). The NDVI tracking approach was able to consistently and accurately identify crop growth stages and convert these into meaningful ET_c values because the NDVI time series progressed smoothly or predictably. Crops included were lettuce, wheat, cotton, corn, sugar beet, and alfalfa. Inclusion of alfalfa is noteworthy because successful resolution of its stages requires frequent satellite overpasses.

‘Alternative identified’ crops (group 2), included citrus and dates. As noted in

Section 8.2.2, NDVI growth stage analysis was confounded by solar illumination effects, but then addressed by incorporating tree maturity information that enables dynamic estimation of ET_c . Using NDVI data over hundreds of citrus sites showed strong correspondence exists between seasonally averaged NDVI values and tree maturity (Figure 8). Which season, winter or summer, to use for averaging may not be important. For this project average mid-winter times were used (corresponding to 'early' and 'late' times) to maximize differences between young and mature trees. Maturity-based K_c values for dates and olives were not available. Maturities were not defined for declining trees, hence ET_c estimates for these cases were assessed by using the K_c Young-Mature scheme.

'Undetermined' crops (group 3) included Bermudagrass , Kleingrass , Sudangrass , and carrots. Data analyzed for these crops did not resolve if K_c and ET_c could be accurately tracked using the proposed growth stage approach. Reasons for uncertainty lie with noisy and hard-to-interpret NDVI patterns. Erratic NDVI signals could be due to remote sensing resolution problems for small ($<$10 acres) or heterogeneous fields, or to variable grass cutting activities. Variability for Bermudagrass and Kleingrass depends in part on irrigation areas- the patterns are irregular for IID (Figure 16) and Coachella, but annually bi-modal for Yuma (Figure 17). These differences mean that sometimes growth stages can be resolved and other times not. Because the LCRAS approach makes no attempt to discriminate between grass cuttings, an alternative NDVI-based approach for ET_c was created for group 3 crops: thresholding (Figure 5, page 23). This method is simple to apply and abandons individual stage identification. If vegetated, the MID-season K_c value is assigned, else it is set to zero. ET_c estimates over Bermudagrass with thresholding are reasonable. Because these crops are significant water consumers, it is important to find an accurate and consistent remote sensing approach. Use of higher spatial resolution data could remove the stage identification problem or, alternatively, the thresholding could be tested.

8.3 Comments on using LCRAS, NDVI, and K_c for ET_c estimation

8.3.1 ET_c from LCRAS

The LCRAS methodology is a well-established and succcessful approach to estimate ET_c over irrigated crops within the Lower Colorado River region. Its achievements, documented in this report, may be due to representative K_c values (updated in 2003) and to the insensitivity of modeling crop growth as static annual patterns. Comparison of LCRAS results with other models for four crops (broccoli, wheat, alfalfa, cotton), showed that its estimation accuracy sometimes exceeds the OpenET model 'SIMS'

(French et al., 2023).

As successful as LCRAS has been, however, it has shortcomings. The LCRAS K_c models are too simple to be representative of actual field conditions. For example, the LCRAS model for wheat (Figure 49) prescribes crop growth on the wrong days, resulting in an inaccurate estimate of total ET_c (e.g., Figure 4C). Notwithstanding remarks by Jensen (2003, pp.16-17), shifting of planting dates does have a significant impact on ET_c . Shifting of planting dates is sometimes much more than 5-10 days- for wheat the shift exceeds 30 days (Figure 50). The LCRAS model also specifies inaccurate growing season lengths (e.g., Figure 30) which further compromises total ET_c estimates.

Also problematic is LCRAS's reliance upon accurate crop classifications. Crop classifications drive the selection of K_c values and the specification of the corresponding crop growth stages. Erroneous classifications affect ET_c estimates at field scales and, if numerous, can significantly bias results for irrigation areas. One potential way to reduce problems from crop mis-classification is to incorporate an Artificial Intelligence (AI) crop classification processing data pipeline. The addition of skilled and knowledgeable GIS personnel could be used to develop and deploy an updated LCRAS system that might not need as many field site visits as currently implemented.

8.3.2 ET_c from NDVI

The NDVI growth stage modeling approach addresses some LCRAS weaknesses and provides a way to accurately model crop ET_c and to adapt to changes in crop management. Satellite remote sensing corrects most errors simply and directly. With online tools such as GEE, NDVI time series for all irrigation areas within the Lower Colorado River Basin can be generated in short times. The NDVI output can be converted to K_c patterns for annual and perennial crops which are then converted to ET_c in the same way as done currently by LCRAS. Outcomes from this study highlighted how the NDVI approach altered LCRAS ET_c estimates:

1. Alfalfa, carrots, sugar beet, and wheat consume significantly lesser amounts of water than estimated by LCRAS.

2. Bermudagrass /Kleingrass , Citrus-Young, grapes, head lettuce, and Sudangrass consume significantly greater amounts.

3. Dates consume about the same water regardless of methodology.

4. Cotton water consumption values are variable and can be greater or less than LCRAS

As is true for LCRAS, the NDVI approach also has shortcomings that need to be acknowledged. Three pre-eminent ones are related to crop classifications, cloudy skies, and field sizes. Even though remote sensing enables crop growth mapping, accurate K_c values still rely upon knowing the crop type. Using remote sensing image data opens opportunities for rich data sets and sub-field analyses, but because NDVI data cannot be observed when skies are cloudy, locating the INI, DEV, MID, and END transitions could be difficult. Regarding field size, freely available satellite data have 10-30 m resolution and cannot resolve small or highly heterogeneous fields.

Opportunities to reduce these shortcomings lie with the use of different remote sensors. Crop classfication errors can be lowered by using AI-tools as noted above, and by using emerging hyperspectral sensors. Data gaps from cloudy skies can be reduced by using radar remote sensing. Problems resolving small fields could be minimized by using 1-4 m image data from commercial providers (e.g., Planet).

8.3.3 ET_c from K_c

Both the NDVI growth stage and LCRAS approaches use crop coefficients to guide ET_c, and it is important to recognize the limits of K_c as a tool. K_c values are empirically derived and geographically and variety-specific. The single K_c approach ignores early season evaporation events and it assumes negligible crop water stress. For vegetable crops, water stress is probably a minor concern. Other crops, notably alfalfa, are managed with seasonal summer-time deficits, and it is unclear if the K_c -approach adequately accommodates those intervals. At the cost of greater complexity and need for soil-related maps, use of the dual K_c approach resolves some problems by improving the modeling early-season evaporation. However, problems from the empiricism and need for geographic and variety calibrations remain.

8.3.4 ET_c from Land Surface Temperatures

For these reasons, some researchers advocate modeling of ET_c using a thermal-based approach. Use of land surface temperature (LST) observations, instead of crop coefficients, address these weaknesses by using vegetation, soil, and air temperature differences to model ET_c. This tactic to look at model physics is compelling and may eventually be the best approach. Five such models are now available via the OpenET platform (`https://etdata.org`) and may provide a more accurate way to map LCRAS evapotranspiration. Preliminary evidence from Yuma studies, however, shows that OpenET isn't as accurate as either LCRAS or the NDVI approach. One reason could be that crop coefficients produce accurate ET_c values for crops that are

fully irrigated, which is likely the case for many Lower Colorado River crops. On the other hand, consistently obtaining accurate LST data is difficult, which means that the resulting ET_c values are sometimes inaccurate. Overall, the NDVI approach produces better outcomes, and the reason may be its superior spatial (10 m) and temporal (3-5 days) resolution. In contrast, the OpenET platform relies upon Landsat, which provides LST observations at ∼100 m at 8 day intervals. Upcoming satellites such as Hydrosat (30 m resolution, https://hydrosat.com) and Trishna (60 m resolution, https://cnes.fr/en/projects/trishna) would greatly improve prospects for ET_c estimation with LST.

8.4 Recommendations

1. Revise crop type mapping at LCRAS

   (a) Update crop type maps to most recently completed year. Current crop type maps are lacking, making it difficult to evaluate the effects of the NDVI approach on estimated consumptive water use and how it compares with the existing LCRAS methodology.

   (b) Test Artificial Intelligence models to improve crop classification at LCRAS. Multiple crop type maps are required within each year to accurately estimate ET_c within LCRAS, but their creation requires time-consuming and costly field verification. Verifications cannot be eliminated, but with use of Artificial Intelligence approaches- now becoming widely accessible– it is possible that they could be reduced, and the subsequent analyses accelerated, by using Machine Learning (ML, e.g., Zhang et al., 2019), Deep Learning approaches (DL, e.g., Sakka et al., 2024).

   (c) Incorporate time series metrics in the ML and DL models. The metrics could include vegetation indices, surface temperatures, radar signals, and weather data.

   (d) Incorporate higher spatial resolution data (<5 m) to increase classification accuracy. One possible source is Planet Labs (https://www.planet.com).

   (e) Test ML and DL models on 2024 results, compare with the existing LCRAS classification approach.

2. Compare NDVI and LCRAS results with OpenET (https://etdata.org).

3. Evaluate reduction of data gaps due to cloudy skies by using active radar sensors to track crop growth stages. Sentinel-1 data are readily available (Sentinel 1 Products).

4. Evaluate efficacy of NDVI thresholding vs. NDVI growth stage mapping. Simple to implement, potentially useful for alfalfa, Bermudagrass , Kleingrass , Sudangrass and could be applicable to wheat, corn, sugar beet.

5. Shift the July field visit to October to improve sampling of fall vegetables. Data for lettuce (Figure 40) shows that many fields have full cover October-November and could be missed in the December field visits.

6. Revise crop coefficients.

   (a) Review FAO-56 updates (Pereira et al., 2021a,b; Rallo et al., 2021).

   (b) Modify LCRAS citrus and dates coefficients.

      i. Ensure continuity across years. Check citrus, dates and deciduous orchards.

      ii. Adjust K_c curves for tree maturity (see Figure 9).

      iii. Evaluate impact of solar elevation angle on NDVI for tree crops.

   (c) Simplify IID and Coachella K_c curves to match the FAO-56 protocol for INI/MID/END (see Figure 1).

   (d) Standardize treatment of K_c values where pre-irrigation and/or salt-leaching events are important. Current LCRAS values sometimes include episodic events (e.g., Figure 1).

7. Evaluate remote sensing signals of 'summer slump' of alfalfa (i.e., the season when the physiological response of alfalfa in maintaining the crown of the plants cause yields to fall significantly). See Alfalfa slump for more details. Do the mid-summer NDVI drops for alfalfa (Figure 15) correspond to K_c drops? Specifically, should K_c MID be decreased from 1.1-1.16 to lower values?

8. Evaluate the potential of indices other than NDVI to reduce solar zenith angle effects and increase the biomass signal for remote sensing of tree crops.

9 Acknowledgements

- Charles A. Sanchez made possible the joint collaboration between USBR, University of Arizona, and USDA, and contributed essential knowledge about farming practices along the Lower Colorado River.
- Cynthia H. Elek provided invaluable editorial assistance.

References

Allen, R., Walter, I., Elliott, R., Howell, T., Itenfisu, D., Jensen, M., Snyder, R., 2005. The ASCE standardized reference evapotranspiration equation. Technical Report. ASCE. Reston, VA, USA. doi:10.1061/9780784408056.

Allen, R.G., Pereira, L.S., Raes, D., Smith, M., 1998. Crop Evapotranspiration, guidelines for computing crop water requirements. Technical Report 56. FAO. URL: http://fao.org/4/x0490e/x0490e00.htm.

Beede, R.H., Goldhamer, D.A., 2005. Olive Production Manual. University of California Division of Agriculture and Natural Resources. chapter Olive Irrigation Management. 3353, pp. 61–69.

Brock, F., 1986. A nonlinear filter to remove impulse noise from meteorological data. Journal of Atmospheric and Oceanic Technology 3, 51–58. doi:10.1175/1520-0426.

Carlson, T.N., Ripley, D.A., 1997. On the relation between NDVI, fractional vegetation cover, and leaf area index. Remote Sensing of Environment 62, 241–252.

Claverie, M., Ju, J., Masek, J.G., Dungan, J.L., Vermote, E.F., Roger, J.C., Skakun, S.V., Justice, C., 2018. The Harmonized Landsat and Sentinel-2 surface reflectance data set. Remote Sensing of Environment 219, 145–161. doi:10.1016/j.rse.2018.09.002.

Erie, L., French, O., Bucks, D., Harris, K., 1982. Consumptive use of water by major crops in the Southwestern United States. Technical Report 29. USDA-ARS. URL: http://cales.arizona.edu/crops/irrigation/consumuse/conusefinal.pdf.

Faber, B., 2015. Drought Tip: Irrigating Citrus with Limited Water. Technical Report 8549. University of California Agriculture and Natural Resources. URL: http://anrcatalog.ucanr.edu/pdf/8549.pdf.

French, A., Sanchez, C.A., Wirth, T., Scott, A.T., Shields, J., Bautista, E., Saber, M.N., Wisniewski, E., Gohardoust, M.R., 2023. Remote sensing of evapotranspiration for irrigated crops at Yuma, Arizona, USA. Agricultural Water Management 290. doi:10.2139/ssrn.4485208.

French, A.N., Hunsaker, D.J., Sanchez, C.A., Saber, M., Gonzalez, J.R., Anderson, R., 2020. Satellite-based NDVI crop coefficients and evapotranspiration with eddy covariance validation for multiple durum wheat fields in the US Southwest. Agricultural Water Management 239, 13. doi:10.1016/j.agwat.2020.106266.

French, A.N., Sanchez, C.A., Hunsaker, D.J., Anderson, R.G., Saber, M.N., Wisniewski, E.H., 2024. Lettuce evapotranspiration and crop coefficients using eddy covariance and remote sensing observations. Irrigation Science doi:10.1007/s00271-024-00921-x.

Gorelick, N., Hancher, M., Dixon, M., Ilyuschenko, S., Thau, D., Moore, R., 2017. Google Earth Engine: planetary-scale geospatial analysis for everyone. Remote Sensing of Environment 202, 18–27. doi:10.1016/j.rse.2017.06.031.

Guillevic, P.C., Aouizerats, B., Burger, R., Besten, N.D., Jackson, D., Ridderikhoff, M., Zajdband, A., Houborg, R., Franz, T.E., Robertson, G.P., Jeu, R.D., 2024. Planet's biomass proxy for monitoring aboveground agricultural biomass and estimating crop yield. Field Crops Research 316, 109511. doi:10.1016/j.fcr.2024.109511.

Hanson, B., Bali, K., Orloff, S., Sanden, B., Putnam, D., 2008. How much water does alfalfa really need?, in: Proceedings, 2008 California Alfalfa and Forage Symposium and Western Seed Conference, UC Cooperative Extension. pp. 1–6. URL: https://alfalfa.ucdavis.edu/sites/g/files/dgvnsk12586/files/media/documents/08-265.pdf.

Hills, F., Winter, S., Henderson, D., 1990. Irrigation of Agricultural Crops - Agronomy Monograph. ASA-CSSA-SSSA, 677 South Segoe Road, Madison, WI 53711 USA. chapter Sugarbeet. 30, pp. 795–810.

Hunsaker, D., Hendrey, G., Kimball, B., Lewin, K., Mauney, J., Nagy, J., 1994. Cotton evapotranspiration under field conditions with CO2 enrichment and variable soil moisture regimes. Agricultural and Forest Meteorology 70, 247–258. doi:10.1016/0168-1923(94)90061-2.

Husman, S., Ottman, M.J., 2015. Irrigation of small grains in Arizona. Technical Report AZ1345. Cooperative Extension, University of Arizona. Tucson, AZ 85721, USA. URL: https://cales.arizona.edu/forageandgrain/sites/cals.arizona.edu.forageandgrain/files/az1345-2015.pdf.

Jafari, M., Kamali, H., Kehavrz, A., Momeni, A., 2021. Estimation of evapotranspiration and crop coefficient of drip-irrigated orange trees under a semi-arid climate. Agricultural Water Management 248. doi:10.1016/j.agwat.2021.106769.

Jensen, M., 1998. Coefficients for vegetative evapotranspiration and open water evaporation for the Lower Colorado River Accounting System. Technical Report. U.S. Bureau of Reclamation. Boulder City, NV, USA.

Jensen, M., 2003. Vegetative and Open Water Coefficients for the Lower Colorado River Accounting System, Addendum to the 1998 Report. Technical Report. U.S. Bureau of Reclamation. Boulder City, NV, USA.

Jiao, X., McNairn, H., Shang, J., Pattey, E., Liu, J., Champagne, C., 2011. The sensitivity of RADARSAT-2 polarimetric SAR data to corn and soybean leaf area index. Canadian Journal of Remote Sensing 37, 69–81. doi:10.5589/m11-023.

Kaffka, S., Tharp, R., 2013. Sugarbeet Production in the Imperial Valley. Technical Report 224142. University of California and Spreckels Sugar Company. URL: https://ucanr.edu/sites/sugarbeets/files/224142.pdf.

Knowles, T.C., Ottman, M.J., 2015. Sudangrass hay production in the irrigated deserts of Arizona and California. Technical Report AZ1664. Cooperative Extension, University of Arizona. Tucson, Arizona, 85721 USA. URL: https://cales.arizona.edu/forageandgrain/sites/cals.arizona.edu.forageandgrain/files/az1664-2015.pdf.

Mayberry, K.S., Meister, H., 2003. Sample Cost to Establish and Produce Kleingrass Hay. Technical Report KG-IM-03. University of California Cooperative Extension. URL: https://coststudyfiles.ucdavis.edu/uploads/cs_public/e2/44/e244021e-fd2e-4bec-8b7a-257420b2a0c8/kleingrass03.pdf.

McNairn, H., Brisco, B., 2004. The application of C-band polarimetric SAR for agriculture: a review. Canadian Journal of Remote Sensing 30, 525–542. doi:10.5589/m03-069.

Meister, H.S., 2004a. Sample cost to establish and produce Bermudagrass Hay. Technical Report BG-IM-04-02. University of California. Imperial County Cooperative Extension, CA, USA. URL: https://coststudyfiles.ucdavis.edu/uploads/cs_public/c9/4e/c94ec5b7-888d-482f-a6cb-b495d65e72e8/bermseed04.pdf.

Meister, H.S., 2004b. Sudangrass. Technical Report SU-IM-04. University of California Cooperative Extension. Imperial County Cooperative Extension, California, USA. URL: https://coststudyfiles.ucdavis.edu/uploads/cs_public/a2/ba/a2ba6644-27fc-4e2a-b70e-611d9c23d636/sudangrass04.pdf.

Montazar, A., Geisseler, D., Cahn, M., 2021. Spatial variability of nitrogen uptake and net removal and actual evapotranspiration in the California desert carrot production system. Agriculture 11. URL: https://doi.org/10.3390/agriculture11080752.

Montazar, A., Krueger, R., Corwin, D., Pourreza, A., Little, C., Rios, S., Snyder, R.L., 2020. Determination of actual evapotranspiration and crop coefficients of California date palms using the residual of energy balance approach. Water 12. doi:10.3390/w12082253.

Mu, X., Yang, Y., Xu, H., Guo, Y., Lai, Y., McVicar, T.R., Xie, D., Yan, G., 2024. Improvement of NDVI mixture model for fractional cover estimation with consideration of shaded vegetation and soil components. Remote Sensing of Environment 314. doi:10.1016/j.rse.2024.114409.

Panella, L., Kaffka, S.R., Lewellen, R.T., McGrath, J.M., Metzger, M.S., Strausbaugh, C.A., 2014. Yield Gains in Major U.S. Field Crops. CSSA. research report Sugarbeet. Special Publication 33, pp. 357–395. doi:10.2135/cssaspecpub33.c13.

Peacock, B., 1995. Water Management for Grapevines. Technical Report IG1-95, 82035. Cooperative Extension, University of California. Tulare County, CA. URL: https://ucanr.edu/sites/Tulare_County/files/82043.pdf.

Pereira, L., Paredes, P., Hunsaker, D., López-Urrea, R., Shad, Z.M., 2021a. Standard single and basal crop coefficients for field crops. updates and advances to the FAO56 crop water requirements method. Agricultural Water Management 243, 1–35. doi:10.1016/j.agwat.2020.106466.

Pereira, L., Paredes, P., López-Urrea, R., Hunsaker, D., Mota, M., Shad, Z.M., 2021b. Standard single and basal crop coefficients for vegetable crops, an update of FAO56 crop water requirements approach. Agricultural Water Management 243, 1–29. doi:10.1016/j.agwat.2020.106196.

R Core Team, 2021. R: A Language and Environment for Statistical Computing. R Foundation for Statistical Computing. Vienna, Austria. URL: https://www.R-project.org.

Rallo, G., Paço, T., Paredes, P., Puig-Sirera, A., Massai, R., Provenzano, G., Pereira, L., 2021. Updated single and dual crop coefficients for tree and vine fruit crops. Agricultural Water Management 250, 1–24. doi:10.1016/j.agwat.2020.106645.

Ramos, A.F., Santos, F.L., 2009. Water use, transpiration, and crop coefficients for olives (cv. cordovil), grown in orchards in southern Portugal. Biosystems Engineering 102, 321–333. doi:10.1016/j.biosystemseng.2008.12.006.

Rouse, J.W., Haas, R.H., Scheel, J.A., Deering, D.W., 1974. Monitoring vegetation systems in the Great Plains with ERTS, in: Proceedings, 3rd Earth Resource Technology Satellite (ERTS) Symposium, pp. 48–62.

RStudio Team, 2020. RStudio: Integrated Development Environment for R. RStudio, PBC. Boston, MA. URL: https://posit.co/products/open-source/rstudio/.

Sakka, M.E., Mothe, J., Ivanovici, M., 2024. Images and cnn applications in smart agriculture. European Journal of Remote Sensing 57, 1–29. doi:10.1080/2279254.2024.2352386.

Wang, H., Muller, J.D., Tatarinov, F., Yakir, D., Rotenberg, E., 2022. Disentangling soil, shade, and tree canopy contributions to mixed satellite vegetation indices in a sparse dry forest. Remote Sensing 14. doi:10.3390/rs14153681.

Wright, G.C., 2021. Irrigating Citrus Trees. Technical Report AZ1151. University of Arizona Cooperative Extension. URL: https://extension.arizona.edu/sites/default/files/2024-08/az1151-2021%2520%25282%2529.pdf.

Zhang, J., He, Y., Yuan, L., Liu, P., Zhou, X., Huang, Y., 2019. Machine learning-based spectral library for crop classification and status monitoring. Agronomy 9. doi:10.3390/agronomy9090496.